The Effect of the Pool and Riffle on Transport in Rivers

by

Ian Halket

A Thesis submitted to the Faculty of Graduate Studies of

The University of Manitoba

in partial fulfilment of the requirements of the degree of

DOCTOR OF PHILOSOPHY

Department of Civil Engineering

University of Manitoba

Winnipeg

Acknowledgements

During the course of my research for this thesis many people gave freely of their time and sage advice. I cannot acknowledge everyone here but I hope they accept my sincere appreciation. I would especially like to thank my supervisors and committee members for their patience and much needed advice. Dr. Peter Rasmussen, Dr. Jay Doering, Dr. David Lobb and Dr. Nazim Cicek were kind enough to offer their criticisms and suggestions during the preparation of the thesis; Dr. Ken Snelgrove gave direction and advice during the initial stage of the thesis. And Dr. Don Trim helped me develop and truth the calculus for the model. Lastly I would like to acknowledge the advice and insightful comments of Dr. Peter Steffler.

I would also like to acknowledge Dwight Williamson and Nicole Armstrong and Manitoba Water Stewardship, my partners in the Assiniboine River Water Quality Study, who offered support and funding; Bob Harrison and Alf Warkenton with Manitoba Water Stewardship, who provided hydrological data for the thesis; and Dennis Lazowski of Water Survey of Canada, who provided the data for the Athabasca River.

I could not have completed my thesis without the support and encouragement that I received from my colleagues at Red River College, especially Ralph Caldwell, Robert Friessen, Ken Webb and Dale Watts.

Lastly, I would like to thank my family, Lisa, Lezlie and Alec for their editorial support, encouragement, understanding and especially their stamina in putting up with my study antics during the time I have been working on this thesis and Ph.D. studies.

For PJ, who always believed.

Abstract

One-dimensional steady flow pollutant transport models assume that the river reach modelled has a uniform cross-sectional shape which manifests as a constant average velocity in the model equations. Rarely do rivers meet this criterion. Their channels are seldom uniform in shape, but rather alternate in a quasi-periodic manner between pool and riffle sections. This bedform sequencing imparts a corresponding variation in the average cross-sectional velocity which is not accounted for in constant velocity transport models. The literature points out that the pool and riffle planform may be the reason for the sometimes poor predictions obtained from these models.

This thesis confirms that the fluctuation in average cross-sectional velocity caused by the pool and riffle planform does have a marked effect on transport in rivers. The pool and riffle planform promotes an enhanced decay of a pollutant when a first order biochemical reaction is simulated. This effect becomes more pronounced as flow declines. The reason for this is that travel time in a pool and riffle channel is greater than for a uniformly shaped channel. Current one-dimensional models assume a uniform channel and therefore overestimate the velocity of a substance moving downstream. To show this an equation is developed that describes the variation in average cross-sectional velocity along a pool and riffle channel. The parameters of the equation can be easily evaluated for any river. The equation is incorporated into a mass balance analysis and a new form of the river transport model is derived.

Analysis shows that the transport of a substance in a pool and riffle channel is governed by travel velocity which is different from the average cross-sectional velocity

used in the traditional advection model. Replacing average velocity with travel velocity provides a simple fix for the traditional model.

The new transport model is tested on the Athabasca River with excellent results. The variable velocity model successfully simulates the DO dynamics on a 550 kilometre stretch of the river. This suggests that the model has good potential for simulating pollutant transport in other rivers. Since analysis shows that the effect of the pool and riffle planform on contaminant transport is magnified at low flow levels, the model has good potential for use in determining TMDLs for contaminants, because these regulatory levels are set for low flow conditions.

Table of Contents

List of Tables

List of Figures

Chapter 1   Introduction

Current one-dimensional steady flow pollutant transport models treat river channels as having a constant cross-sectional shape. However, river channels are characterized by a rhythmic bedform sequence of river bottom highs and lows, riffles and pools, which result in zones of accelerating flow and of decelerating flow. This sequence creates obvious physical and biogeochemical differences between riffles and pools which are not accounted for in current river transport models. Incorporating this non-uniformity of shape is critical to accurately modelling the transport of pollutants in a river.

The difference between pools and riffles are numerous. Pools experience a relatively lower average velocity than riffles under normal flow conditions. The sediment comprising the bed of a riffle is courser than the bed material of the adjacent pool (Keller,

1971; Milne, 1982; Clifford, 1993 and Sear, 1996). At moderate flows riffles tend to be wider and shallower than pools, which results in more turbulence and mixing in the riffle than in the pool. This difference in velocity and sediment strata also causes marked differences in reaeration potential between pools and riffles. Another difference is the abundance of benthic invertebrates which is also influenced by mean flow velocity and bed particle size. Areas experiencing fine particle sedimentation, the pool deeps at moderate flow, show relatively sparse populations, while areas of relatively high velocity and shallow flow show an increase in invertebrate communities (Mermillod-Blondin et al., 2000; Jowett, 2003; Ward et al., 1998). Another difference can be found in solute exchanges between the hyporheic zone and the stream, which are governed by the river bottom high to low bedform undulation of the pool and riffle sequence. Water enters the hyporheic zone along the bed up-slope, between the tail of the pool and the mid-point of the riffle, and exits the hyporheic on the bed down-slope (Elliot and Brooks, 1997; Harvey and Bencala, 1993).

Current one-dimensional transport equations, like the Streeter–Phelps equation and the advection-dispersion equation employed by QUAL2K and MIKE 11 use constant physical parameters to describe the character of the river reach being investigated (i.e., average velocity, cross-sectional area, average depth and roughness). As a result, these equations cannot account for differences that occur between the flow in pools and riffles along a reach. The purpose of this thesis, therefore, is to derive an alternative formulation of the transport equation that can account for differences between pool and riffle sections, and determine whether this new model improves upon the constant parameter approach.

If one sets about determining a new transport equation that can account for the differences between pool and riffle sections then the three major challenges are to:

- Derive an equation that can adequately describe the difference in hydraulics between the pools and riffles mathematically;

- Incorporate this equation into a mass balance analysis and derive a new form of the advection equation that describes non-uniform transport through pool and riffle sequences; and

- Validate the predictions from this new transport model.

These challenges form the outline of this thesis.

The classic equation describing substance transport in rivers is the constant parameter advection-dispersion (AD) equation

$$\frac{\partial c}{\partial t} = -u \frac{\partial c}{\partial x} + D \frac{\partial^2 c}{\partial x^2} + R \ . \tag{1.1}$$

This equation suggests that the average cross-sectional concentration (c) at any time t, and place x, is a function of the velocity u, dispersion D, and biochemical reaction R. However, the velocity, dispersion and the other physical parameters used to evaluate the reaction term – depth and roughness for instance – are assumed to be constant along the particular channel of interest. Although the next two chapters will establish that these physical parameters vary along river channels, this thesis concentrates on the effect of the variation in average velocity on the advection component of the AD equation. Recognizing that average velocity varies between pool and riffle sections, a novel mathematical expression that can describe these quasi periodic fluctuations in average velocity is derived. Differences between a constant advection models and a varying advection model are discussed and compared with transient storage models.

Chapter 2 looks at the literature surrounding transport of pollutants by advection and dispersion in rivers. It points out that the constant parameter assumptions implicit in the formulation of the transport equations may not adequately describe the transport phenomenon in rivers.

Chapter 3 examines the literature on the pool and riffle sequence. Support for its importance as the predominant bedform in rivers is presented and its periodic nature is established. Also in Chapter 3, hydraulic geometry, the empirically derived relationships between flow level and average velocity and cross-sectional area of the channel are explored, especially in the light of the hydraulic reversal hypothesis put forward by Keller (1971). The historic flow records at nine hydrometric stations along a 450 kilometre stretch of the Assiniboine River upstream of Brandon, Manitoba are analyzed. Each station contains over 20 years of recorded flow, water level and cross-sectional data. There is a marked variation in the exponents and coefficients of the power law relationship used to describe the individual station hydraulic geometries. However, when these variations are classified as pool or riffle, a pattern to the average velocity-discharge curves emerge that depicts the velocity reversal pattern. Examination of the hydraulic geometry data from other river studies reported in the literature confirms similar patterns exist.

In Chapter 4, a periodic function that can describe the average velocity variation between pools and riffles with distance downstream is developed. This function is incorporated into a theoretical mass balance analysis for a pollutant moving in a river and a new form for the one-dimensional transport equation derived. The analytical and

numerical solutions are examined for this new differential equation. Both solutions

provide the same result when tested on the Assiniboine River.

Chapter 5 is concerned with the validation of the proposed new pollutant transport

model. The model is used to simulate dissolved oxygen (DO) levels on a 550 kilometre

section of the Athabasca River, from Hinton to Athabasca. Since the model results are

compared to measured DO levels, a new form of the Streeter- Phelps equations with a

variable velocity component is developed and employed. Excellent results are obtained

with the new model when compared to measurements of DO collected along the river for

four sample periods.

Chapter 6 summarizes the findings of the thesis and concludes with

recommendations for use of the new approach to transport modelling and future

directions for additional research.

Chapter 2   Transport of Pollutants in Rivers

The most widely used river transport model is the advection-dispersion (AD) equation.

This equation describes the movement of pollutants by advection and turbulent dispersion

coupled to chemical and biological reactions. The AD equation is derived from a mass

balance around a representative element of the channel. The classic one-dimensional

form of the equation, as proposed by Taylor (1954), is

$$\frac{\partial c}{\partial t} = -u\frac{\partial c}{\partial x} + D\frac{\partial^2 c}{\partial x^2} - kc \ . \tag{2.1}$$

The first term ($\partial c/\partial t$) describes the pollutant concentration with time, the accumulation term. The advection term ($u\,\partial c/\partial x$) and the dispersion term $D\,\partial^2 c/\partial x^2$ describe the net effects of transport, where u is average cross-sectional velocity and D is the longitudinal dispersion coefficient, while the last term kc describes a first order reaction for the pollutant. Good reviews of the AD equation's derivation are given in Chapra (1997, p. 160-163) and Nazaroff and Alvarez-Cohen (2001, p. 257-265). Analytical solutions for a variety of boundary conditions are widely available (see Chapra, 1997; Fischer, 1967; Ogata and Banks, 1966; Thomann and Mueller, 1987; Runkel, 1996). The solution of the AD equation for an instantaneous spill of a conservative substance evenly distributed across a river at x and $t = 0$ is

$$c(x,t) = \frac{M_a}{2\sqrt{\pi D t}}e^{\left(-\frac{(x-ut)^2}{4Dt}-kt\right)}. \tag{2.2}$$

where M_a is the mass of pollutant per unit cross-sectional area. The solution models the concentration distribution at any time t as a normal probability density function, the spread of the contaminant pulse as it moves downstream increasing in proportion to the distance traveled.

The AD equation has become the universally accepted method of modelling pollution transport in rivers. For a continuous spill, it is used to assess transport under two separate conditions: steady state and non-steady state or dynamic conditions. In a steady-state system, $\partial c/\partial t$ is zero in Equation 3.1 and the solution for a continuous spill with boundary conditions

$$c(x = 0) = c_0 \text{ and } c(x) \to 0 \text{ as } x \to \infty \text{ is}$$

$$c(x) = c_0 e^{\left(\frac{ux}{2D} \left[1 - \left(\frac{4k}{u^2/D} + 1 \right)^{\frac{1}{2}} \right] \right)}.$$
(2.3)

This steady-state solution is used to simulate situations where continuous discharge of pollutants occur, either from end-of pipe or distributed sources, while the dynamic condition applies to pollutant spill modelling. Qual2K employs the AD equation under the steady-state condition and this model is widely used to determine total maximum daily loads (TMDL) for many pollutants in Canada and the USA. DOSTOC, based on the Streeter-Phelps equation, which drops the dispersion term, is used to model dissolved oxygen for the steady-state condition. It is this aspect of modelling, the steady-state condition, that this thesis concentrates on.

Good results have been achieved when the AD equation is used to simulate transport in canals, laboratory flumes and pipes -- all channels with uniform cross-sectional shape and therefore constant average velocity. However, difficulties persist with the application of the AD equation to a river. In many cases the predictions of the model do not agree with field measurements. It works some of the time, but not always. The literature identifies three main areas of concern. They are:

1. the inability to derive a formula that can accurately determine the dispersion coefficient for rivers,

2. the spread of a pollutant pulse as it travels downstream does not conform to the Fickian dispersive behavior predicted by the AD equation, and

3. time-concentration curves measured from tracer studies have a different shape than those predicted by the AD equation.

Good initial discussions of these topics can be found in Beltaos and Day (1978), Fischer et al. (1979) and Czernuszenko and Rowinski (1998). These three difficulties suggest that there are other mechanisms at work in rivers which are not accounted for in the constant parameter AD equation. Apart from closing statements in many papers that allude to the possible unaccounted for effects of the pool and riffle planform on transport there are no investigations that the author is aware of that look at the effect of the pool and riffle on advection, which is the purpose of this thesis.

2.1   Longitudinal Dispersion

The idea of a single bulk coefficient that describes dispersion in a river is attractive from an engineering point of view because of its simplicity. It accounts for, in one fell swoop, all of the hydrodynamic mechanisms that affect dispersion in rivers: velocity fluctuations, irregular channel shape, sinuosity, and transient storage in backwater areas. However, the accurate determination of the dispersion coefficient is a formidable problem in river transport studies. Many theoretical and empirical equations have been proposed for determining the value of the dispersion coefficient, each an improvement on its precursor, but the most recent only provides an accuracy of one and a half to two times the actual value 90% of the time. Excellent reviews on the subject are found in Fischer et al. (1979), Rutherford (1994) and Kashefipour and Falconer (2001).

In 1954, Taylor in applying his analysis of turbulent diffusion to flow in a circular pipe of radius *r*, proposed that the dispersion coefficient could be calculated as

$$D = 10.1 r V_f \qquad\qquad\qquad (2.4)$$

where V_f is the frictional velocity. Elder (1959) in stretching Taylor's analyses to an infinitely wide, open channel of depth d, proposed that the dispersion coefficient could be evaluated by

$$D = 5.9dV_f .$$ (2.5)

Fischer (1966, 1967, 1968,) improved on Elder's formula by deriving an equation for a prismatic channel with a large width to depth ratio, a situation more akin to that of a river channel. He proposed that

$$D = \frac{0.11\bar{u}^2 w^2}{u*d}$$ (2.6)

where $u*$ is average shear velocity.

Unfortunately, the evaluation of the dispersion coefficient using Fischer's formula does not often correspond with the results from tracer studies. This inconsistency has resulted in many attempts to improve upon Fischer's equation; see papers by Deng et al. (2002), Mcquivey and Keefer (1976) Liu (1977), Petersen (1977) Seo and Cheong (1988), Thackston and Krenkel (1967), Kashefipour and Falconer (2002) to name but a few. However, when the results of these "improved" formulae are also compared with the results from tracer studies, they still under-predict the dispersion coefficient, often by one to three orders of magnitude (Sooky, 1969; Godfrey and Frederick, 1970; Chatwin, 1971; Nordin and Sabbol, 1974, Liu, 1977, Seo and Chung, 1998; Deng et al. 2002). A formulation proposed by Deng et al. (2002), which is a slight improvement on its predecessors based on comparisons with other formulae, still only manages an accuracy of one half to two times the values found from tracer studies in 90% of the cases examined. Seo and Baek (2004) propose an equation based on the transverse velocity profile in streams which is only a slight improvement on the previous formulations. In a

meta-study of reported dispersion measurements in rivers, Toprak and Savci (2007), report an improved formulation based on fuzzy logic analysis. However, this type of analysis, also used by Noori et al. (2009), only improves slightly on previous formulations. Norri et al. (2009) report a correlation coefficient for their improved equation of 0.73.

The inability to provide an equation that can accurately determine the dispersion coefficient is usually blamed on the presence of other non-accounted for dispersive mechanisms at work in rivers, such as the role of irregular channel cross-sections, sinuosity, spiral currents and storage in dead zones. For example, Fukuoka and Sayre's (1973) experimenting with a rectangular shaped sinuous laboratory channel found that a sinuous channel sets up a periodicity in dispersion behavior. This was further investigated by Guymer (1998), who reported that in laboratory studies the dispersion coefficient can differ by as much as 150% between a sinuous channel with uniform prismatic cross-section shape and the same channel with alternating pool and riffle type cross-sections. Nordin and Sabol (1974), revisiting the calculations of compiled longitudinal dispersion coefficients used as benchmarks for applied investigations, found that they are average values, and that constancy of these dispersion coefficients was rare with values of dispersion varying with position along the rivers in question. Guymer's (1998) study suggests that the variation in the value is because of the effect of a varying cross-sectional shape along the river channel.

2.2   The Spread of a Pollutant Pulse

The second facet of the debate regarding the AD equation's application to rivers is the spreading of a pollutant pulse as it moves downstream.   Aris (1956) showed that the moments of the AD equation converge to a Gaussian type function. Importantly, he also determined that the variance, σ^2, of the concentration distribution increases linearly with time and downstream distance. Essentially,

$$\sigma_x^2 = 2Dt \ \ \text{and} \ \ \sigma_t^2 = \frac{2D}{u^3}x . \tag{2.7a,b}$$

These expressions are often used to calculate the dispersion coefficient from measurement of a tracer plume. Expressions 2.7a and 2.7b imply that the increase in the spread of a pollutant pulse, as measured by the variance, increases linearly (Fig. 2.1). Or if measured by the standard deviation, the common measure of spread used in the studies reported in the literature, the increase in the spread is related to $x^{0.5}$. A value of the
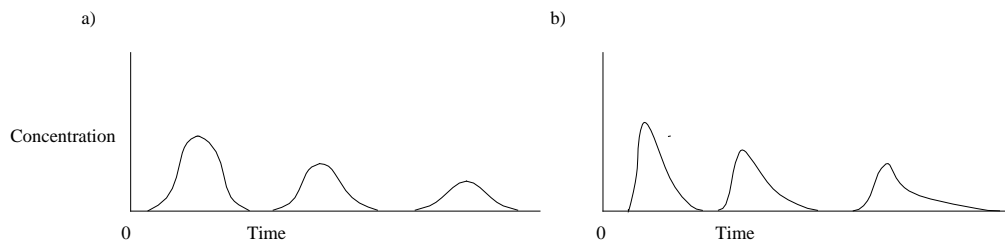
Figure 2.1. Typical representations of time-concentration curves from a) the advection-dispersion equation and b) measurement of a tracer release.

exponent greater than 0.5 implies that *D* increases exponentially. Measurements of tracer

releases in rivers show that the increase in the spread as measured by the standard

deviation is non-linear (Nordin and Sabol, 1974; Day, 1975; Day and Wood, 1976;

Beltaos and Day, 1978; Chatwin, 1980).   In a study of large numbers of field results,

Nordin and Sabol (1974) calculate that the spread of a contaminant pulse increases on an

average conforming to $x^{0.7}$ and varying between 0.5 and 1.0, implying a non-linear

increase in the variance. In a study of mountain streams in New Zealand, Day (1975)

reports that the exponent is closer to one and in some cases greater than one.

An insightful study into the spread of a tracer pulse in a river was devised by

Beltaos and Day (1978). Noting that laboratory studies of uniform channels support the

Fickian nature of dispersion -- the increase in the spread of a tracer pulse moving

downstream, as measured by the variance, is linear -- while studies of mountain streams

and rivers with non-uniform cross-sections exhibit non-linear behavior, the authors

postulate that a river with restricted irregularity in channel geometry and flow regime

should show a variance behavior somewhere in between these extremes. They chose a 24

kilometre reach of the Lesser Slave River in Canada, beginning at the outlet from Lesser

Slave Lake. They note that although the river has a somewhat high sinuosity (1.8), its

channel shape is close to prismatic and there is little variation in downstream cross-

sectional geometry. The flow regime of the reach which is governed by the water level

of Lesser Slave Lake is also somewhat dampened when compared to rivers with

headwater stream systems suggesting a muted pool and riffle effect. The results from the

tracer study confirm their hypothesis; the behavior of the tracer pulse in the Lesser Slave

River, although not Fickian, did not deviate from Fickian behavior nearly as much as

other rivers and streams studied by Day (1974, 1975) and Nordin and Sabol (1976) which exhibited more irregularity in their cross-section shape.

Without exception, measurements from tracer studies on natural rivers convincingly show that the dispersion behavior in rivers is non-Fickian in nature (Day, 1975; Beltaos and Day, 1976,1978; Guymer, 1998; Nordin and Sabol,1976; Chatwin, 1980 et al., for example). Although the exact interplay of mechanisms contributing to the non-Fickian nature of dispersion observed in natural rivers is unknown, Beltaos and Day (1978, p 573) suggest that: "natural rivers are far from prismatic in cross-sectional shape, they very rarely exhibit extended reaches of uniform flow, and meanders, dead zones, and pool and riffle sequences could influence the dispersive process, in a way that suppresses fulfillment of the conditions necessary for Fickian process."

The weight of evidence in the literature regarding the increase of the spread of a contaminant plume as it moves downstream supports the contention that other non-Fickian dispersion mechanisms are at work in the natural river. Fischer (1976) actually warns that when the variance shows a non-linear increase with distance or time, then the basic assumptions of uniform cross-section, steady flow and constant mass balance used to derive the AD equation are invalid, and it no longer applies. However, although this caveat is recognized, engineering studies continue to apply the AD equation where non-Fickian behavior is apparent because of the lack of a better alternative.

2.3   Time-Concentration Curves and Transient Storage

Time-concentration curves obtained from the results of tracer studies point out that the front of a pollutant pulse is steeper, and its tail is thicker and longer than the shape of the

Gaussian pulse predicted by the AD equation (Figure 2.1).   Investigators speculate that this deviation is the combined result of the bypassing, trapping and release of tracer in stagnant flow zones within the channel (Aris, 1959; Beer and Young, 1983; Day, 1975; Day and Wood, 1976; Nordin and Troutman, 1980; Pedersen, 1977; Thackston and Schnelle, 1970; Valentine and Wood, 1977). These zones are regions within a river's channel that are isolated from the main flow stream. They are formed on the inside of meander bends and other regions of the channel where flow separation occurs, for instance behind an obstruction to the flow. In a pool and riffle sequence, a non-circulating eddy usually occurs on the inside bank of the meander, slightly downstream from the point bar where flow separation occurs. These zones are also referred to as dead zones or transient storage zones.

These zones alter the profile of pollutant transport in a river. Initially, some of the pollutant mass may bypass these non-circulating eddies and arrive at a downstream point much more rapidly than calculated using the AD equation. However, a portion of the pollutant may also be sequestered in these zones and released later, causing a much longer residence time in the system than the AD equation would calculate. The interaction of the main channel with these transient zones alters the shape of the time-concentration curves from the Gaussian type shapes expected in a uniform channel.

An alternative formulation which describes the additional dispersion behavior attributed to dead zones is the Transient Storage Zones (TSZ) model proposed by Hays (1966). The TSZ model divides the flow in a river into two regions: the main stream and the adjoining dead zone. A system of two equations is necessary to describe this transport process: the first equation simulates transport processes in the main channel,

while the second simulates the trapping and releasing of pollutants in the dead zones. An

example of an operational form of the TSZ model is the United States Geological

Survey's One–Dimensional Transport with Inflow and Storage or OTIS (Runkel et al.,

1996; Runkel, 1998). The two equations that describe this interaction are:

$$\frac{\partial c}{\partial t} = -\frac{Q}{A_m}\frac{\partial c}{\partial x} + D\frac{\partial^2 c}{\partial x^2} + \alpha_s(c_s - c) - k_m c \quad \text{and,}$$

(2.8a)

$$\frac{\partial c_d}{\partial x} = \alpha_s\frac{A_m}{A_s}(c - c_s) - k_s c_s$$

(2.8b)

where c and c_s are the concentrations in the main stream and the dead zone, respectively.

The storage zone exchange coefficient, α_s describes the mixing between the dead zone

and the main channel, while A_m and A_s are the cross-sectional areas of the main channel

and storage zone, respectively. The coefficients k_m and k_s describe the reaction rate of the

pollutant in the main channel and storage zone. Essentially, the dead zone model is the

AD equation coupled to an extra term that describes the mixing mechanics between the

main channel and dead zone.

An interesting thesis that marginalizes the role of Fickian dispersion in the TSZ

model is proposed by Beer and Young (1979). They suggest that the dispersive behavior

of a river is totally embodied within the dead zone mechanics and drop the Fickian

dispersion component in Equation 2.8a. They then test and show that their abbreviated

TSZ model, essentially a plug-flow system, simulates transport in a river just as

accurately as the Hays model.

Investigators have demonstrated that the TSZ model fits tracer release data from

rivers far better than does the AD equation (Czernuszenko et al., 1998; Thackston and

Schnelle, 1970; Nordin and Troutman, 1980; Pedersen, 1977). The effect of transient

storage zones on the calculation of TMDLsis examined by   Chapra and Runkel (1999)

under a plug-flow scenario coupled to a first order reaction for primary and secondary

pollutants, BOD and DO deficit respectively.   They show that the effect of the storage

zones is to increase the rate of exponential decay of the pollutant concentration along the

river channel.

The success of the TSZ model in more accurately simulating pollutant transport in

rivers is unfortunately tempered by the difficulty in determining physically realistic

values for α_s and the ratio A_m / A_s .   These parameters have to be estimated from

calibration with a tracer study or by statistical best fit methods. Since the values of now

four unknowns – α_s , A_m / A_s and D – are required for the application of the transient

storage equations, considerable uncertainty surrounds the particular weighting given to

each of these parameters. For example, OTIS provides two methods for estimating the

dead zone parameters: calibration with tracer measurements, and a non-linear regression

package that optimizes the estimates of the dead zone parameters and the dispersion

coefficient by minimizing the squared difference between simulated and measured

concentrations. However, whether these are the real values of the parameters (area of the

channel, area of storage, mixing rate and dispersion) is always in doubt, since they can

not be verified.

The TSZ model demonstrates that transient storage of pollutant within dead zones

does play a crucial role in the overall transport behavior of rivers. The initial bypassing

and later trapping of contaminant within the dead zones more closely replicates the non-

Fickian dispersion behavior observed in tracer release studies on rivers. The TSZ model

also provides insight into the role of the pool and riffle sequence in the dispersion

behavior of rivers. Pools are areas where transient storage is most likely to occur while

riffles are zones where advection and mixing predominate. This combined effect of

transient storage potential in the pool and pure advection dispersion behavior in the riffle

is a very different dynamic than that of the constant channel geometry envisaged by the

constant parameter AD equation.

Singh (2002) persuaded by the arguments of theTSZ approach to transport

modeling modifies the AD equation to account for transient storage in the following

fashion:

$$(1-\eta+k)\frac{\partial c}{\partial t}=-u\frac{\partial c}{\partial x}+D\frac{\partial^2 c}{\partial x^2}-kc\,.$$
(2.9)

The equation uses two additional parameters, η and k, a stagnant zone and an

adsorption parameter, respectively. The stagnant zone parameter is the ratio of the area

of the stagnant zone to the flow, while adsorption is represented by k. Singh suggests that

transient storage zones decrease the cross-sectional flow area of the river and therefore

increase the average velocity. He also suggests that adsorption of solute on soil particles

suspended in the flow and in transient storage zones acts to effectively decrease average

velocity. Therefore, he proposed Equation 2.9, a modification to the AD equation. From

an operational perspective the equation is cumbersome since it requires a parameter

balance that is nearly impossible to validate.

2.4   Discussion

The sum of the evidence is this: the absence of a universally accepted formula that can

accurately evaluate the dispersion coefficient in the AD equation for rivers, the non-

Fickian behavior of a pulse of pollutant as it spreads downstream, and the non-conformity of time-concentration and distance-concentration curves predicted by the AD equation to those measured from tracer release studies persuasively show that the constant parameter form of the AD equation does not adequately model a river's transport dynamic. Therefore, the discrepancies between the results of the AD equation and field measurements of pollutant transport are not surprising.

Natural channels never meet the required assumption of uniform cross-sectional shape which manifests itself as constant cross-sectional velocity in the AD equation. Instead, meandering river channels where the pool and riffle bedform is the norm would, based on continuity, experience a quasi-rhythmic change in average velocity as flow moves between pool and riffle sections. Many scientists including Aris (1959), Beer and Young (1983), Day (1975), Day and Wood (1976), Deng et al. (2002), Nordin and Troutman (1980), Pedersen (1977), Singh (2002), Thackston and Schnelle (1970) and Valentine and Wood (1977) recognize the role of irregular cross-sections along sinuous channels in influencing the transport mechanics in rivers. It is this irregularity in channel shape that is most commonly cited as the reason for the inability of the constant parameter form of the AD equation to model transport in rivers.

Recognizing this limitation of the constant parameter AD equation, raises the question of whether the fluctuating average cross-sectional velocity imparted by the pool and riffle sequence affects the transport of solutes in rivers. The AD equation models two transport components, advection and dispersion. In rivers, advection is the primary mechanism of transport whereas dispersion is usually of minor significance. This statement is supported by a comment on Seo and Baek's (2004) paper by Lowe and

Groninger (2005). The authors point out that the business of assessing dispersion in rivers is not really a worthwhile endeavor for water quality modellers since it is usually one of the least sensitive parameters that need to be evaluated in a water quality study. They demonstrate that dispersion is usually four to five orders of magnitude less significant than the advective and reactive components in the AD equation using the average values for these parameters found in the literature. The point is also supported by Beer and Young (1983) and is substantiated by a Peclet number analysis of the Assiniboine and Athabasca Rivers which demonstrates that dispersion is of minor significance.

Since advection is the primary component of transport in a river, a good starting point is to examine whether a fluctuating velocity has an effect on advection, the plug-flow scenario. The first step to accomplish this requires an equation that can describe the change in average velocity as flow moves through a pool and riffle sequence. This is the subject of the next chapter.

Chapter 3   Pool and Riffle

The extensive literature on river channel morphology establishes that the pool and riffle

planform develops and is maintained in both meandering and straight river channels

(Knighton, 1998; Leopold and Wolman, 1957). Although the pool and riffle sequence is

most commonly associated with gravel and sand bed rivers (e.g. Hudson, 2002), Keller

and Melhorn (1978) believe that the pool and riffle sequence is the fundamental macro-

scale bed-form of rivers irrespective of bed material type. Indeed the presence of the

sequence has also been reported in bedrock streams (Hack, 1957; Keller and Melhorn,

1978; Shepherd and Schumm, 1974; Wohl and Legleiter, 2003), as well as, in

supraglacial streams (Dozier, 1974 and 1976). Yalin (1971) states that "Past experimental

and theoretical studies have shown that any fluid moving along an inclined boundary will

develop alternating zones of fast accelerating, and slow decelerating flow, with

subsequent sediment erosion and deposition creating a sequence of topographic lows (pools) and highs (riffles)."

In a meandering river channel, pools are usually located at the apex of bends in association with point bars, which form on the inside of the bend (Fig.3.1). This generally lends an asymmetrical cross-sectional shape to pools. Riffles, on the other hand, form in the transition between meander bends and tend to be wider and shallower than their counterpart pools. However, the three dimensional morphology of pools and riffles varies, depending on local scour conditions, channel obstructions and type of bar formation (Church and Jones, 1982).
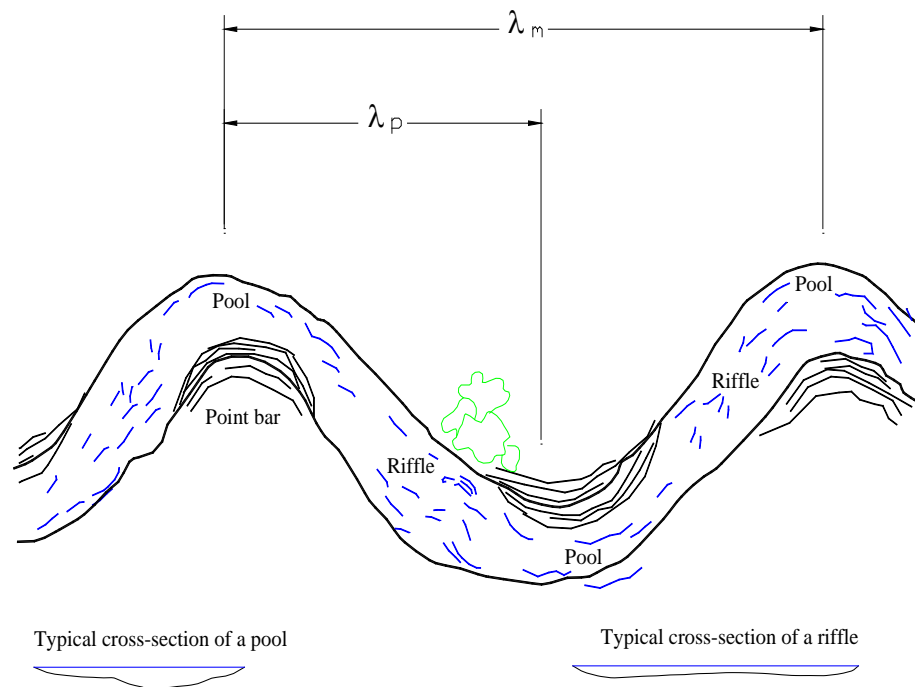
Figure 3.1 Typical pool and riffle sequence.

There are evident physical and hydraulic differences between pool and riffle

sections. Ecologically significant is the difference in bed strata. The sediment

comprising the bed of a riffle is courser than the bed material of the adjacent pool (Keller,

1971; Milne, 1982; Clifford, 1993; and Sear, 1996). The pool bed is made up of much

finer material and is subject to fine particle sedimentation during low to moderate flows.

This substrate variation between pools and riffles is crucial to the health and abundance

of benthic invertebrate communities (Jowett, 2003), and the health and diversity of the

ecology of the stream as a whole (Rutherford and MacKay, 1985).

During low to average flow stages, riffles are generally wider, about 15% to 30%

wider (Keller, 1978; and Richards, 1976b) than their counterpart pools. The average

cross-sectional area of the riffle is less than that of the adjacent pool. Also, the average

velocity in the riffle is greater than in the pool. Water surface slopes are steeper over the

riffle than the upstream pool (Richards, 1976a and 1978; and Leopold, 1982), the riffle

acting hydraulically as a weir and controlling the water surface elevation of the upstream

pool.

That pool and riffle sequences have a regular spacing over a wide range of scales

is well established (Church and Jones, 1982). Keller and Melhorn (1978) report that

$$\lambda_p = 5.42w^{1.01}, \tag{3.1}$$

where λ_p is pool-to-pool length along a line measured parallel to the channel meander

axis (Fig. 3.1), and w is channel width, for 250 measured pool-to-pool sequences along

eleven streams flowing in both bedrock and alluvium. This supports the results of an

earlier study by Leopold and Wolman (1960), which related meander wavelength, λ_m, to

channel width by the equation:

$$\lambda_m = 10.9 w^{1.01} \tag{3.2}$$

because pool-to-pool spacing is half of the meander wavelength.

Keller and Melhorn's data was reanalyzed and split into two distinct data sets, one set representing alluvial rivers and the other set for bedrock rivers by Roy and Abrahams (1980). They suggested that the mean pool spacing for alluvial rivers was significantly different than the spacing for bedrock rivers. Alluvial rivers have a spacing of 5.6 times channel width while for bedrock rivers, the spacing is 6.7 times channel width.

On the other hand Carling and Orr (2000) found that the spacing of pools on the River Severn in England was approximately half of that shown by the previous studies. They suggested

$$\lambda_p = 3w. \tag{3.3}$$

The differences in the formulae derived from field studies is also reflected in the results from laboratory studies and theoretical arguments concerning the average spacing of pools. Richards' (1976 and 1978) theoretical work suggests that pool-to pool spacing is

$$\lambda_p = 2\pi w \ \text{ or } \ \lambda_p \cong 6w, \tag{3.4a,b}$$

while Yalin (1971) theorizes that meander spacing is

$$\lambda_{ma} = 2\pi w, \tag{3.5}$$

which would suggest that pool-to-pool spacing is

$$\lambda_p = \pi w. \tag{3.6}$$

While there are differences in opinion regarding the exact spacing of the pool and riffle sequence, the rhythmic nature of the sequence is clearly evident in all the studies.

Another facet of the pool and riffle sequence that is important to this paper is the ratio of the length of the pool to the length of the riffle. Carling and Orr (2000) and Thompson (2001) demonstrate that there is not a great deal of variability in the ratio of pool length to riffle length and that for modelling purposes it can be assumed to be 1:1.

In summary then, from a water quality modelling point of view, the pool and riffle are considered the predominant macro-scale bedform in a river channel. The sequence is regularly spaced and can be determined, either by using the aforementioned relationships, or derived from field measurements. The literature also points out that a pool and riffle are for the most part equal in length. These two constructs suggest that a periodic function could be used to model the rhythmic fluctuations in average velocity between pools and riffles.

3.1 Hydraulic Geometry

The basis for hydraulic geometry is the identity

$$Q = uA = uwd, \tag{3.7}$$

where Q is discharge, u is mean sectional velocity, A is channel cross-sectional area, w is width and d is mean depth. Hydraulic geometry (Leopold and Maddock, 1953) describes the relative strength of the independent variables by examining the empirically derived power relationships:

$$u = aQ^b \ , \ w = eQ^f \ \text{and} \ d = gQ^h. \tag{3.8a,b,c}$$

The exponents b, f, and h sum to one, while the product of the coefficients a, e, and g is also one.

25

Leopold and Wolman proposed these relationships as a way to characterize and contrast the downstream changes in a river. Today, water quality programs, like QUAL2E, DOSTOC and WASP, use hydraulic geometry to characterize the flow along a particular reach of river. A reach is defined as a length of river having a similar geomorphologic condition and constant flow. In practice this usually means that a reach is a major section of river, between the confluences of major tributaries encompassing many pool and riffle sequences. However, there is substantial body of evidence in the geomorphologic literature that shows hydraulic geometry varies between pools and riffles. In fact it is this very variation that is posited as the cause for the stability of the pool and riffle bedform year after year and flood after flood.

3.2   The Velocity Reversal Hypothesis

The reason for the stability of the pool and riffle planform in a river channel has often puzzled hydrologists. In 1971 Keller proposed "velocity reversal" as the mechanism responsible for the maintenance of pools and riffles through multiple flood cycles. Basically, Keller noted from a study of Dry Creek, California, that the rate of increase in the near-bed velocity in a pool as flow increased was greater than in the rate in the downstream riffle as shown in Figure 3.2. These different rates of change in velocity cause a difference in the sediment transport dynamic between pools and riffles. At low flow stage, the overall sectional velocities are low and therefore sediment transport competence is also low. However, the velocity in the riffle is greater relative to the
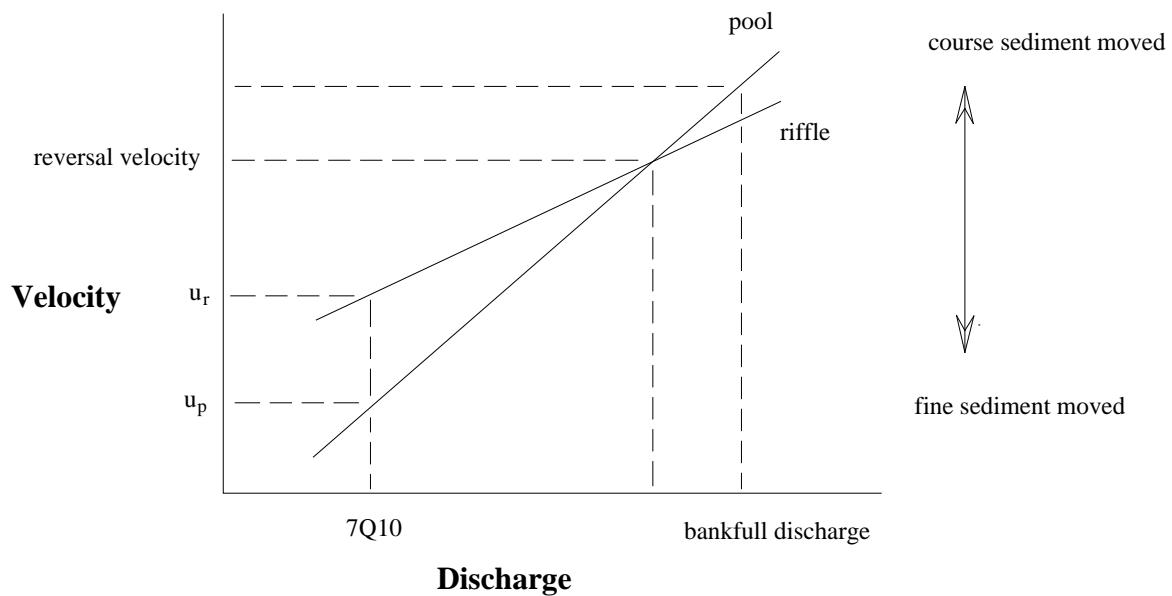
Figure 3.2 The velocity reversal hypothesis (Keller, 1971)

velocity in the adjoining pool (Fig. 3.2). Sediment movement occurs as a winnowing of

fines from the riffle bed with subsequent deposition on the bed of the downstream pool.

As discharge increases, mean velocity in the pool and riffle converge, while mobility of

fine bed material increases.

The intersection of the velocity-discharge curve for the pool with that of the riffle

occurs at 60 to 90 per cent of the bank-full discharge. As flow increases to this stage, the

movement of the bed material in the riffle commences. As flow continues to increase

past the point of intersection, the velocity in the pool surpasses the velocity in the riffle.

The larger bed particles of the riffle are now mobile and move downstream through the

higher velocity pool to settle on the next riffle where transport competence is reduced.

Meanwhile, in the pool, where the velocity is now greater than in the riffle, scouring of

the bed ensues and thus these deeps are maintained during high flows. As discharge

27

declines the sediment transport competencies of the pool and riffle return to the low flow regime and thus the pool-riffle bed form is maintained over time and space.

The velocity reversal hypothesis has been the subject of intense investigation and debate in fluvial studies since Keller's article in 1971. However, the phenomenon was alluded to as early as 1900 by Seddon when he noted in a study of the Mississippi River that during low flow levels the water surface slope is greater over riffles than in pools, but during high flows the situation reversed with greater slope observed over pools. The debate has mainly centered on whether a reversal in average velocity or other surrogate measures of stream competence occurs. Keller (1971) actually measured near bed velocity. That there are marked differences in the rate of change in average velocity as discharge increases from low flow stage is established without doubt.

A review of twenty studies reported in the literature confirms that as flow increases the curves depicting the rate of change in velocity between a pool and riffle converge or reverse (Andrews, 1979; Ashworth, 1987; Booker et al. 2001; Bhowmik and Demmissie, 1982a,b; Carling, 1991; Carling and Wood, 1994; Clifford and Richard, 1992; Jackson and Beschta, 1982; Keller, 1970, 1971, 1972; Keller and Florsheim, 1993; Lisle, 1979; Milan et. al., 2001; O'Connor et al., 1986; Petit, 1987; Richards 1976a, b, 1978; Robert, 1997; Sear, 1996; Teissyre, 1984; Thompson et al., 1999).

An interesting aspect of the debate regarding velocity reversal is the number of different measures of stream transport competence that have been employed to test the hypothesis. Keller and Sear (1992a,b,c, 1996) measured near bed velocity while Andrews (1979), Richards (1976a,b,1978) and Jackson and Beschta (1982), employed average cross-section velocity. Shear stress calculated from Du Boys formula has also

been used to assess reversal by Ashworth (1987), Petit (1987) and Lisle (1979), while

Clifford and Richards (1992), Carling (1991), Milan et al. (2001) and Tessyre (1984)

examine simultaneous variations in velocity and shear stress. Other measures have

included stream power (O'Connor et al., 1986), the Froude number (Bhowmik and

Demissie, 1982) and water surface slope (Thompson et al., 1999). The multitude of

parameters employed, besides making it difficult to compare studies, add an extra degree

of confidence to the overriding consensus that there is a difference in hydraulic geometry

between the pool and riffle.

Perhaps the most widespread criticism of the reversal hypothesis is the lack of

field studies or the lack of measured data points that actually record reversal. The

reasons for the lack of observations of the reversal phenomenon are succinctly elucidated

by Booker et al. (2000). To paraphrase, they cite the need for and difficulty of measuring

flow simultaneously at discrete cross-sections along the river. This difficulty of

measuring flow parameters simultaneously along contiguous pools and riffles has led to

computer simulation studies of flow in pool and riffle channels. All of these studies

support the reversal concept.

O'Connor et al. (1986), Keller and Florsheim (1993) and Carling and Wood

(1994) use HEC-2 to simulate flow through pool and riffle sections and these studies

support the reversal hypothesis. More importantly, these three flow simulation studies,

based on the pool and riffle morphology of three different streams, conclusively show

that at low flow stages the mean velocity in the riffle is greater than in the pool, but as

flow increases the rate of change of velocity in the pool and riffle converge. Using a

different hydrodynamic model Richards (1977) was also able to simulate the converging

average velocities of pool and riffle sequences as discharge increased. Richards modified

a computer routine developed by Fread and Harbaugh (1971) to solve a gradually varied

flow model based on the Bernoulli equation. The model was applied to two streams,

Bronte Creek in Ontario, Canada, and River Fowey, Cornwall, England. Results of these

studies show a definite convergence on Bronte Creek but a more detailed simulation on

the River Fowey lacked calibration with observed data.

It is worth noting three more studies by Booker et al. (2001), Wikinson et al.

(2004) and Harrison and Keller (2007) that use computer flow simulation models to

investigate the cause of pool and riffle maintenance. Booker et al. (2001), using a three-

dimensional computational fluid dynamics model, are able to show that average sectional

velocity in a pool reacts differently than in the riffle when discharge increases. Their

simulation of a section of the Highland Water in England show that near-bed velocities

and bed shear stresses decrease on riffles and increase in pools as discharge increases.

Wilkinson et al. (2004) use HEC-RAS to model four pool and rifle sequences on the

Stevenson River in Australia. They purport an upstream phase shift in the region of

maximum shear stress as stage increases. For low flow stages maximum shear stress is

experienced just downstream of the riffle crest, but at high flow stages the region

experiencing maximum shear is located upstream of the riffle crest. They argue that that

it is not the location of maximum and minimum shear stress that is important to the

maintenance of the pool riffle bedform but the areas of increasing and decreasing shear

stress gradient that are important. At low flow stages, an increasing shear stress gradient

is found over the riffle while a decreasing shear stress gradient is found over the pool.

However, as flow increases these gradients migrate upstream until at high flow stages the

30

region experiencing the increasing shear stress gradient is located over the pool, thus

causing scour in this area. The authors suggest that it is the upstream migration of these

regions as flow increases that explains the stability of the pool and riffle bedform. The

two-dimensional modelling of a pool and riffle sequence on a mountain stream,

Rattlesnake Creek, by Harrison and Keller (2007) also supports the observations of

Wilkinson et al. (2004) and show reversal in shear stress and velocity due to the

confining presence of large boulders.

What is strikingly apparent from a review of all studies on reversal is that they all

confirm that there is a marked difference between the average velocity in a pool and riffle

at low to medium flow levels (Fig. 3.2).

The reason for the difference in behavior of the average velocity-discharge curves

for pool and riffle sections is well established in the hydraulic literature. The different

behaviors are a result of the hydraulic role of the riffle.   The riffle crest acts as a

hydraulic control on flow through the upstream pool at low to medium flow levels.

(Richards, 1978; Harrison and Keller, 2007; Pasternack et al., 2008; Cao et al., 2003;

Thompson and Wohl, 2009; Sawyer, 2010; Caamano et al., 2009). At low flows, the

riffle crest controls backwater conditions in the upstream pool. This creates a difference

in the water surface slopes over the riffle and pool. During low flow, the energy slope is

at its maximum over the riffle tail and a minimum at the tail of the pool (Cao et al.,

2002). The direct result of this difference in slope, the driving force behind flow in the

river, is observed differences in the respective velocities. As discharge increases, the

extent of the backwater migrates upstream, dampening the role of the upstream riffle as a

control. At bankfull stage flows, the riffle is drowned out and functions more as a large-scale roughness element.

From a water quality modelling perspective, the velocity reversal hypothesis presents a quandary. One-dimensional water quality models treat the river channel as a uniform section having constant average velocity. The hydraulic studies on reversal establish that at high flow levels the average velocities, and by continuity, the average cross-sectional areas, between pools and riffles are roughly equal and a river can be modelled at these high flow levels using a constant average velocity for the whole reach. However, the literature on velocity reversal also establishes that there is a marked difference between average velocity in the pool and in adjoining riffle at low to medium flow stages, the stages at which total maximum daily loads (TMDL) for many pollutants are calculated. This leads to the questions of:

1. Are constant parameter transport models appropriate for usage at these low flow stages?

2. Can the differences in velocity and shape be accounted for in a river transport model? And,

3. What is the effect of these differences on water quality predictions?

The answer to these questions lies in the derivation of a set of functions that can describe the downstream variations in hydraulic geometry at any flow stage between riffles and pools. This set of functions can then be used to re-examine the one-dimensional constant velocity advection equation and perhaps derive a new form of the equation for non-uniform flow conditions in a river.

A study by Halket (2003) of the Assiniboine River in Manitoba provides the background analysis of hydraulic geometry necessary to assess Keller's reversal hypothesis. The metering records for seven hydrometric stations along the River were analyzed. The station operator's main concern is flooding and this is reflected in the number of high stage flows measured at each site. Although the hydrometric sites are not located in contiguous pool and riffle sequences, the station metering site position within the pool and riffle sequence was established from interpretation of cross-sections and aerial photographs. This enabled a detailed analysis of the velocity reversal concept on the Assiniboine River, especially at high flow levels which are difficult to measure and where information is lacking in the literature.

3.3   Assiniboine River Study

The Assiniboine River stretches 1287 kilometres, from its headwaters in eastern Saskatchewan to its confluence with the Red River at Winnipeg, Manitoba. The focus of this study is the section of river between the Shellmouth Dam on Lake of the Prairies and the confluence with the Little Saskatchewan River, a distance of 387 kilometres (Fig. 3.3). Here, the river flows in a wide deep valley, a former glacial spillway, incised into the Saskatchewan Till Plain.

Andres and Thompson (1995) divide this section of Assiniboine River into two distinct reaches: an upper reach extending from the outlet of the Shellmouth Dam downstream to the confluence with the Qu'Appelle River (Reach 1), and a lower reach extending from this confluence downstream to the confluence with the Little Saskatchewan River (Reach 2).
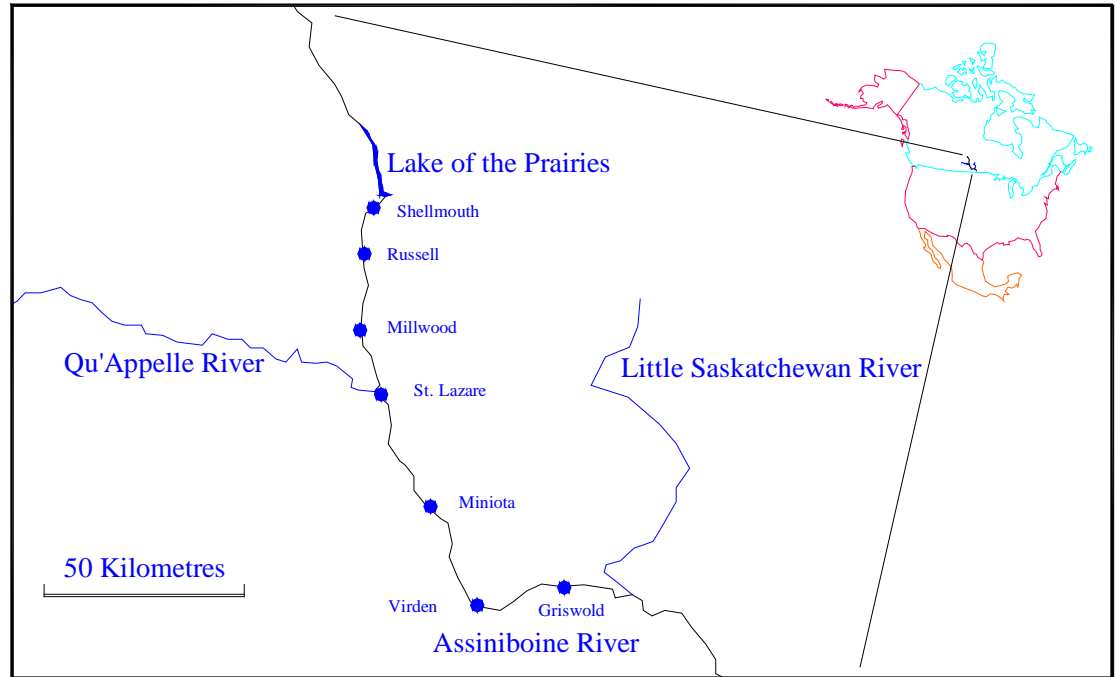
Figure 3.3 Assiniboine River Study Area.

The bank-full stage flows for each of these reaches are 44 cms and 74 cms, respectively (Harrison, 2002). The average bed slopes along the upper and lower reaches are 0.00022, and 0.000083, representing the steepest and shallowest sloped reaches along the entire river. These two reaches also exhibit high sinuosity, 1.90 and 2.3, respectively, and the highest degree of channel confinement along the river (Andres and Thompson, 1995). The alluvium of the riverbed of both reaches is similar in composition, being predominantly composed of sand. The average grain size distribution of this alluvium is approximately 95 per-cent sand and 5 per-cent gravel (Galay, 1974).

34

Table 3.1 Hydraulic geometry coefficients and exponents for the hydrometric stations on the Assiniboine River ($U = aQ^b$ $d = gQ^h$ $w = eQ^f$).

Station	b	h	f		a	g	e
Shellmouth	0.36	0.41	0.23		0.18	0.30	19
Russell	0.28	0.38	0.34		0.37	0.23	12
Millwood	0.21	0.31	0.48		0.30	0.50	7
St Lazare	0.41	0.26	0.32		0.11	0.57	15
Miniota-pool	0.51	0.28	0.21		0.08	0.74	16
Miniota-riffle	0.22	0.63	0.15		0.24	0.16	25
Virden	0.19	0.60	0.22		0.26	0.22	17
Griswold	0.32	0.54	0.14		0.17	0.21	28

The hydraulic geometry relationships for the hydrometric stations along the river are summarized in Table 3.1. The first three stations in the table are located along the upper reach, while the bottom four stations are located along the lower reach. The table illustrates the great deal of variation in hydraulic geometry between the stations. These data were compiled from an analysis of the metering records at the seven hydrometric stations located along the river. Metering records were collected for each of the stations for the period 1975 to 2002. Water Survey of Canada conducts on average four to six flow measurements per year at each station. At least 20 measurement records were initially selected for analyses at each site. These records were picked to show as wide a variation of flow as possible. Also, records were selected so that both open-channel flows and ice-covered flows could be analyzed. This analysis is discussed in a report submitted to Manitoba Conservation in 2003.

Cross-section drawings were drawn to scale in AutoCAD for each of the metering records. These drawings not only depict the cross-sectional form of the channel at the time of the measurement, but also allow for the calculation of channel properties

such as cross-sectional area, wetted perimeter and hydraulic radius. The cross-sectional

areas derived from the drawings were compared to the calculated areas from the metering

notes – a check on the accuracy of the drawings.

At each station, drawings were compared for cross-sectional similarity. Cross-

sections showing anomalous bed and bank configurations were laid aside and other

records showing similar cross-sectional shape substituted. The anomalous cross-sections

were, more than likely, the result of measurements being made at alternative sites

upstream or downstream from the station. Sections showing unusual water stage versus

discharge, due to backwater condition, were also put aside and, where possible, other

records substituted.

Analysis of the flow measurement data began with the four stations along the

lower reach of the Assiniboine River. This reach extends downstream from the

confluence of the Qu'Appelle River to the confluence with the Little Saskatchewan

River. The Qu'Appelle River with a mean July flow of 11.1 cms adds a significant
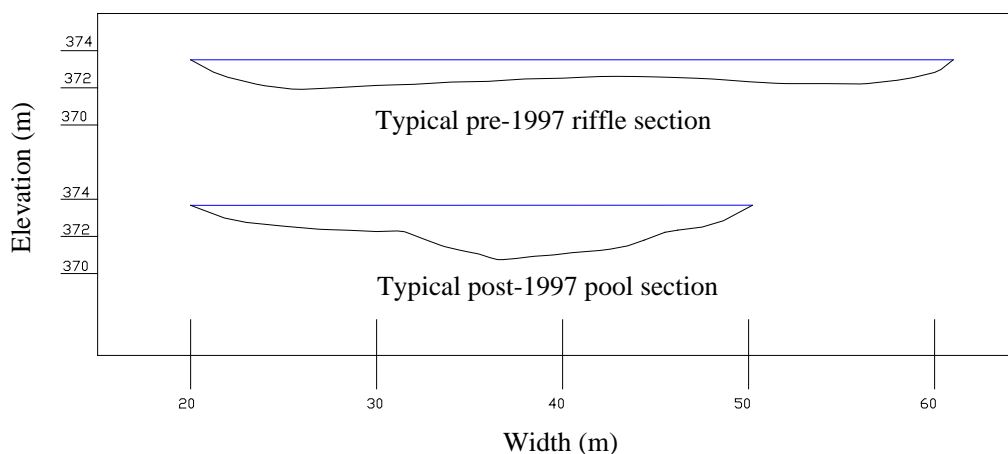
Figure 3.4 Comparison of pool and riffle cross-sections at Miniota for a 23 cms flow level.

discharge to the Assiniboine River, which has mean July flow of 18.3 cms above the confluence.

The Miniota station, located along the lower reach of the Assinboine River, has what proves to be an illuminating operational history. The station was located at a riffle section until 1997, when it was moved upstream approximately 100 m to the tail of a pool, because of the building of a new bridge. The difference in shape of the sections between these two locations is compared in Figure 3.4. The cross-sections are drawn for the same flow level of 23 cms. The Miniota station data plotted in Figure 3.5 illustrate the difference that cross-sectional shape has on hydraulic geometry for an adjacent pool and riffle. This data span the time period from 1993 to 2007.
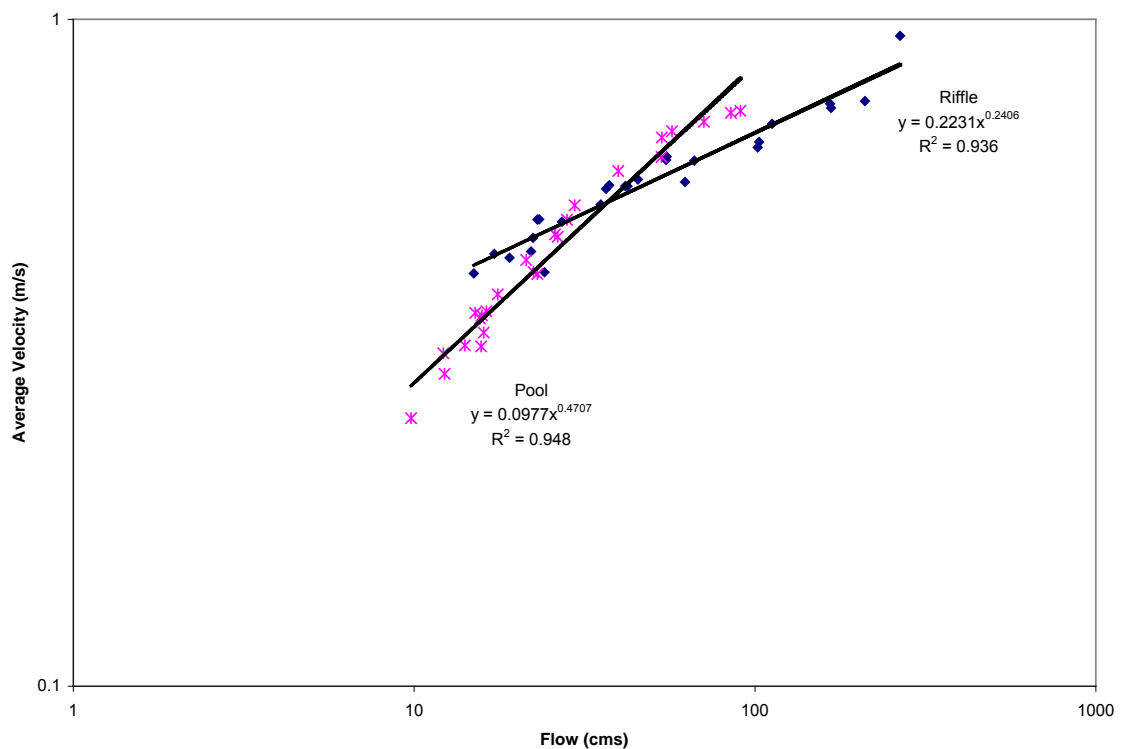
Figure 3.5. Velocity–discharge curves for the Miniota Station.

The mean velocity-discharge relationships for both of the sections are markedly different and lend support to the velocity reversal hypothesis (Fig.3.5). The pool's velocity curve exhibits a steeper slope and lower y-intercept than does the riffle's, with the point of reversal occurring at a flow of 36 cms, which is approximately 50% of the bank-full discharge for this reach. The relationships are statistically strong with regression coefficients upward of 0.93. Interestingly, the measurement data for the Miniota station indicates that, for the period before 1997, higher flood flows were measured than for the period after 1997. This is illustrated by the different data ranges of the curves plotted in Figure 3.5. This difference is not entirely due to the vagaries of nature, the metering conventions employed at the two sites have also influenced the type of data available for this analysis. Flow measurements at the old station were made using the cableway for flow levels ranging from medium to high on the river, but at very low flow stages the measurements were made by wading the river at sections downstream of the cableway. The location of these wading sections varied and therefore these measurements are not included in the analysis. The lowest flow measured at the cableway for the pre-1997 record is 14.97 cms. After the cableway was moved in 1998, flow measurements were not only made from the cableway, but also from the downstream side of the new bridge, especially at high flows. Again the measurements made from the bridge are excluded, thus eliminating many of the high flow measurements. This combination of factors has combined to give the measurement record at Miniota its overall character.
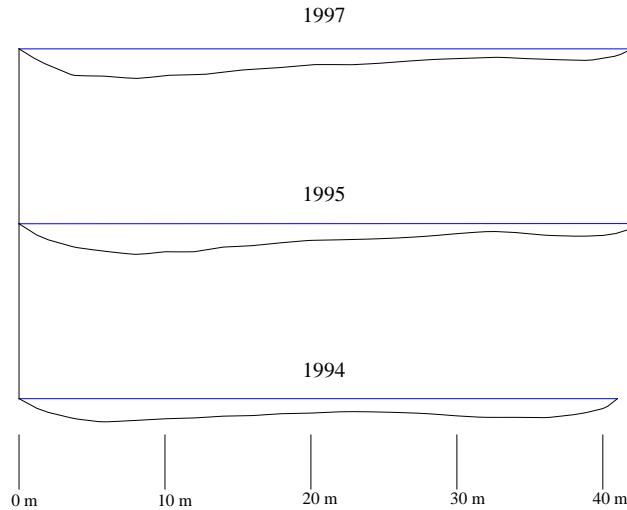
Figure 3.6. Comparison of river channel cross-sectional shape at Miniota Station for 1994, 1995, and 1997 at a 22 cms flow stage.

Another facet of the measurement data is the variance of the measurements about the best fit curves in Figure 3.5. To investigate this variance the channel cross-section shape measured during each metering are compared. This analysis revealed that the channel bed changed slightly on a year to year basis. The riffle cross-section shows the most variation on an annual basis, the pool having a more stable form. The extent of the variation in the riffle section is shown in Figure 3.6 for the years 1994 to 1995 and 1997 for a flow stage of approximately 22 cms. A measurement at this flow was not conducted in 1996. As can be seen in the figure, the cross-sections vary ever so slightly from year to year, but their stability of form is impressive, considering that three intervening large spring floods occurred in the time span with peak flows of: 463 cms in 1995, 237 cms in 1996 and 165 cms in 1997. This is consistent with the ideas of pool and riffle maintenance in the geomorphologic literature, but also illustrates that the river bed is a dynamic environment, undergoing both erosion and deposition.
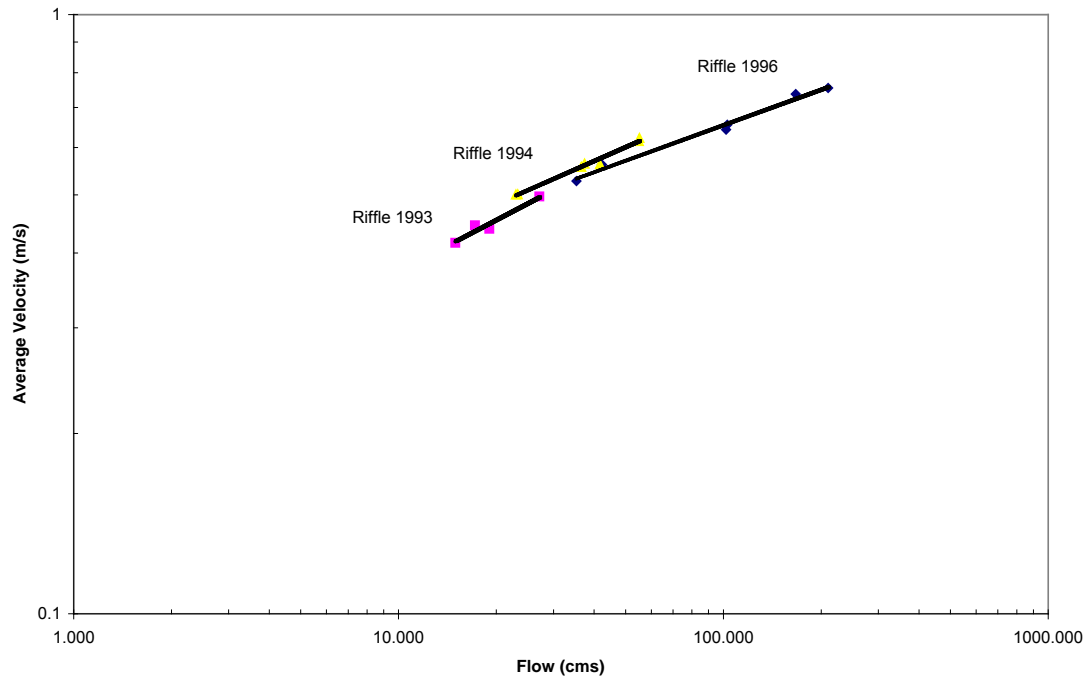
***Figure 3.7. Comparison of annual Velocity-discharge curves at Miniota Station
for 1993, 1994, and 1996 at the riffle section.***

The effect of this gradual change in cross-sectional shape on the hydraulic

geometry at the riffle from year to year is illustrated in Figure 3.7 where the annual

hydraulic geometry curves for measurements made during 1993, 1994 and 1996 at the

riffle section are plotted.   The fit of the curves to the yearly data is much closer than the

fit of the composite curve for the riffle shown in Figure 3.5. When the annual curves are

compared for the riffle, a drift in the hydraulic geometries is evident owing to the slight

change in cross-sectional form from year to year. This accounts for the greater scatter in

the data points around the best fit curves that depict the composite hydraulic geometry

relationships plotted in Figure 3.5 when multiple years of data are combined.
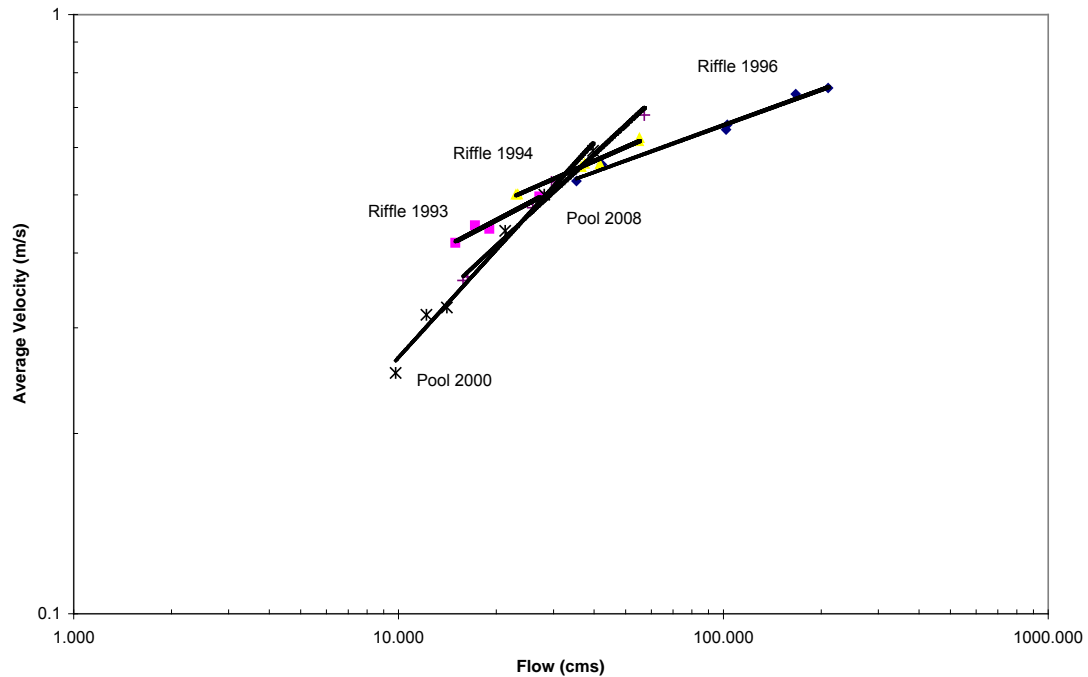
Figure 3.8. Comparison of annual hydraulic geometry curves at Miniota Station between the pool and riffle sections.

What is more striking about these annual relationships is the evidence they provide for the velocity reversal hypothesis. Figure 3.8 combines the riffle curves of Figure 3.7 with the pool curves for the years 2000 and 2008. As can be seen the curves definitely support the velocity reversal hypothesis, the pool curves showing a higher slope and lower y-intercept than the curves for the riffle. Reflecting back to the literature review on the velocity reversal, hypothesis, this is only the fifth study where velocity reversal is measured in a river and the only investigation with multiple measurements occurring above the reversal point.

41
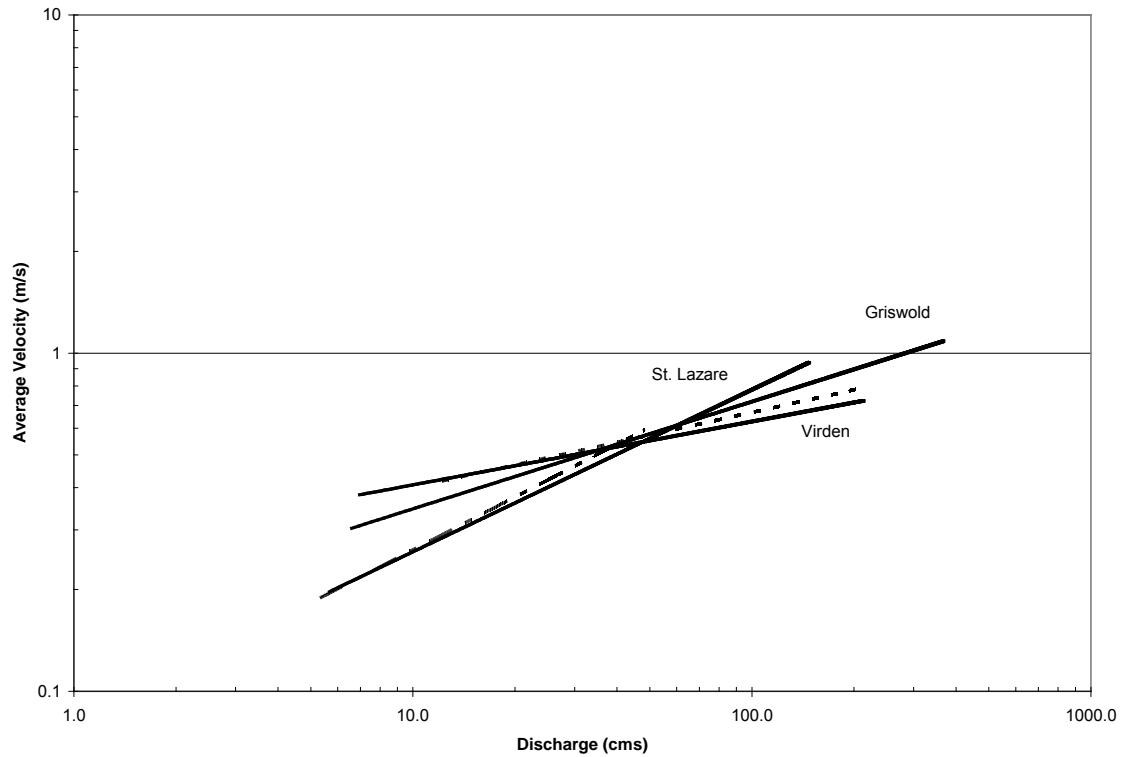
Figure 3.9. Velocity-discharge curves for the hydrometric stations at Griswold, St. Lazare and Virden.   The curves for Miniota are shown as dashed lines.

Adding to the Miniota station's evidence in support of the velocity reversal hypothesis is the analysis of the data gathered for the other hydrometric stations in this lower reach of the Assiniboine River. When the mean velocity-discharge curves for the stations at Griswold, St. Lazare and Virden are plotted (Fig. 3.9) with the Miniota curves (dashed lines), the velocity reversal pattern is evident. The curves representing Griswold, St. Lazare and Virden practically overlie the Miniota curves (dashed lines in Fig. 3.9). Because the hydrometric stations span the entire reach, the particular reversal pattern may be representative of the entire reach.

The splay of the family of curves that form the reversal pattern is governed by each stations location along the pool riffle continuum. The curves that have the flattest

42

slopes in Figure 3.9 depict the riffle sections at Virden and Miniota, while those with the

steeper slopes represent the near-pool sections at Miniota and St. Lazare. The curve for

the Griswold station represents an intermediate pool-riffle section. The cross-over point

of the curves has moved slightly from that depicted by the Miniota station analysis, and

occurs at a flow of 55 cms which is 61% of the bank-full discharge (74 cms) for this

reach.

     The pattern of this family of curves firmly establishes the existence of the velocity

reversal pattern for the pool and riffle sequences along this reach of the Assiniboine

River. It is similar to the pattern of curves that Andrews (1979) describes for the pool

and riffle sections along a reach of the East Fork River in Wyoming and the patterns

found in all the studies on velocity reversal reviewed earlier in this thesis. What is more,

this pattern is not only established at one particular site on the reach, but is supported by

the curves for other stations along the reach and therefore would seem to be a

characteristic of the reach as a whole

     However, the curves in Figure 3.9 do not show the maximum range in the mean

average velocities between the pools and riffles along this reach. This is because the

hydrometric stations along the river are located at sites considered to be relatively stable

and this is usually on or close to a riffle section. Therefore, to find the maximum range to

the splay of the pattern shown in Figure 3.9, six cross-sections were surveyed that span a

typical pool and riffle sequence near Virden. The cross-sections are shown in figure on

the next page.
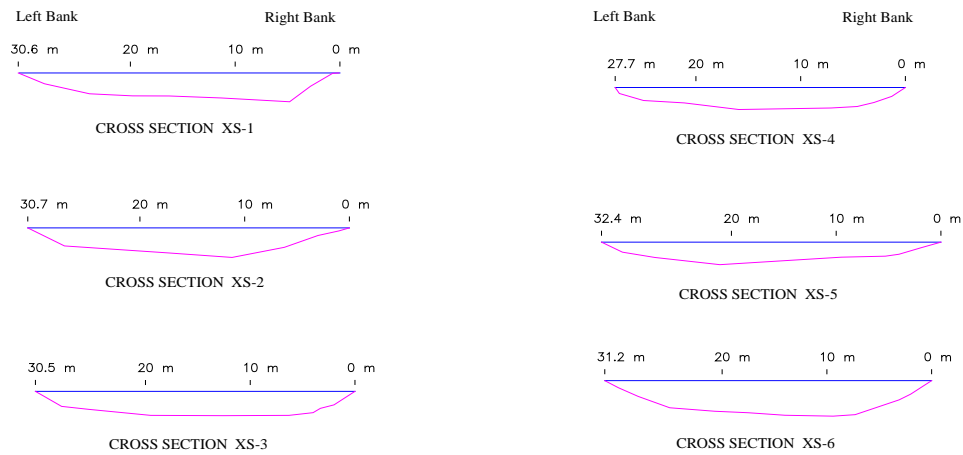
Figure 3.10. Channel cross-sections near Virden, Manitoba.

The surveys were conducted at a flow stage of 22.4 cms. The average velocity

for each section was determined and these points are plotted in Figure 3.11 below.
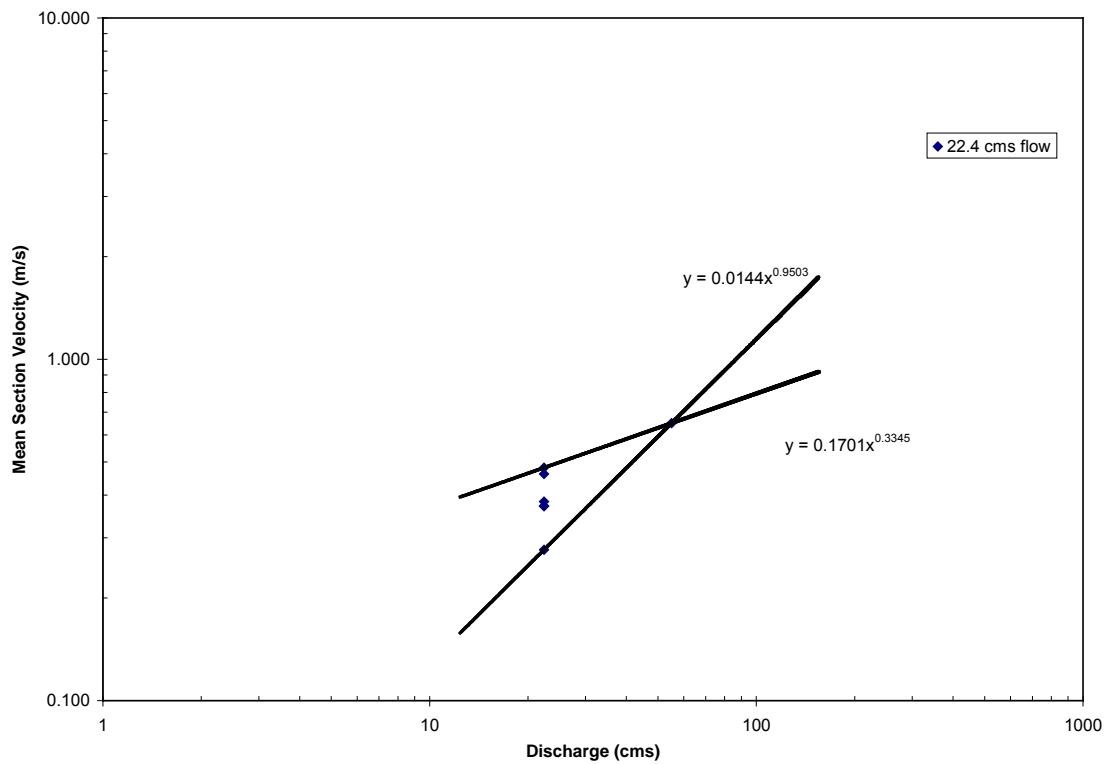
Figure 3.11. Full range of the velocity reversal pattern at Virden, Manitoba.

The points range from highest average velocity at the riffle section to lowest at the pool in the following order: XS-4, XS-5, XS-2, XS-1, XS-3 and XS-6. Note the flow-velocity points for XS-1 and XS-3 overlap, they have the same average velocity of 0.37 m/s, while XS-2 is close to these with a velocity of 0.38 m/s. Assuming that curves can be extended from the maximum (22.4 cms, 0.48 m/s) and minimum points (22.4 cms, 0.28 m/s) through to the point of reversal at 61% of bank-full stage discharge for this reach, the full splay of the velocity reversal pattern can be determined for the reach as depicted in Figure 3.11.

Analysis of the data from the four hydrometric stations along the lower reach of the Assiniboine River adds firm support for the velocity reversal hypothesis, but how
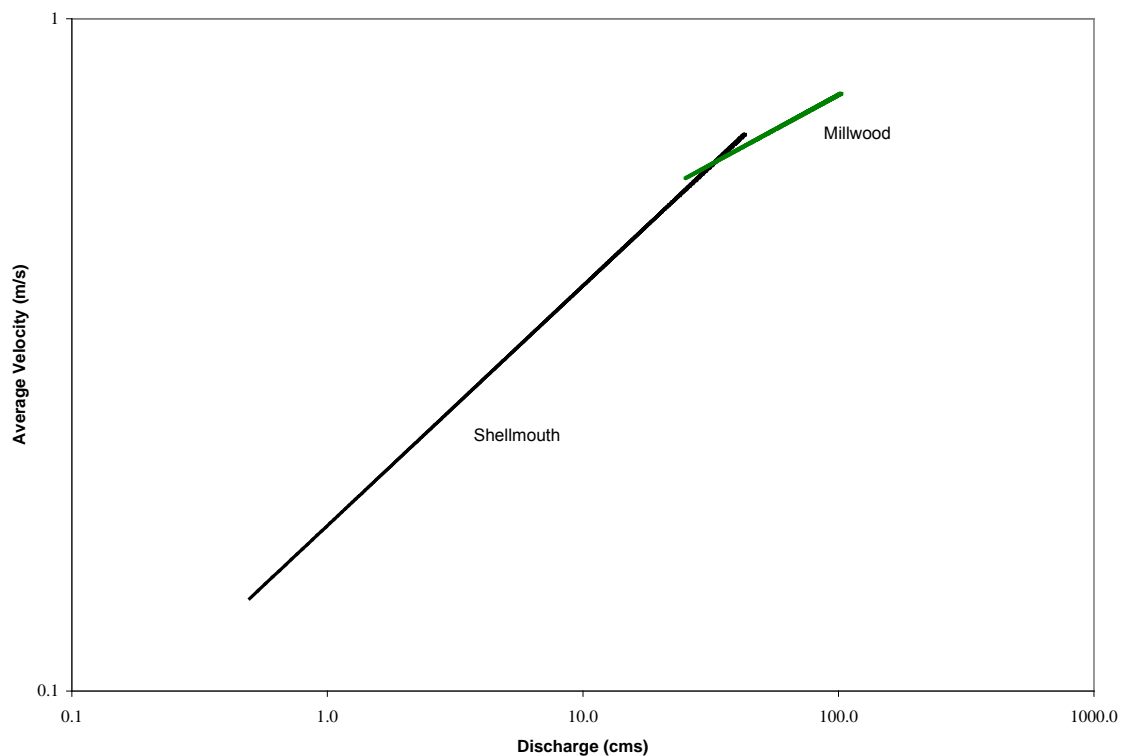
Figure 3.12.   Velocity reversal pattern established from analysis of the records at Shellmouth and Millwood stations.

about the three stations along the upper reach of the Assiniboine River? The analysis of

these station's records also shows support for reversal. The curves for the Shellmouth

and Millwood stations definitely show the reversal pattern (Fig. 3.12). The lengths of

each curve reflect the range of flows measured at each station. The Shellmouth station is

located at the top of the reach, just below the dam and its flow measurement record

reflect a series of low to medium flow measurements, while the Millwood station, located

near the end of the reach, has a much more varied flow record, measuring many high

flow events. The pattern for this reach is not as well defined as that of the lower reach

because it is only represented by these two stations which are located at a riffle and near

pool section. Additional cross-section measurements, similar to those surveyed at

Virden, are needed to establish the full splay of the reversal pattern.
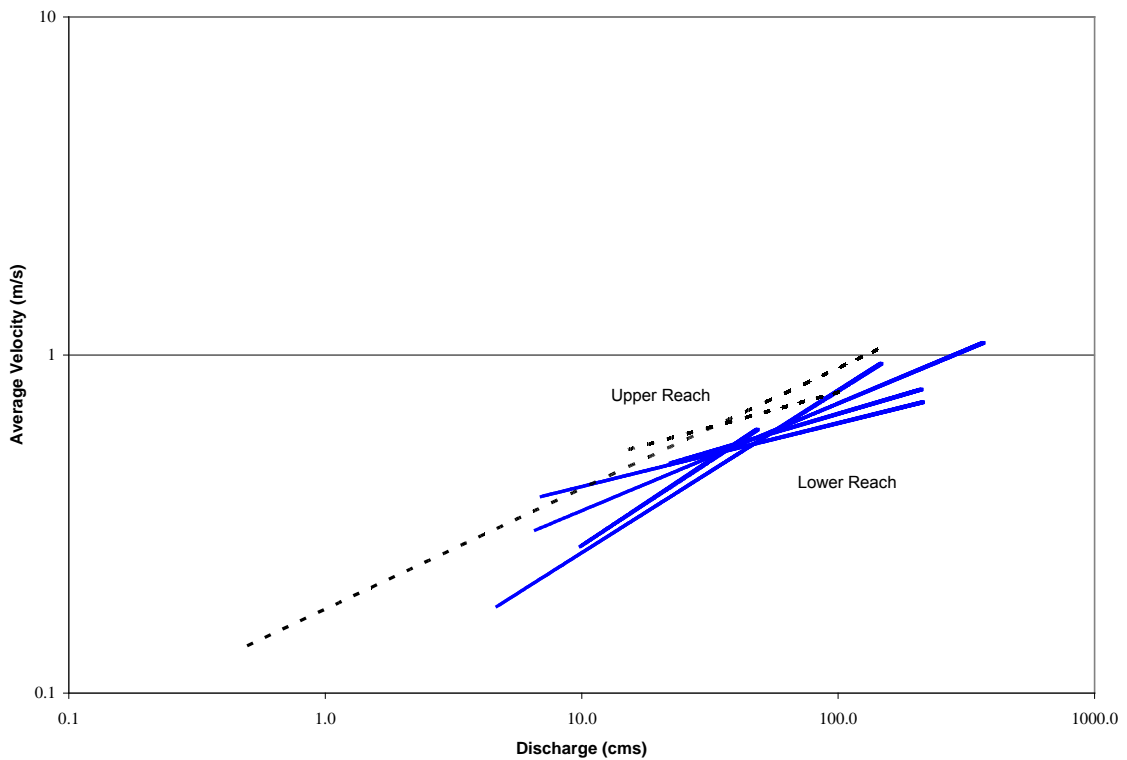
*Figure 3.13. Comparison of velocity reversal patterns for the upper and lower
reaches on the Assiniboine River.*

The reversal pattern for the upper reach plots above and to the left of the pattern of curves representing the lower reach, as shown in (Fig. 3.13).   This is not surprising since the upper reach of the Assiniboine River is much smaller above its confluence with the Qu'Appelle River. This is similar to the finding of Beven and Carling (1992) in an examination of the reversal hypothesis for two reaches on the Severn River in England.

Russel, located approximately at the mid-point of the upper reach, is the third station located in this reach. However, the short section of the river at Russel is strikingly different in its geomorphology than the rest of the upper reach. The Assiniboine has a braided channel in this short section and therefore it should be regarded as an anomalous
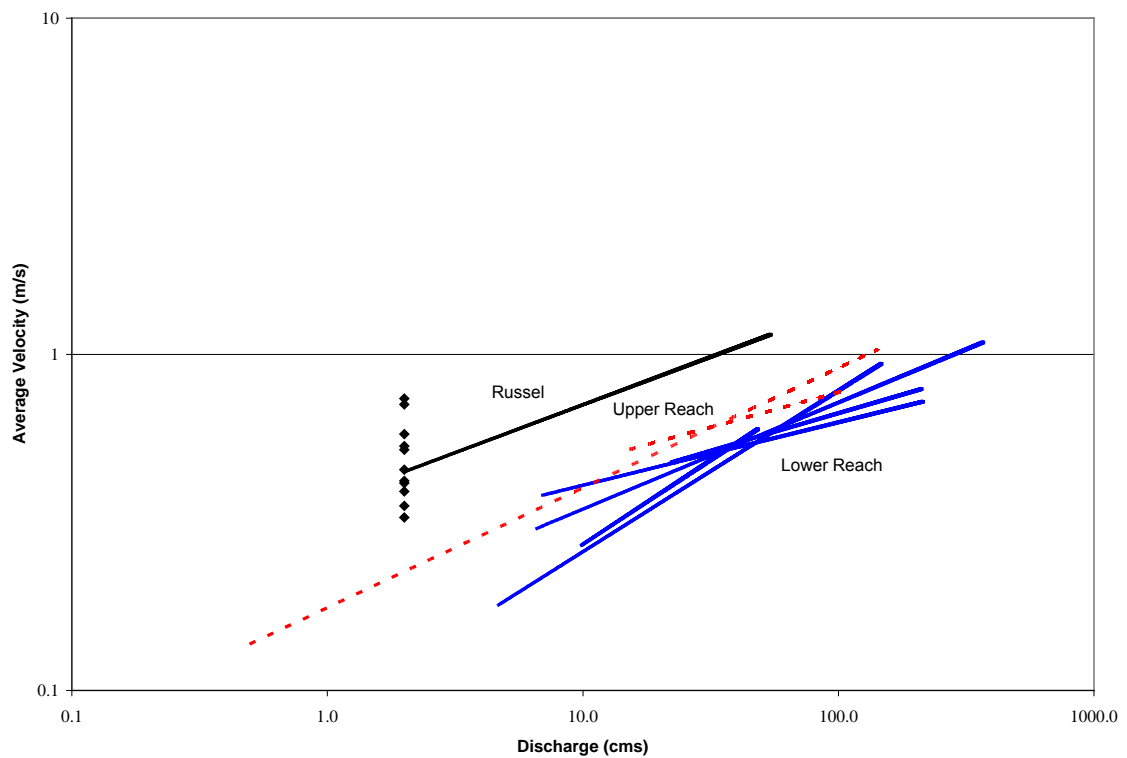
Figure 3.14.   Comparison of velocity reversal patterns for the upper, lower and Russel reaches on the Assiniboine River.

section. The reason for the braided channel is sediment overload. Here, two tributaries,

with inordinately large gravel loads empty into the Assiniboine River. The gravel is

deposited immediately and a series of gravel bars are formed in the main channel,

extending downstream for a kilometre. This difference in geomorphology is illustrated by

the hydraulic geometry curve at Russell which plots further to the right of the pattern of

curves for the upper and lower reaches as shown in Figure 3.14.

In order to establish the full splay of the reversal pattern for the anomalous reach

at Russel, 13 cross-sections were surveyed at a flow of 2 cms. The cross-sections were

sited to capture the full range of the pool and riffle sequences in this braided section of

the river. Average velocities for each cross-section were calculated and these points are

plotted in Figure 3.14. The range of these points shows the full splay of the velocity

reversal pattern at Russell.

3.4   Discussion

Of particular note in Figure 3.14 are the shifts in the reversal patterns for the three

reaches of the Assiniboine River. Taking the significance of the velocity reversal

hypothesis one step further, it is proposed that these reversal patterns are distinct

signatures of each reach and that their location and spread are governed by the reach's

pool and riffle character. This hypothesis is supported by examination of the data

reported by a number of river studies in the literature. In a study of two reaches of the

River Severn in England, Beven and Carling (1992) establish similar patterns for the two

reaches investigated.   A similar pattern is also established for the reach of the East Fork
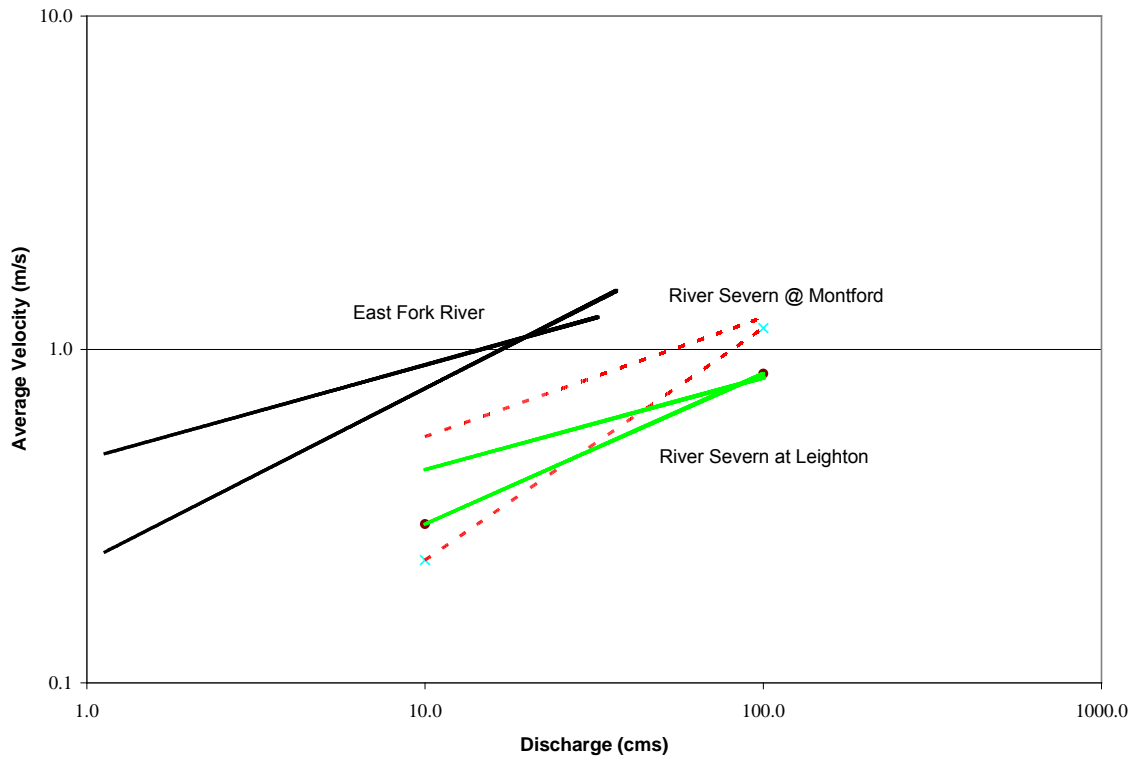
Figure 3.15. Comparison of Average Velocity-discharge curves for the East Fork River and Severn River.

River in the USA when the curves established for the twelve cross-sections are overlaid. Both of these studies results are shown in Figure 3.15.

It should be mentioned here that two of the curves for the East Fork River are excluded because they are not typical of the reach. They are located between a bridge crossing and a bed-load sediment trap and, not surprisingly, plot outside of the pattern shown in Figure 3.15.

It is proposed that the velocity reversal pattern is indicative of a reach's hydraulic regime. The location and splay of the pattern are determined by the hydrological and physical characteristics of the pool and riffle sequences along a river. Each pool and riffle sequence exhibits a reversal pattern that is a microcosm of the reach pattern. The full variability of the pool and riffle sequences along the reach is expressed in the

composite pattern for the reach. There is certainly a difference in the location of the

patterns for different reaches on the Assiniboine River. Support for this hypothesis is

found when the data from other reversal studies is considered. Similar shifts are shown

between reaches along the River Severn in Beven and Carling's (1992) study and a

similar composite pattern is established for the East Fork River by Andrews' (1979)

study data. The measurements of Keller (1971, 1972, 1977, 1978) , Keller and Florshiem

(1993), Keller and Melhorn (1973), Carling and Wood (1994), Clifford and Richards

(1992), Lisle (1979), Radecki-Pawlick (2002), Robert (1997), Teissyre (1984),

Thompson et al. (1999) and Wilkinson et al. (2004) also show reversal patterns. These

studies add strength to the contention that the location and spread of the pattern when

plotted on log-log paper are unique signatures of a reach's hydraulic regime.

Furthermore, these reversal patterns can be established relatively easily compared

to traditional approaches for determining river hydraulic geometry. The traditional

approach dictated by constant parameter transport models is to condense channel survey

measurements into reach average statistics, because constant parameter transport models

rely on reach averaged hydraulic statistics. These averages are calculated from a large

number of surveyed cross-sections. The overriding tenet is the more cross-sections the

better the estimate of average conditions. However, as the reversal pattern illustrates, the

variation displayed by the individual cross-sections is lost when this approach is used.

The analysis of the Assiniboine River firmly supports Keller's velocity reversal

hypothesis. However, the significance of the velocity reversal pattern to river transport

modelling lies in its ability to predict average velocity at any section along the pool riffle

continuum for any flow level. For instance, at a particular discharge level, the average

flow velocity would increase as one moves from a pool to riffle and then decrease as one

moves down to the next pool. This fluctuation, bounded by the velocity reversal pattern,

is described mathematically and incorporated into a new stream transport model in the

next chapter.

Chapter 4   Model Development

The different velocity response of pool and riffle to change in flow level in a river is firmly established in the literature on velocity reversal. This pattern, which can be established by plotting the measurements on a log-log graph, shows a relative increase in the difference in average velocity between a pool and riffle as discharge declines when compared to the reach average velocity (Fig. 3.2). This suggests that the pool and riffle influence on river hydraulic behavior is more pronounced as river flow declines. How this behavior affects river transport is unknown. Since the TMDL for many pollutants are set at low flow levels, an investigation of the effect of varying velocity along a river on transport seems prudent.

Water quality investigations are concerned with forecasting the effects of a change in the quality or quantity of point and non-point pollutant discharges to rivers. The forecast is commonly based on low flow conditions, because the assimilative capacity of the river is at its lowest and stress on aquatic life is at its highest under these conditions. The 7Q10 flow stage, the lowest flow over seven consecutive days in a ten year period is commonly used as the criteria. Importantly, the previous chapter has shown that the relative difference in the average velocity of flow between pool and riffle sections is close to maximum at this flow stage, reflecting the relatively increasing influence of the pool and riffle bedform on transport.

Current one-dimensional steady flow river transport models, which are based on the constant parameter advection-dispersion equation, do not address this quasi-periodic fluctuation in average velocity between pool and riffle sections at low flow conditions. Instead, they treat the river channel as a uniform section with constant flow velocity and cross-sectional area (Eq. 2.1). To address this inadequacy, a new transport equation will be developed in this chapter that can describe the effect of a variable velocity on the advection component of transport is examined. In order to do this, an equation that can describe the average velocity fluctuation through a pool and riffle is developed. Then this equation is used in a mass balance analysis to develop a new advection equation that can describe transport along a pool and riffle channel, a channel whose transport hydraulic is governed by a variable average velocity along the channel.

This new advection model may provide additional insight into the transport processes within a non-uniform river channel. Guymer (1998, p. 33) calls for exactly this type of research in his concluding remarks on a study of dispersion in sinuous channels of

53

varying cross-sections when he suggests the "need for an improved method for incorporating the effects of longitudinal variations in cross-sectional shape" on transport in rivers. This sentiment is also echoed by Singh (2003) in his paper proposing an alternate form of the advection-dispersion equation based on channel irregularities.

4.1   Average Velocity Equation for a Pool and Riffle

If the velocity reversal pattern is established for a river reach, in the manner described in Chapter 3, then a mathematical expression that describes the downstream variation in average velocity can be derived in the following fashion.

On the basis of the evidence presented in Chapter 3 on the nature of the pool and riffle planform, the following assumptions are made in the derivation of a velocity expression:

1. Pools and riffles are of equal length, and

2. Their distribution along the channel follows a rhythmic pattern.

If the average length along the channel between pools L_p, is known, then position x along the sequence in radians is given by $2\pi x / L_p$.

Assuming that the average cross-sectional velocity between pool and riffle varies in a sinusoidal manner, then the average cross-sectional velocity at any point along the river channel $u(x)$ under steady flow conditions is given by a periodic function of the form

$$u(x) = \left(\frac{u_r + u_p}{2}\right) + \left(\frac{u_r - u_p}{2}\right)\cos\left(\frac{2\pi x}{L_p}\right) , \qquad (4.1)$$

where u_r is the maximum mean section velocity at the riffle and u_p is the minimum mean

section velocity at the pool. The equation starts ($x = 0$) at the mid-point of the riffle, the

point of maximum average cross-sectional velocity within the channel. A more succinct

form for the equation 4.1 is

$$u(x) = a + b\cos\left(\frac{2\pi x}{L_p}\right),$$
(4.2)

where a is the average cross-sectional velocity between the pool and riffle while b is one

half the amplitude of the variation in velocity between the pool and riffle. This form of

the equation is used in the next section in the derivation and analysis of a river transport

equation that takes into account a fluctuating flow velocity.

The variation in average cross-sectional area of the channel as a function of

downstream distance, x, can also be stated in a similar fashion. Or, alternatively, cross-

sectional area at steady flow is related to discharge, Q, by,

$$A(x) = \frac{Q}{u(x)}.$$
(4.3)

Equations 4.2 and 4.3 can be readily evaluated for any flow level from the velocity

reversal pattern.

These two equations provide a conceptually meaningful and efficient basis for

determining the variation in average cross-sectional velocity and cross-sectional area of a

reach of river for a water quality study. Current practice for water quality investigations

requires the surveying of many cross-sections of the river channel. This cross-sectional

data is usually used in two ways:

1. The cross-sections are amalgamated on a reach basis and average values for cross-sectional area and average velocity are computed. These average reach values are then used as the governing values for the river transport equations.

2. The cross-sections are used by hydraulic routing models like HEC-RAS and MIKE 11 to simulate flow within the channel from which hydraulic geometry and other physical parameters required by the water quality models are determined. Since the numerical water quality models are limited by the number of segments of channel that can be linked in any simulation, the hydraulic modelling is again forced to report segment or reach averaged parameters.

Both procedures require an inordinate amount of cross-sectional data, the over-riding tenet being "the more the better". Although true for the hydraulic modelling, this does not carry through to the water quality modelling in all cases, because of the limitation on number of channel segments that can be used in the water quality models. Another facet of traditional studies is that the surveyed cross-sections are usually arbitrarily situated along the river, more often than not, their location governed by surveying control criteria. The business of river surveying is extremely difficult, time consuming and expensive work and therefore can exhaust the budget of a water quality study. Therefore judicious arrangement of cross-sections is required. To capture the full impact of the pool and riffle planform on hydraulic regime, cross-sections that straddle the bedform in a fashion similar to the investigations at Virden and Russel discussed in Chapter 3 are suggested.

The discussion so far has focused on a sinusoidal function being used to describe the transition in channel shape between a pool and riffle. This, however, is not the only type of function that could be used. Other functions that immediately spring to mind that could describe the transition dynamic are the step function and the saw-tooth function. The difference caused in water quality modelling by the choice of function is discussed in Section 4.4.

This study's findings offer a new and intuitive method of determining a reach's physical and hydraulic characteristics. In realizing that average cross-sectional velocity and cross-sectional area do vary in step with the pool and riffle bedform and that the velocity reversal pattern typifies a reach's hydraulic and physical character, another method of establishing average velocity along the channel is proposed. This method follows exactly the analysis of the velocity reversal pattern shown in Figures 3.11 and 3.14. It can be applied to any river reach, based on analysis of its historic hydrometric record from which the hydraulic geometry of the reach can be constructed. From the measurement of a few astutely situated cross-sections, the full splay of the velocity reversal pattern can be established.

What is more, for river water quality studies, this method can not only simulate average conditions but also provide insight into extreme conditions. For example, comparisons can be made between pool-like channels and riffle-like channels.

4.2   A Pollutant Transport Model

This section begins with the derivation of an equation that models transport by advection in a non-uniform channel. The solution to this variable advection equation is applied to the lower reach of the Assiniboine River for a theoretical situation and its results are compared to the predictions from the constant velocity advection equation to gain an understanding of the differences between them. Chapra and Runkel (1999) used a similar approach when evaluating the results of the TSZ advection model. They used a theoretical scenario on Uvas Creek, California, to compare predictions between models.

The derivation of a new transport model uses the average cross-sectional velocity equation that describes the average velocity fluctuation through a regularly varying pool and riffle channel and, therefore, the assumptions that govern its usage must also hold for this new model's derivation. These assumptions are:

1. The lengths of pools and riffles along a reach are equal.

2. The distribution of pools and riffles along the reach follows a regular repeating pattern given by the cosine function.

3. The average velocity along the reach is given by Equation 4.2.

4. A steady flow condition exists along the reach.

5. Transport of pollutants along the reach is dominated by advection, in other words a plug-flow system characterizes the reach adequately.

6. Mixing of a pollutant varies only in the downstream direction, lateral and vertical mixing is complete.
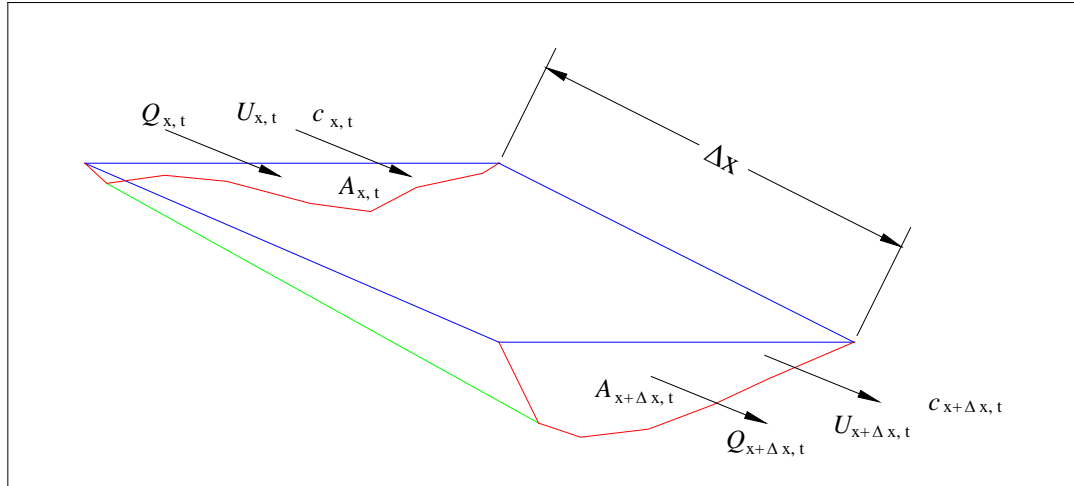
Figure 4.1. Schematic for deriving the one-dimensional general mass-balance equation for a pool and riffle channel.

Figure 4.1 illustrates a control volume within a pool and riffle river channel. The control section is located at position x, has length Δx, and cross-sectional end areas A_x and $A_{x+\Delta x}$ and average area $\bar{A}$. The volume of the unit is $\bar{A}\,\Delta x$. Consider a pollutant with concentration $c(x, t)$. The flow Q, entering the element, is equal to the flow out of the element, implying a steady flow condition. The pollutant mass loading rate, $W(x,t)$ is equal to $Qc(x,t)$ and is a function of position and time, t. The principal assumption in the derivation is that the solute concentration varies only in the x direction, or in other words, mixing is complete in the lateral and vertical directions. Consider what happens over a time interval of Δt, beginning at t.

The mass-balance principle maintains that the change in the amount of pollutant in the control volume over some time interval must equal the amount of pollutant that flows into the unit minus the amount that flows out plus the net amount of pollutant produced within the unit. Translating this into a mathematical expression gives:

$$A(x,t+\Delta t)\Delta x c(x,t+\Delta t) - A(x,t)\Delta x c(x,t) = W(x,t)\Delta t - W(x+\Delta x,t)\Delta t + \bar{A}\Delta x r \Delta t \ . \quad (4.4)$$

The product on the left-hand side, $(A \Delta x c)$ is the total amount of pollutant in the control

volume. The two terms on the left then represent the net increase in pollutant contained in

the volume from the start t, to the end, $t + \Delta t$ of the time interval. On the right hand side

of the equation, the first term represents the total net flow of pollutant into the unit while

the second term represents the total net flow of pollutant out of the unit. The third term

expresses the net rate, r, of pollutant produced in the unit.

Next, dividing both sides by $\Delta x \Delta t$ yields

$$\frac{Ac(x,t+\Delta t) - Ac(x,t)}{\Delta t} = \frac{W(x,t) - W(x+\Delta x,t)}{\Delta x} + \bar{A}r \,. \tag{4.5}$$

Taking the limit as Δx and Δt approaches zero and realizing that $\bar{A}$ approaches $A(x)$ gives

$$\frac{\partial \left(A(t)c(t)\right)}{\partial t} = -\frac{\partial W(x)}{\partial x} + A(x)r \,. \tag{4.6}$$

The difference terms are transformed into partial derivatives. If a steady-flow condition,

is assumed, then discharge is a constant and can be taken out of the differential on the

right-hand side, yielding

$$A(x)\frac{\partial c(t)}{\partial t} = -\frac{Q\partial c(x)}{\partial x} + A(x)r \,. \tag{4.7}$$

Dividing both sides of equation 4.7 by $A(x)$ gives

$$\frac{\partial c(t)}{\partial t} = -u(x)\frac{\partial c(x)}{\partial x} + r \tag{4.8}$$

since $Q = u(x)A(x)$. Recalling that the average cross-sectional velocity along a pool and

riffle sequence is described by Equation 4.2 which is

$$u(x) = a + b\cos\left(\frac{2\pi x}{L_p}\right) \tag{4.2}$$

Substituting this equation into Equation 4.8 and abridging the notation gives

$$\frac{\partial c}{\partial t} = -\left[a + b\cos\left(\frac{2\pi x}{L_p}\right) \right]\frac{\partial c}{\partial x} + r .$$

(4.9)

If a first order reaction with rate coefficient k is assumed for the reaction term r, then the

equation becomes

$$\frac{\partial c}{\partial t} = -\left[a + b\cos\left(\frac{2\pi x}{L_p}\right) \right]\frac{\partial c}{\partial x} + kc .$$

(4.10)

Equation 4.10 is the new pollutant transport model proposed in this thesis. This model

describes the transport of a pollutant under steady-flow and steady-state conditions in a

pool and riffle channel, a channel experiencing a rhythmic fluctuation in average

velocity. This is the new variable velocity advection model.

The steady-state solution to the differential equation where $\partial c / \partial t = 0$ is

$$c = c_0 e^{\Psi}$$

(4.11)

where c_0 is the initial concentration. The exponent

$$\Psi = \frac{\left[kL\arctan\left(\frac{(a-b)\tan\left(\frac{\pi x}{L}\right)}{\sqrt{a^2 - b^2}} \right) \right]}{\pi\sqrt{a^2 - b^2}} .$$

(4.12)

This solution is analyzed for the theoretical case of a continuous and constant

release of pollutant at the head of the lower reach of the Assiniboine River. Assuming

steady-state condition and immediate and complete mixing across the channel at the point

of discharge, the initial concentration of pollutant, c_0, is 2.0 mg/l. The pollutant removal

rate, k, is 0.0001 sec^{-1}. The values of the parameters for average velocity, a, and

amplitude of the variation in average velocity, b, are based on field measurements at a
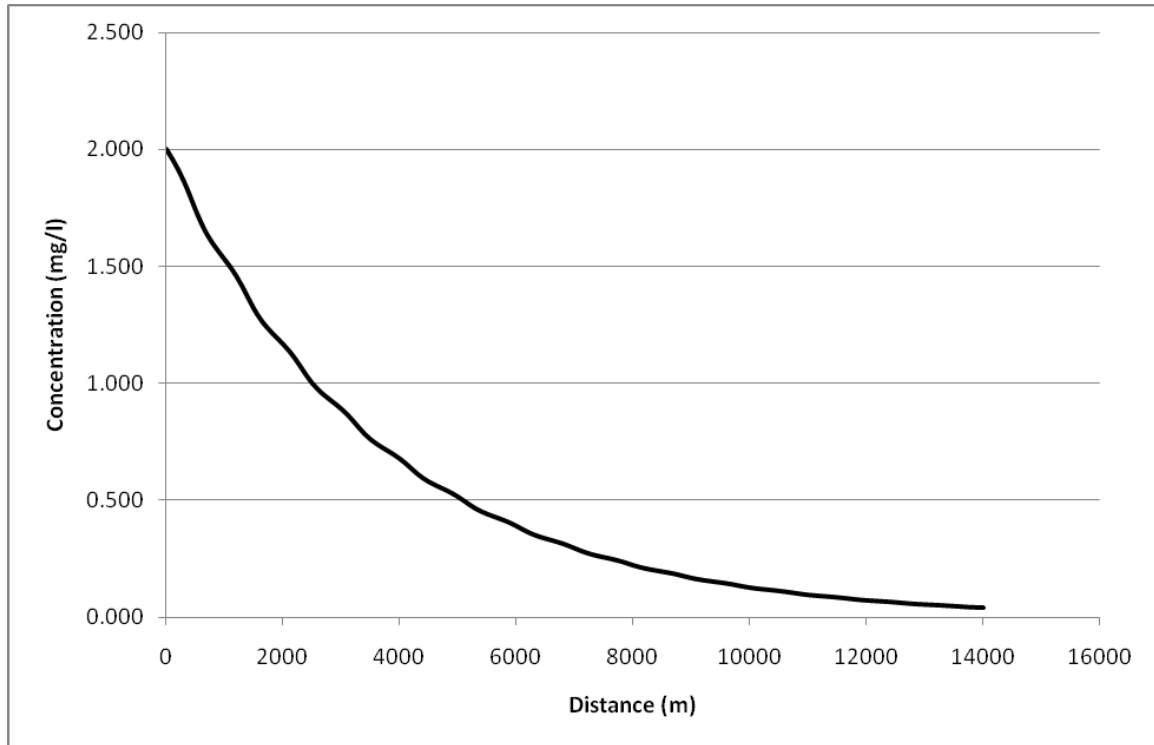
Figure 4.2. Plot of analytical solution to Equation 4.10 for the lower reach of the Assiniboine River at a 22.4 cms flow stage.

flow stage of 22.4 cms (Fig. 3.11). The average velocity of flow over the pool and riffle

sequence is 0.38 m/s with amplitude of ±0.1 m/s. The sinuosity of this reach is 2.34 with

an average meander wavelength of 800 m. This implies that the length of the pool-to-pool

spacing, *L,* is 936 m. This scenario, referred to as Scenario 1, is used to analyze the new

model's results and contrast them to the results of the traditional one-dimensional

pollutant transport model, the constant velocity advection equation.

The analytical solution to Equation 4.11 is plotted in Figure 4.2. The function

plots as a slightly oscillating exponential decay function.   At 5000 m downstream the

concentration of pollutant has decayed from 2.0 mg/l to 0.516 mg/l. At 10000 m the

concentration is 0.129 mg/l. The oscillation is the effect that the pool and riffle bedform
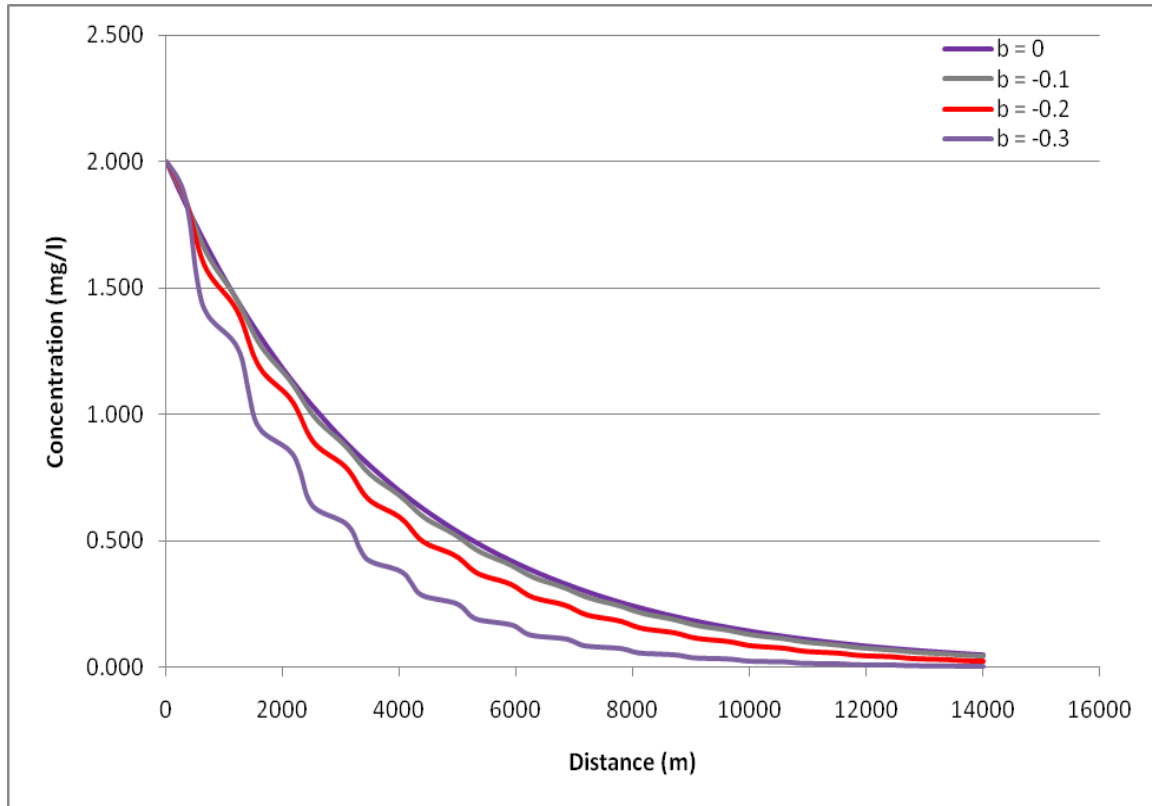
Figure 4.3. Comparison of distance-concentration curves for amplitudes varying from 0 to ±0.3 on the Assiniboine River at a flow of 22.4 cms.

has on transport of a pollutant in rivers. It clearly depicts the periodic fluctuation in average velocity for flow through the pool and riffle sequence.

An important feature of the variable velocity advection equation is the role that the amplitude, *b,* plays in the decay of the pollutant. Recall that amplitude represents the variation in average velocity about the mean channel velocity as flow moves between the pool and riffle. If *b* is zero, then the varying velocity differential reverts to the constant average velocity form of the advection equation. The plotted solution is shown in Figure 4.3. (Note that the slight oscillation of the functions as seen in Figure 4.2 has been left out so as to illustrate just the decay). However, as velocity amplitude increases, the rate of decay of the pollutant is more rapid as depicted by the array of exponential curves for

63

Table 4.1. Comparison of concentrations for variations in amplitude.

Concentration (mg/l)				
Amplitude (m/s)	Distance downstream (m)			
	0	5000	10000	20000
b = 0	2.000	0.536	0.144	0.010
b = ±0.1	2.000	0.516	0.129	0.009
b = ±0.2	2.000	0.436	0.088	0.004
b = ±0.3	2.000	0.250	0.025	0.000

incremental values of amplitude, *b*, shown in Figure 4.3. Table 4.1 presents the

concentrations for the situations depicted in Figure 4.4.

This data shows the marked difference that can occur in overall decay of a

pollutant where a pool and riffle bedform is encountered. For amplitude of ±0.2 m/s, the

data show that the overall decay of a pollutant will increase by approximately 19% at

5000 m downstream and 39% at 10,000 m downstream over the values predicted by the

constant velocity equation. This is a significant difference, and illustrates the effect that

pool and riffle planform can have on transport in rivers.

The extent of the effect that pool and riffle geometry have on first-order decay is

further detailed by the differences between a constant velocity and a variable velocity

approach at the 7Q10 flow level on the Assiniboine River in Figure 4.4. The 7Q10 flow

on the lower reach of Assiniboine River is 5 cms. The average velocity at this flow level

is 0.18 m/s with amplitude of ±0.11 m/s. In Figure 4.4, the curves for both approaches

are shown. Note that the undulation of the VVM curve is not shown.
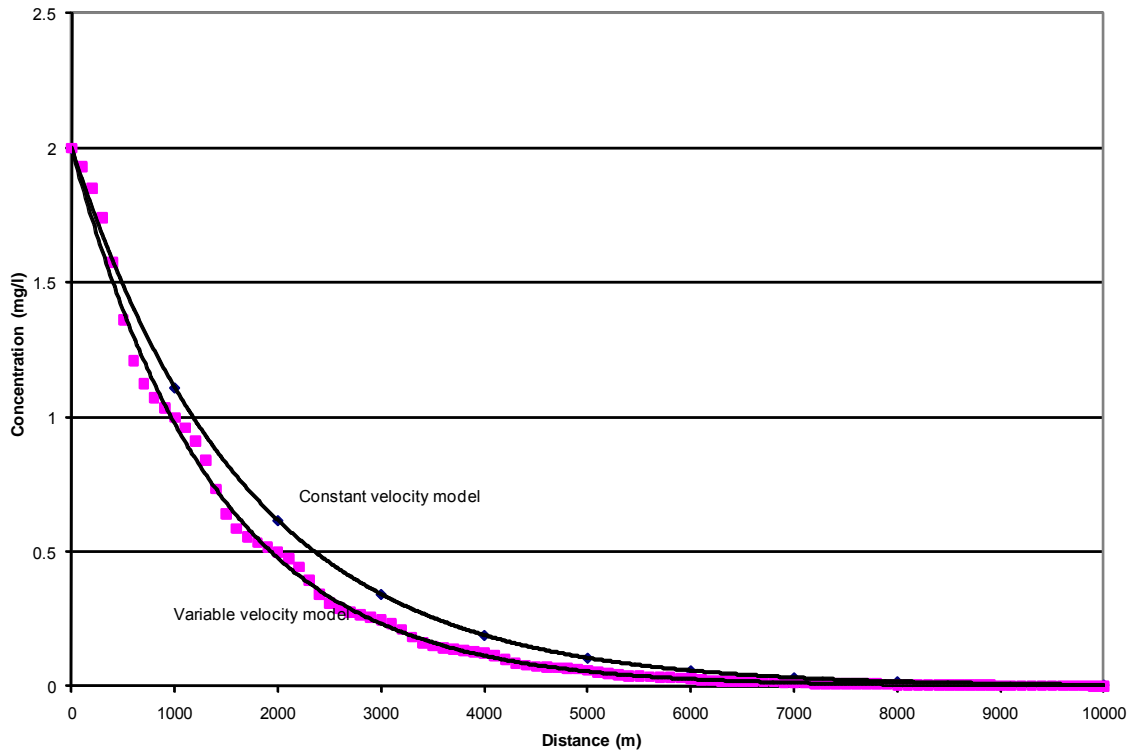
Figure 4.4. Comparison of distance-concentration curves for the constant velocity model versus the variable velocity model at the 7Q10 flow stage on the Assiniboine River.

The variable velocity model has a more rapid decay. For instance, at the 3000 metre mark, there is a 36 per cent difference between the concentrations predicted by both models. This is clearly a substantial difference between the models.

The examples presented by Figures 4.3 and 4.4 at flows of 22.4 cms and 5 cms, respectively, raise the question of what is causing the difference in the overall decay. The next section, a theoretical analysis of the solution to the variable velocity model provides insight into the reason for the difference in decay.

4.3   Theoretical Analysis.

In this section the cause for the enhanced decay experienced in a pool and riffle channel is examined. The examination starts with a comparison of the solutions for the constant parameter equation and the variable velocity equation. Both solutions have a similar structure as shown in Equation 4.11. The difference between them lies in the exponent ψ. For the constant parameter model ψ is equal to k/u, the decay coefficient divided by average velocity, whereas for the variable velocity model ψ is given by Equation 4.12. Since the decay term is common to both these terms, the difference between the terms is in their advective components shown below:

$$\frac{1}{u} \quad \text{and} \quad \frac{L\arctan\left[\dfrac{(a-b)}{\sqrt{a^2-b^2}}\tan\left[\dfrac{\pi x}{L}\right]\right]}{\pi\sqrt{a^2-b^2}}. \qquad (4.13\text{a,b})$$

The constant velocity model assumes that the channel is of uniform cross-sectional shape and therefore u is the average velocity experienced at any cross-section along the channel. However, for a pool and riffle channel the average cross-sectional velocity varies with position, x (Equation 4.2). A feature of the term 4.13b is the role of the arctangent-tangent structure. On the inside of the tangent function is the term π/L. On the outside of the arctangent function is the inverse of this term, L/π. If b is zero these terms cancel, but if b does not equal zero then the effect of the pool and riffle bedform is simulated by the imbedded range term

$$\frac{a-b}{\sqrt{a^2-b^2}} \qquad (4.14)$$

which determines the range of the slight oscillation in the decay curve (Fig. 4.2). As is

shown next, the denominator of this term is the average velocity of flow through a

complete pool and riffle sequence while the numerator is the minimum velocity

experienced in the pool. Thus this term represents the minimum velocity divided by the

average velocity. Taking the arctangent of this ratio does not make a great difference to

the outcome, but does cause a fluctuation. It nears unity at 0, $\pi/2$, π, $3\pi/2$, 2π, and so on,

while the variation is at a maximum at every $\pi/4$, $3\pi/4$, $5\pi/4$, $7/4\pi$, and so on. This

corresponds to the maximum variation occurring at the end of the riffle, and every $\pi/2$

units there-after (i.e., the start of the pool, end of the pool, start of the riffle and end of the

riffle). This term also implies that as the difference between the velocities in the pool and

riffle become more severe the effect of the periodicity of the pool and riffle becomes

more pronounced. Therefore, the oscillation of the decay curve in Figure 4.2 is the result

of the interplay of the arctangent tangent structure with the embedded parameters shown

in term 4.15 below:

$$\frac{L\arctan\left[\frac{(a-b)}{\sqrt{a^2-b^2}}\tan\left[\frac{\pi x}{L}\right]\right]}{\pi}. \tag{4.15}$$

A more important facet of the variable velocity solution is the role of the term

$\sqrt{a^2-b^2}$ in the denominator of ψ and in the term above. Comparison with the constant

parameter model suggests that this term may represent the average velocity of the flow

through an entire pool and riffle sequence, a new velocity term called that will be referred

to as travel velocity, u_T from now on. Insight into the workings of the term is given by an

examination of the curves presented below.

67

a)
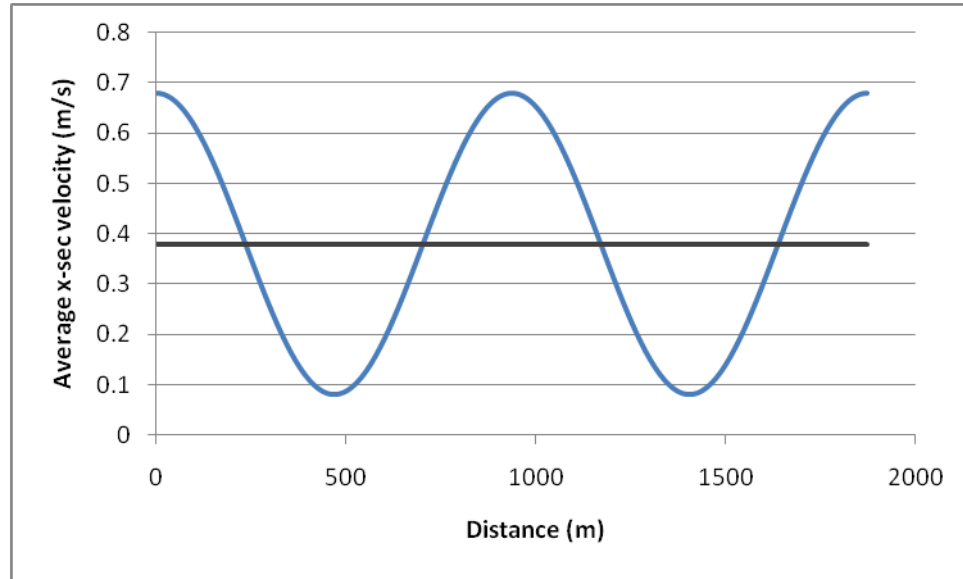
b)
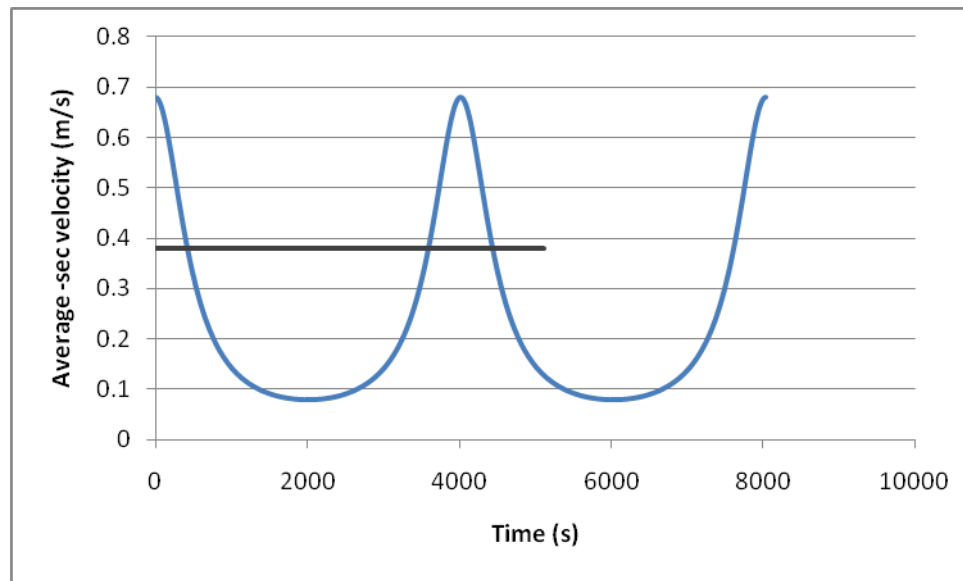
Figure 4.5a and b. Velocity-distance(a) and velocity-time(b) graphs for a 22.4 cms flow at Virden on the Assiniboine River.

In Figure 4.5a the average cross-sectional velocity, as given by Equation 4.2, is plotted with downstream distance for a flow level of 22.4 cms. If the case where *a* is equal to 0.38 m/s and *b* is equal to 0.3 m/s is considered, the average velocity versus

distance relationship (Fig. 4.5a) plots as a cosine curve fluctuating between 0.8 m/s and

0.68 m/s. However, the average cross-sectional velocity versus time graph (Fig. 4.5b)

shows a completely different picture. The cosine curve is now distorted.   It is

compressed around the riffle and stretched over the pool. The reason is that the time it

takes for flow to traverse the riffle is shorter than the time it takes to travel through the

pool. This distortion clearly establishes that travel time through the pool takes longer

than through the riffle. Whatismore, the travel velocity over a complete pool and riffle

sequence, u_T, is the length of the sequence divided by travel time and calculates to 0.23

m/s. This is different from the average cross-sectional velocity, a, which is 0.38 m/s.

Evaluating Term 4.15 of Equation 4.12 also yields 0.23 m/s. This suggests that Term

4.15 is a new velocity quantity that describes the time-based motion of a particle through

a pool and riffle channel, a sort of Lagrange velocity.

As a matter of fact, for the general case where the average cross-sectional velocity

is described by the function

$$u(x) = a + b\cos x,$$ (4.16)

it can be shown that the travel velocity over a complete pool and riffle sequence is given

by

$$u_T = \sqrt{a^2 - b^2}$$ (4.17)

Proof for this assertion is found by reviewing the mathematics behind Figure 4.5b.

In this figure, the time it takes to travel each metre along the pool and riffle sequence was

calculated. Each discrete time was found by dividing the unit distance by the average

velocity over the particular unit distance. The total travel time then is the total of all

these discrete times. The average velocity over the pool and riffle sequence is the length

of the sequence divided by the total travel time. This is akin to saying that the travel time

T over a pool and riffle sequence of length 2π is given by the definite integral

$$T = \int_0^{2\pi} \frac{dx}{a + b\cos x} \tag{4.18}$$

where dx is the distance of a infinitesimally small unit and $a + b\cos x$ is the average

cross-sectional velocity at any point x along the sequence. Integrating this expression

(CRC Standard Mathematical Tables, 1981,*341) results in

$$T = \left[\frac{2}{\sqrt{a^2 - b^2}} \arctan\left[\frac{\sqrt{a^2 - b^2}\ \tan\frac{x}{2}}{a + b} \right] \right]_0^{2\pi} . \tag{4.19}$$

Since the arctangent function only returns values between $-\pi/2$ and $\pi/2$ for any value of x,

a suitable counter must be entered for values of x outside this range. Realizing this and

evaluating the integrand between its bounds yields

$$T = \frac{2}{\sqrt{a^2 - b^2}}(\pi - 0), \tag{4.20}$$

which can be simplified to

$$T = \frac{2\pi}{\sqrt{a^2 - b^2}} . \tag{4.21}$$

 The above expression evaluates the travel time through a pool and riffle sequence that is

2π units in length. Since the length of a complete sequence is 2π units, then the travel

velocity of a pollutant u_T is

$$u_T = \sqrt{a^2 - b^2} . \tag{4.22}$$

Therefore, travel time through a pool and riffle sequence of length L_p is given by

$$T = \frac{L_p}{\sqrt{a^2 - b^2}} \ . \qquad\qquad (4.23)$$

This analysis demonstrates that the presence of a pool and riffle planform increases travel time when compared to a uniform channel. The increase in the travel time (given by Equation 4.23) for a pool and riffle channel is a direct result of the magnitude of the velocity amplitude b. The end result for river transport mechanics is that the increase in the overall decay of a substance in a pool and riffle channel depends on the magnitude of the velocity amplitude. When this is severe enough to be of concern in a river is the topic of the next section.

This analysis also suggests that the constant velocity model could be amended to account for the presence of the pool and riffle planform by simply replacing the velocity term with Equation 4.22. However, the slight oscillation of the decay would be lost.

4.4 Non-Dimensional Analysis.

Table 4.2 presents the changes in the velocities and areas between the pool and riffle as flow declines from bankfull stage to the 7Q10 level. As flow declines the area of the pool increases relative to the area in the riffle. This is shown by the ratio A_p/A_r which is the area of the pool divided by the area of the riffle. In conjunction with this, the relative difference in the velocity between the pool and riffle compared to the average cross-sectional velocity is given by the ratio *2b/a*. As flow declines, this ratio increases. This implies that residence time in the pool relative to the residence time in the riffle will increase as flow level declines.

Table 4.2. Comparison of hydraulic parameters and flow for the upper reach of the Assiniboine River.

	Q cms	u pool m/s	u riffle m/s	a m/s	b m/s	2b/a	A pool sq. m	A riffle sq. m	Ap/Ar
Bankfull	74	0.86	0.72	0.79	-0.07	-0.18	86.0	103.1	0.83
	60	0.70	0.67	0.69	-0.02	-0.05	85.1	89.7	0.95
Reversal	55	0.65	0.65	0.65	0.00	0.00	84.7	84.6	1.00
	50	0.59	0.63	0.61	0.02	0.06	84.3	79.4	1.06
	40	0.48	0.58	0.53	0.05	0.20	83.4	68.5	1.22
	30	0.36	0.53	0.45	0.08	0.37	82.2	56.5	1.45
Metered	22.4	0.28	0.48	0.38	0.10	0.54	81.0	46.5	1.74
	20	0.25	0.46	0.36	0.11	0.60	80.6	43.2	1.87
	10	0.13	0.37	0.25	0.12	0.96	77.9	27.2	2.86
7Q10	5	0.07	0.29	0.18	0.11	1.26	75.2	17.2	4.38

Table 4.3 presents the travel times for a complete transit of a pool and riffle sequence.

This table shows that as flow stage declines the transit time in the pool relative to the

riffle, as shown by the ratio t_p/t_r , grows. Importantly, the travel time ratio is greater than

2 for the 7Q10 flow, indicating that the travel time in the pool is more than twice the time

spent in the riffle. This corresponds with the ratio, *2b/a*, which is greater than one at the

7Q10 level, as shown in Table 4.2. At this flow level, the role of the pool and riffle in

affecting travel time and hence decay of pollutants becomes quite marked. This is

Table 4.3. Comparison of travel times for the upper reach of the Assiniboine River.

	Q cms	Travel time (s)	Time in pool (s)	% Time in pool	t_p/t_r
Bankfull	74	1189	561	47	1
	60	1357	666	49	1.0
Reversal	55	1440	720	50	1.0
	50	1535	784	51	1.0
	40	1774	940	53	1.1
	30	2114	1177	56	1.3
Metered	22.4	2553	1493	58	1.4
	20	2731	1635	60	1.5
	10	4268	2814	66	1.9
7Q10	5	6569	4660	71	2.4

illustrated by the data in Table 4.4 which compares concentrations of a substance as it

decays along the Lower reach of the Assiniboine River for the constant parameter model

and the variable velocity model.   The concentration differences in per cent between the

constant velocity model and the variable velocity model are shown. The values are

calculated for downstream stations along the lower reach of the Assiniboine using

Scenario 1 data. The results of the analysis show that at low flow levels the differences

in predictions between the two models is significant. The difference is of particular

concern at or near the 7Q10 level.

If a ten per cent difference is considered to be significant, then the variable

velocity model should be used to predict concentrations along the lower reach of the

Assiniboine for flow levels below 20 cms. This corresponds in Table 4.2 with a 2b/a

ratio of 0.6 and in Table 4.3 where travel time in the pool compared to travel time in the

riffle is a sixty-forty split. In general then, when the ratio 2b/a is greater than 0.6, the

variable velocity method should be used because the pool and riffle planform has a

significant effect on transport. It has increased the travel time and thus lowered the

Table 4.4. Comparison of differences in concentration between variable velocity and constant velocity advection equations.

		Distance Downstream and Per cent Concentration Change						
	Q cms	**1000 m**	**2000 m**	**3000 m**	**4000 m**	**5000 m**	**7500 m**	**10000 m**
Bankfull	74	0%	0%	0%	0%	0%	0%	0%
	60	0%	0%	0%	0%	0%	0%	0%
Reversal	55.1	0%	0%	0%	0%	0%	0%	0%
	50	0%	0%	0%	0%	0%	0%	0%
	40	0%	0%	0%	0%	0%	1%	1%
	30	0%	0%	1%	1%	1%	3%	4%
	22.4	1%	1%	2%	3%	4%	7%	10%
	20	1%	2%	3%	4%	6%	10%	14%
	10	4%	9%	13%	17%	22%	34%	45%
7Q10	5	12%	22%	31%	40%	48%	66%	78%

average velocity which has increased the overall decay.   This generalization can also be

stated in terms of cross-sectional area.   In other words, when the pool cross-sectional

area is approximately twice the riffle area, the pool and riffle bedform has a significant

effect on transport and the variable velocity model should be employed to predict

transport.

This finding may also help to explain the wide variation in the values between the

predictions from the constant velocity advection-dispersion model and those determined

from tracer studies on rivers, discussed in Chapter 2. The role of the pool and riffle on

transport is not accounted for in these comparisons and therefore the enhanced decay

attributable to the bedform at low flow levels is not reflected. This study's findings

suggest that as the flow stage increases to bankfull level, the enhanced decay attributable

to the pool and riffle planform on the river becomes less and less a factor. However, at

low flow levels it is a factor that needs to be considered. Since the comparisons between

modeled and tracer results in the literature are made across a wide range of flow

conditions, discrepancies in the comparisons would be expected in light of this finding.

This analysis conclusively shows that at low flow levels the pool and riffle

bedform increases the travel time of a contaminant when compared to travel time in a

uniform channel. This effect is not accounted for in the traditional constant parameter

advection model. The phenomenon becomes more severe as flow levels decline to the

7Q10 stage and therefore the effect of the bedform should be considered when modelling

water quality at low flow stages. The next chapter will test the new variable velocity

approach to modelling on the Athabasca River, but first an analysis of other functions

that could be used to describe the channel shape transition between a pool and riffle is

presented.

4.5   The General Case.

So far the transition in channel shape between the pool and riffle has been modelled with

a periodic function. But this is not the only type of function that could be used to model

the transition. The two other functions that immediately spring to mind are the step

function and the saw-tooth function. If the transition is modelled by one of these

functions or another type of function, its effect on travel time can be seen by rewriting

Equation 4.18 to reflect the use of any velocity function. It becomes

$$T = \int_0^{L_p} \frac{dx}{u(x)} \ . \tag{4.24}$$

Replacing the velocity function with its composite area function leads to

$$T = \frac{1}{Q} \int_0^{L_p} A(x)dx \ . \tag{4.25}$$

The integral is simply the volume of the pool and riffle unit at a particular flow stage,

$V(q)$, and can be written as

$$T = \frac{V}{Q} \ . \tag{4.26}$$

Then the travel velocity of a pollutant through the system becomes

$$u_T = \frac{QL_p}{V} \ . \tag{4.27}$$
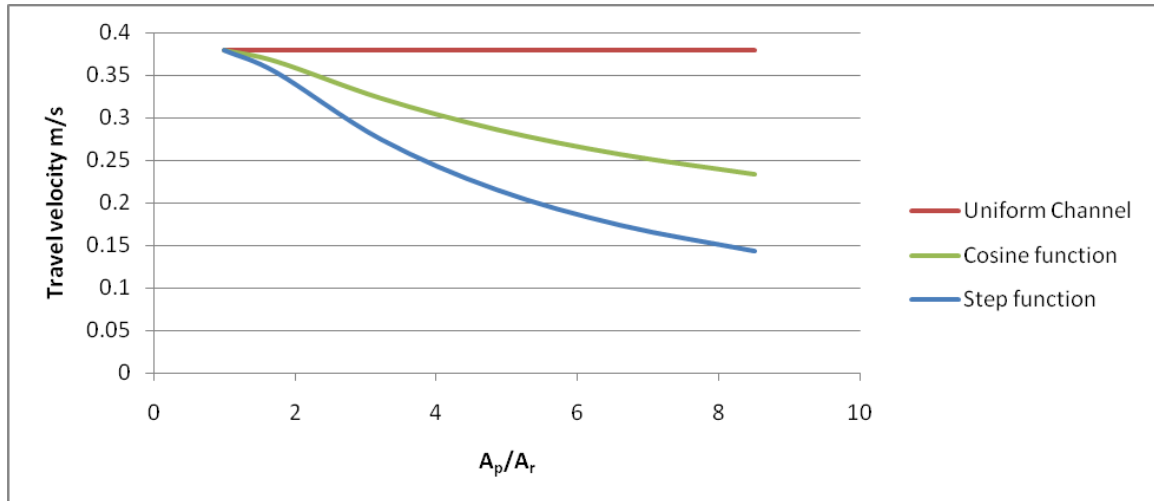
Figure 4.6. Travel velocity versus the ratio of the area of the pool to the area of the riffle.

This expression can be used to evaluate the travel velocity when a function other than a periodic function is used to simulate the transition between a pool and riffle.

A comparison of travel velocities between a simple step function where the pool steps to the riffle at the half way point and back again, the cosine function and constant average velocity approach is shown in the following analysis which uses the case on the Assiniboine River shown in Figure 4.3 and Table 4.1. Figure 4.5 presents the travel velocity curves for the three cases. As can be seen the constant velocity approach forms the upper bound for travel time, whereas the step function forms the lower bound. The cosine function describes an intermediate travel time domain.

More study of the pool and riffle planform over the complete discharge regime of a river is required before a more definitive recommendation on the appropriateness of the transition function is made. In this thesis the periodic function is adopted because not all pool and riffle sequences in a channel will develop to their full, but instead a series of well developed and less developed couplets randomly distributed along the channel

would be the norm. Therefore, as shown in Figure 4.5, the cosine function is used to

model the transition between pool and riffle because it calculates a travel velocity

between the limits of the other two approaches.

Chapter 5   Model Calibration and Validation

This thesis proposes that transport of pollutants in rivers is affected by the pool and riffle bedform which in turn sets up a corresponding fluctuation in average velocity along the river channel. This velocity variation along a channel is not accounted for in current one-dimensional transport equations. Accordingly, an equation has been developed that can describe the periodic fluctuation in average velocity through pool and riffle sections (Chapter 3). This equation is incorporated into a mass balance analysis and a new pollutant transport model that simulates this variable advection phenomenon derived (Chapter 4). This new transport model incorporates the quasi-periodic changes in channel cross-sectional shape due to pool and riffle planform in a velocity expression that can be readily ascertained from stream flow records and surveyed cross-sections.

Preliminary theoretical analysis, using measured data from the Assiniboine River,

suggests that the proposed variable velocity advection model (Equation 4.10) has

promise: it is intuitively simple in architecture, yet complex enough to model the effect of

the riffle and pool sequence on the transport of pollutants. In this chapter, the model will

be tested by comparing its results with measured data and an assessment of the model as

a predictive tool discussed. This is usually referred to as model validation. Also, the

validation exercise provides a methodology for applying the model to other rivers.

Because model validation requires a comparison of the models predictions with

measured data, a complete historical data set with the following qualities is necessary:

1. Hydraulic data that includes continuous flow levels and commensurate metering
   data along separate but contiguous reaches of a river. Surveyed cross-sections
   progressing downstream from the start to the finish of the river section to be
   validated.

2. Water quality measurements for the main channel of the river coupled to data
   from all tributaries and municipal/industrial point sources. These data must be
   sampled in a manner that follows a parcel of water as it passes along the river.

3. Field or laboratory measurements of rate coefficients that describe the addition or
   decay of the substance being modelled.

There are not many rivers in Canada that have such an extensive data record.

Originally, the Assiniboine River was considered for the validation exercise, but after

examination of its database, it was ruled out for two reasons. One, there is a question

about the timing of sampling and therefore the ability to accurately portray the change in

quality of a plug of water moving down the river, and two, there are not enough

hydrometric stations along the river to fully assess its hydraulic geometry. For these two

reasons it was necessary to look at data sets for other rivers. One river that stood out for

the completeness of its data base is the Athabasca. The river was part of the Northern

River Basins Study (NRBS), a multipurpose study that looked at the cumulative effects of

industrial, agricultural, municipal and other development on the Athabasca, Peace and

Slave River basins. One of the goals of the NRBS was to model dissolved oxygen (DO)

levels in the Athabasca River during the winter, the period thought to be the most

stressful to aquatic organisms. It is this data-base collected by Alberta Environment for

DO modelling, coupled to the extensive hydraulic data measured on the river by collected

by Water Survey of Canada that is used for the validation of the new transport model.

Validation of the new transport model requires a number of steps. Because the

validation of the new transport model is focused on DO prediction in the Athabasca

River, the first step is to modify the transport model to simulate DO mechanics in the

river along the lines of the Streeter-Phelps equations. Second, the hydraulic geometry of

the river must be established. Third, the hydraulic structure linked to the river's

hydrology and BOD and DO inputs must be established. Fortunately, because the

Athabasca has already been the focus of modelling studies by MacDonald and Hamilton

(1989) and Chambers et al. (1996), the hydraulic structure and inputs that they

established can be used in this validation exercise. This is followed by a discussion of

sources of uncertainty within the measurements used in the modelling structure. After
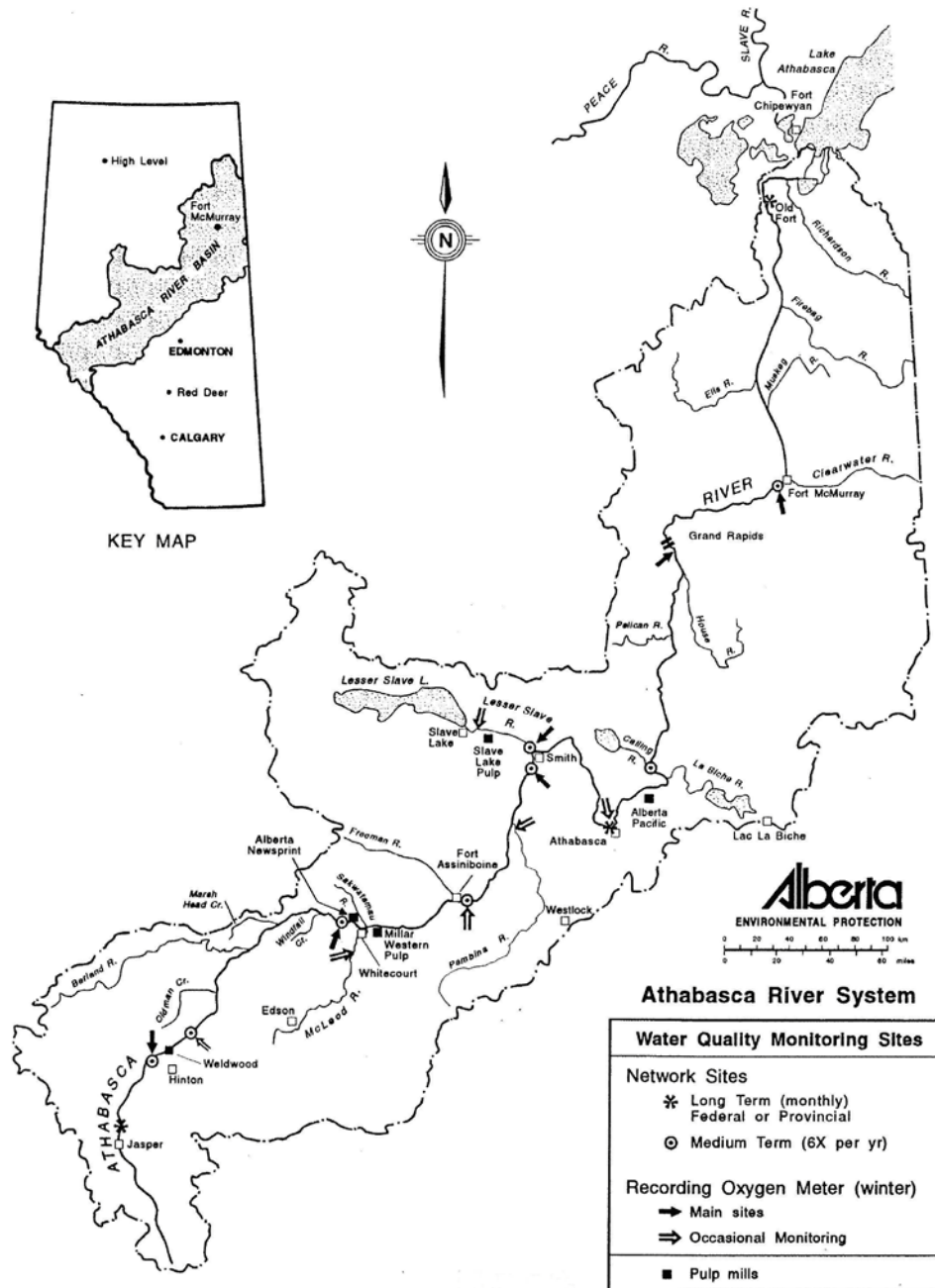
Figure 5.1. Athabasca River Basin. (Noton and Allan, 1994).

completion of these steps, calibration of the model begins. Calibration involves adjusting

the set of parameters in the model to reflect the environmental conditions in which the

model is being tested. The fifth step utilizes a sensitivity and non-dimensional analysis to

gain an appreciation of the role that each of the models' parameters plays in determining

the outcome. The final step is to compare the model's DO predictions to measurements

of DO along the river.

Before embarking on this endeavor, a discussion of the Athabasca River's

watershed and hydrology plus a review of DO studies on the river is presented.

5.1   Athabasca River

From its headwaters draining the Columbia Ice Field near Jasper, the Athabasca River

flows northeastward through Alberta to its terminus at Lake Athabasca (Fig. 5.1). It is the

second largest river in Alberta with a length of 1,231 kilometres and a drainage area of

138,412 square kilometres. The river is not regulated, and has the typical regime

associated with northern rivers, peak flows occurring during the late spring with low

flows occurring in the winter under ice conditions.

The 555 kilometre long section of the Athabasca River between Hinton and

Athabasca is selected for this validation study. Between Hinton (1003 m asl) and

(Athabasca 533 m asl), the river descends approximately 470 metres. Four major

tributaries, the Berland, McLeod, Pembina and Lesser Slave Rivers, along with seven

creeks and three springs join this section of river. These tributaries contribute

substantially to the river's flow. At Hinton the mean annual flow is 173 cms while the

7Q10 flow is 16 cms. Contributions from tributaries have increased the mean annual

flow to 433 cms and the 7Q10 to 53 cms at Athabasca. Average flows in the river during the months of January and February for the calibration and validation periods range between 25 cms and 32 cms, close to twice the 7Q10 levels.

5.2   History of studies on the Athabasca River.

DO is essential for the health of all aquatic organisms. In Canadian rivers, these organisms usually experience the most DO stress in winter when flows are at minimum levels and ice cover limits interaction with the atmosphere. Further increases in stress can be caused by further depletion of DO levels due to seepage of low DO groundwater and by oxidation of organic matter, usually stemming from municipal and industrial effluent discharges. The importance of these factors in depleting DO levels in ice covered streams has long been recognized, but their interaction in northern rivers is still not well understood. Many Canadian rivers are experiencing the effects of increased development activities in their basins stemming from agriculture, mining, oil and gas development and urbanization. One method to better understand the combined impacts of these changes on rivers is to apply a water quality model. This was recognized by the Northern River Basins Study and one of their major objectives was to develop a water quality model that could be applied to Alberta's rivers.

Concern with DO levels in the Athabasca River dates back to the 1950s with the start-up of the first pulp and paper mill on the river at Hinton. Above Hinton, DO levels in the river are close to saturation (13 mg/l) even under ice conditions in winter. However, below Hinton, DO levels decline, reaching about half this value at Grand Rapids before recovering. Modelling of DO levels in the Athabasca started in the 1980s

with the dual studies by Charles Howard and Associates (1984) using the WQRS (Water Quality model for Rivers and Reservoir Systems) model and the initial application of the DOSTOC (Dissolved Oxygen Simulation Model) by Hamilton et al. in 1988. Further attempts using DOSTOC to model river DO levels were conducted by Macdonald and Hamilton (1989), Macdonald and Radermacher (1992, 1993) and Chambers et al. (1996). A number of complimentary studies examining DO trends (Noton and Allan, 1994), rate coefficients (Shaw and MacDonald, 1993), sediment oxygen demand (SOD) (Casey and Noton,1989; Casey, 1990; Noton, 1995) and a review of rate coefficients on the Athabasca (Shaw and MacDonald, 1993) were also completed.

Alberta Environment conducted extensive water quality surveys along the river during the winters of 1988 and 1989. DO and BOD levels were measured upstream of Hinton and at other points along the main channel down to the town of Athabasca. They also measured all tributary contributions of BOD and DO just upstream of their confluences with the river. The general idea was to sample a parcel of water as it moved down the river combined with the sampling of all inputs as the parcel passed them. All samples were collected from holes drilled through the ice usually in the centre of the channel. Four separate winter water quality surveys are used in this validation analysis. The February, 1988 survey was used in calibration of the model while the March, 1988, January, 1989 and February-March, 1989 were used for validation.

During this period (1988 to 1989) two pulp and paper mills were operating on this section of river. The Weldwood of Canada mill at Hinton discharged effluent continuously over the period, while the Millar Western, at Whitecourt, started up operations in 1989.   Also, discharging effluent during this period were the two

municipal waste water treatment plants at Whitecourt and Athabasca. Effluent samples

collected from the pulp and paper mills were 24-hour composites, while the municipal

waste-water samples were grab samples; all samples were collected from these facilities

just upstream of their discharge points. This data was collected and analyzed by Alberta

Environment. The methodology for the collection and analysis of the BOD and DO

samples is discussed in Chambers et al. (1996, p.2.5). For all samples, BOD_5 and DO

levels are measured. The results are the averages of duplicate samples. The conversion

procedure and analysis of BOD_5 measurements to BOD_U levels is also discussed in

Chambers et al. (1994, p.4.4). Basically, the technique measured daily levels of BOD

over 120-day periods for a select number of samples. Using the 120-day sample as

representative of the BOD_U, the average BOD_U/BOD_5 ratio is used to convert all other

BOD_5 levels to BOD_U levels.

BOD levels and rates of decay were measured by the Mills and Alberta

Environment. There are discrepancies between the sample results. It is not clear why

the discrepancy exists, both agencies claiming to have used standardized scientific

methods of analysis and standardized handling procedures for the samples. This is

discussed more fully by MacDonald and Hamilton (1988). Since the mill discharges are

the largest point sources of BOD to the river, this discrepancy causes some uncertainty in

the modelling.

5.3   Variable Velocity DO Model

The classic engineering approach to modelling DO levels in rivers is the use of the

Streeter-Phelps model. The model uses two equations that relate biological oxygen

demand (BOD), B, and oxygen deficit, D, to distance, x, downstream from the source of

the effluent. It assumes nearly instantaneous mixing at the point of discharge. The

oxygen deficit is the difference between the dissolved oxygen saturation level and the

dissolved oxygen level in the river:

$$0 = -u\frac{dB}{dx} - kB - s \quad \text{and} \tag{5.1}$$

$$0 = -u\frac{dD}{dx} + lB - nD. \tag{5.2}$$

These two equations use the first order rate coefficients, $k, l,$ and n, where k is the

removal rate of BOD in the river, which is the sum of the BOD decay rate, l, plus the

BOD settling rate, m. The reaeration rate constant, n, describes the rate of oxygen

replenishment in the river while s is the sediment oxygen demand (SOD).

Levels of DO have been previously modelled on the Athabasca River with the

DOSTOC model (Dissolved Oxygen STOCastic model), basically a numerical form of

the above Streeter-Phelps equations. A good discussion of this model and its governing

equations is found in Chambers et al. (1994). Using this form of the Streeter-Phelps

model and modifying it to reflect the variation in average velocity that is experienced

along a pool and riffle channel like the Athabasca results in the following two equations:

$$0 = -\left(a + b\cos\left(\frac{2\pi x}{L}\right)\right)\frac{dB}{dx} - kB - s, \text{ and} \tag{5.3}$$

$$0 = -\left(a + b\cos\left(\frac{2\pi x}{L}\right)\right)\frac{dD}{dx} + lB - nD. \tag{5.4}$$

As before, a is the average velocity of flow along the channel reach, b is the amplitude of

the velocity variation between pool and riffle, and L is the river distance between

adjacent pools. The coefficients k, l and n are the rate coefficients for removal of BOD,

decay of BOD and reaeration, respectively. The last term in Equation 5.3 is the sediment

oxygen demand, *s*. These two equations form the variable velocity model to be tested on

the Athabasca River. If B equals B_0 and D equals D_0 when t and x equal to 0, then these

equations can be solved for B and D. The numerical ODE solver in Maple 10 is used to

solve this system of equations.

5.4   Velocity Reversal Patterns

Hydrometric stations, operated by Water Survey of Canada, at Entrance, Hinton,

Windfall and Athabasca, provide the metering data necessary to establish the hydraulic

geometry along the 555 km section of the river.   This section is composed of five distinct

reaches, defined by the confluences of major tributaries (Fig. 5.1). These reaches from

upstream to downstream are: Hinton to the Berland River; Berland to the McLeod River;

McLeod to Pembina River; Pembina to Lesser Slave River; and Lesser Slave to

Athabasca. The stations at Hinton and Entrance are located at the start of the upper reach

while the station at Windfall lies between the Berland and McLeod Rivers and the station

at Athabasca lies in the middle of the lower reach.   This leaves the two reaches between

the McLeod and Pembina and Pembina and Lesser Slave without representation.

However, the cross-section data surveyed by Trevor et al. (1988) provides insight into the

hydraulic geometry of these reaches as well as supporting the hydraulic geometry

analysis of the other three reaches.   These 42 surveyed river cross-sections, located

randomly at approximately 12 kilometre intervals between Hinton and Athabasca, were

required for HEC-2 modelling of the river. Their purpose was to characterize the

variability in channel shape along this section of the river, the traditional means of
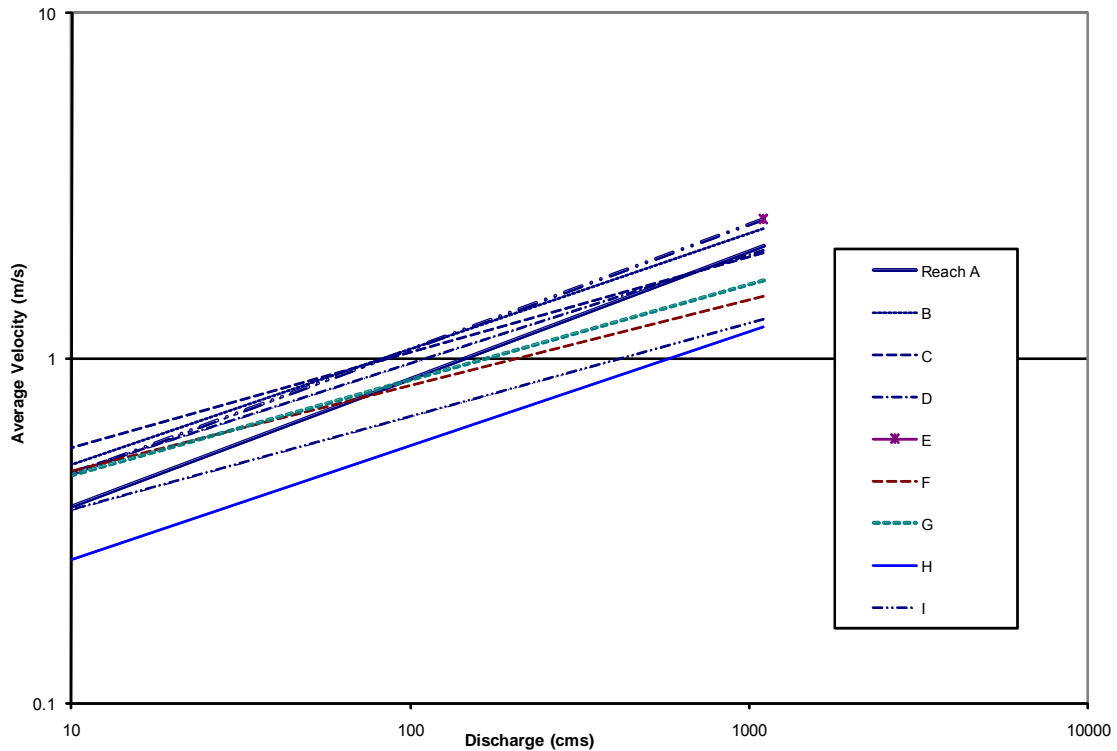
Figure 5.2. Velocity-discharge curves for the Athabasca River used by MacDonald and Hamilton (1988) and Chambers et al. (1996).

defining hydraulic geometry for water quality studies. The cross-sections were surveyed

at flow levels gradually increasing in the downstream direction from 105 to 200 cms.

An important point of note here is the hydraulic geometry that was determined by

the HEC-2 analysis and used in the DOSTOC modelling by MacDonald and Hamilton

(1989), MacDonald and Radermacher (1993) and Chambers et al. (1996). As can be seen

in Figure 5.2, the Athabasca was divided into 9 reaches. An average velocity-discharge

relationship, represented by a line on the graph, characterizes the hydraulics of each

reach. What is interesting to note is the general parallelism of these velocity-discharge

lines which will be discussed later. This is a good example of the type of hydraulic

geometry results found in water quality studies that use the traditional constant parameter
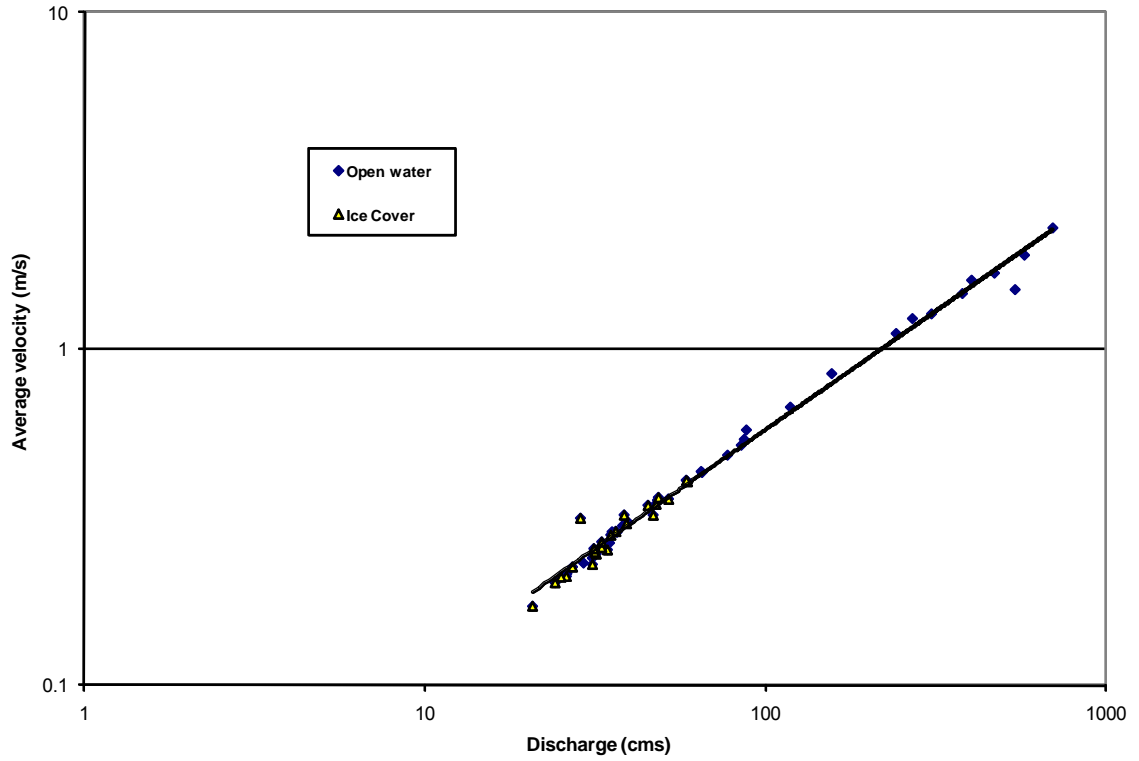
Figure 5.3a. Hydraulic Geometry at Hinton on the Athabasca River.
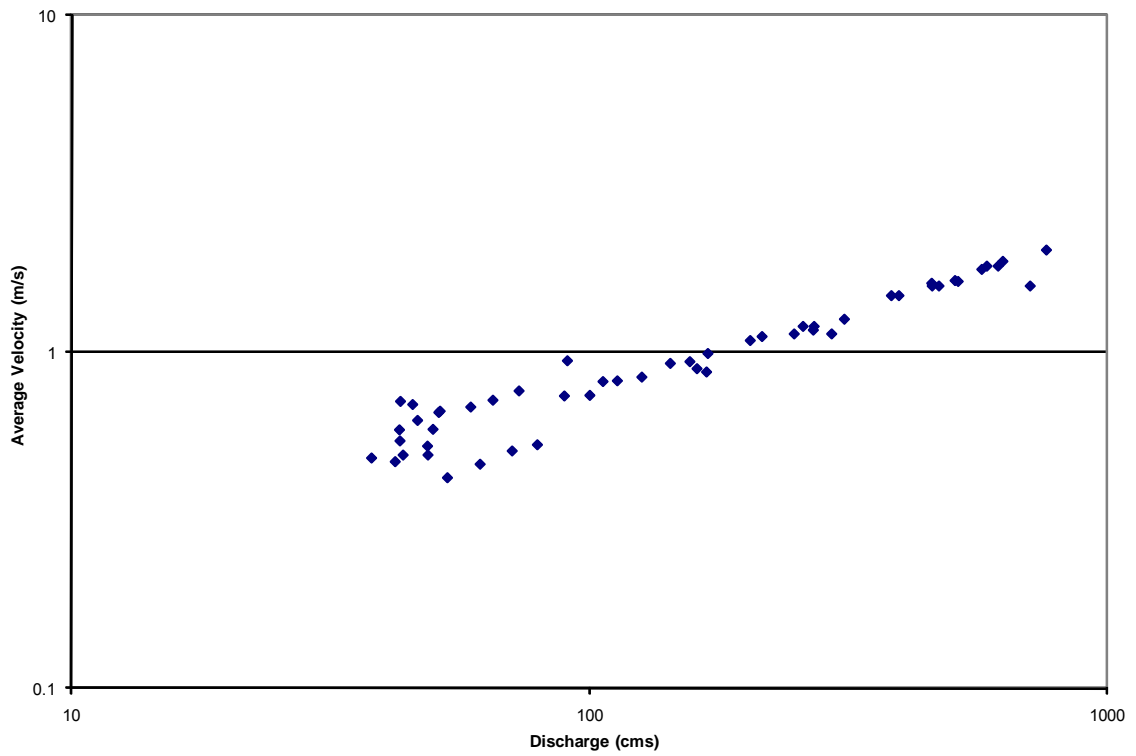
Figure 5.3b. Hydraulic Geometry at Windfall on the Athabasca River.

Figure 5.3c. Hydraulic Geometry at Athabasca on the Athabasca River.

advection type of model. This is because hydraulic models are forced to report reach

average conditions to fit the requirements of the constant parameter transport models.

The historic records for the stations at Hinton, Windfall and Athabasca were

analyzed for the period of 1988 to 1991, the start of the time period coinciding with the

water quality surveys. The four year length at each station encompasses a minimum of

fifty flow measurements, enough data to establish the hydraulic geometry at these

stations. Average velocity versus discharge plots were constructed on log-log graph paper

for each station (Fig. 5.3 a, b, and c). The plot of the velocity-discharge at Hinton is a

very good fit to a straight line, suggesting a strong power relationship between velocity

and discharge. However, there is a wider variation in the discharge versus velocity data

for the stations at Windfall and Athabasca.

Figure 5.3d. Hydraulic Geometry at Entrance on the Athabasca River.

The station at Entrance proved to be particularly insightful in explaining the differences between the graphs. The station at Entrance was located approximately a kilometer upstream of the station at Hinton. Although it was abandoned in 1961, the period of record from 1958 to 1961 was examined and the velocity-discharge relationship plotted. Similar to the Hinton station, a plot of the velocity versus discharge data describe a strong power relationship (Fig. 5.3d). Importantly, when the curve for Entrance is overlain with Hinton's curve, the familiar velocity reversal pattern that describes the difference between riffle and pool is evident (Fig. 5.4). The upper curve depicts the relationship for a riffle section while the lower curve depicts the relationship for a pool section.
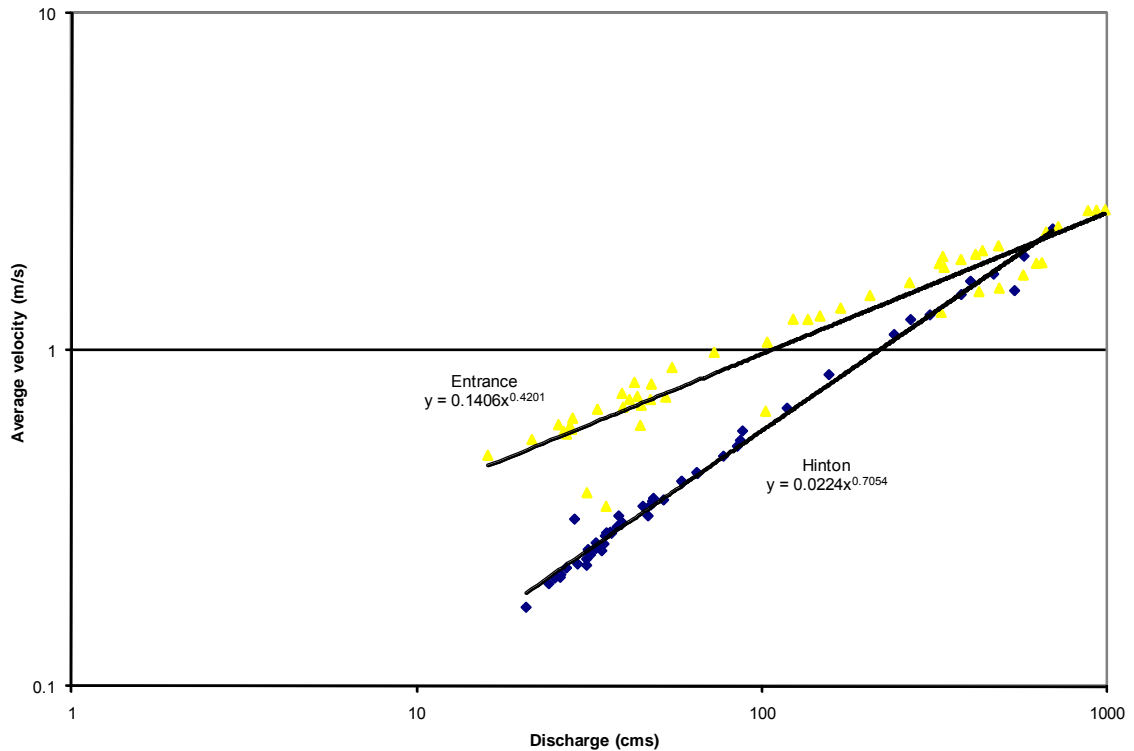
Figure 5.4. Velocity-discharge curves at Hinton and Entrance.

Lending further credence to the existence of the pattern are the results of the ten

surveyed channel cross-sections of Trevor et al. (1988). These channel cross-section

surveys were conducted at flows of 105 to 110 cms from Hinton downstream to the

confluence with the Berland River. When the average velocity versus discharge data is

plotted for these cross-sections, they form a vertical line that straddles the Hinton and

Entrance curves (Figure 5.5). Not only does this support the velocity reversal pattern, but

also, because the measured cross-sections of Trevor et al. (1988) extend from Hinton to

the Berland River, supports the idea that the pattern represents the reach's hydraulic

geometry.

$$y = 0.1406x^{0.4201}$$

$$y = 0.0224x^{0.7054}$$
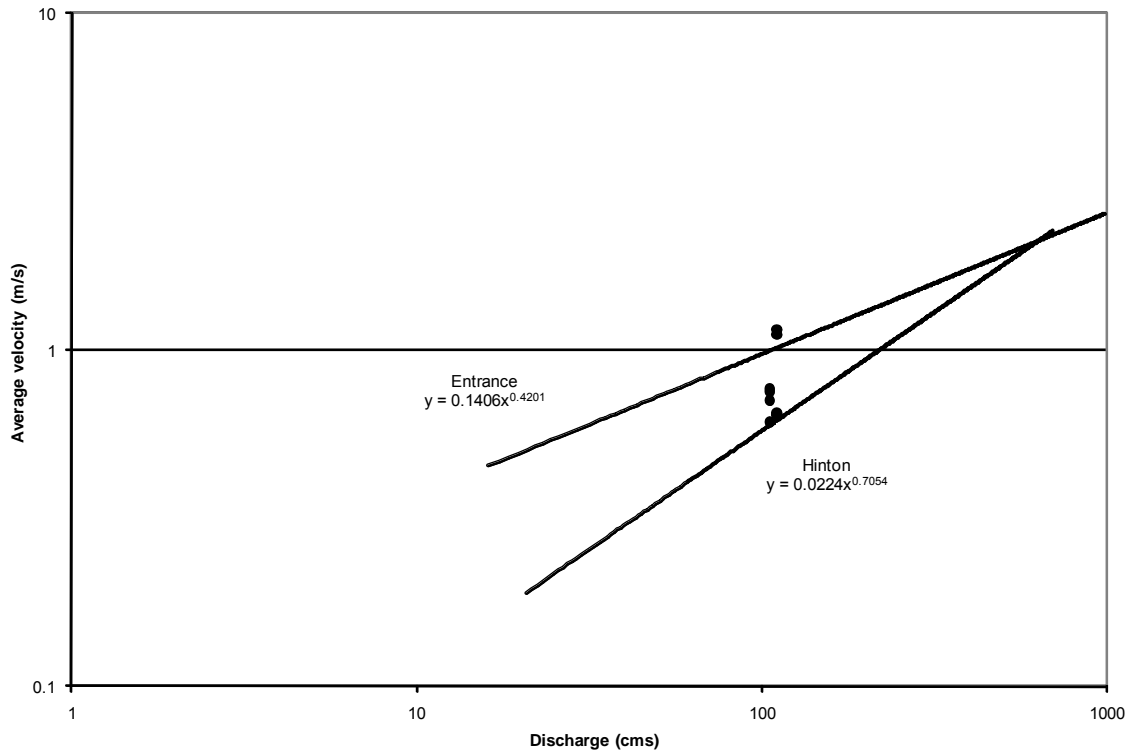
Figure 5.5. Trevor et al. (1988) measurements for Hinton reach.

The uncovering of the velocity reversal pattern on the upper reach of the river

helps with the interpretation of the average velocity–discharge data for the stations at

Windfall and Athabasca.   The spread of the data at the two stations suggests that the flow

meterings may have been measured at different locations. Dennis Lazowski,

Hydrological Service Supervisor at Water Survey of Canada in Edmonton, confirms that

this was indeed the case. As a matter of fact, Lazowski was the technician in charge of

measuring the flow at Athabasca during this time. He confirms that the location of the

meterings at the Windfall and Athabasca stations varied by up to a kilometer around the

station depending on the local conditions encountered at the site at the time of

measurement. Therefore, flow measurement recorded at these sites would encompass the

full range of cross-sections spanning the pool and riffle planform at the site, because the

93
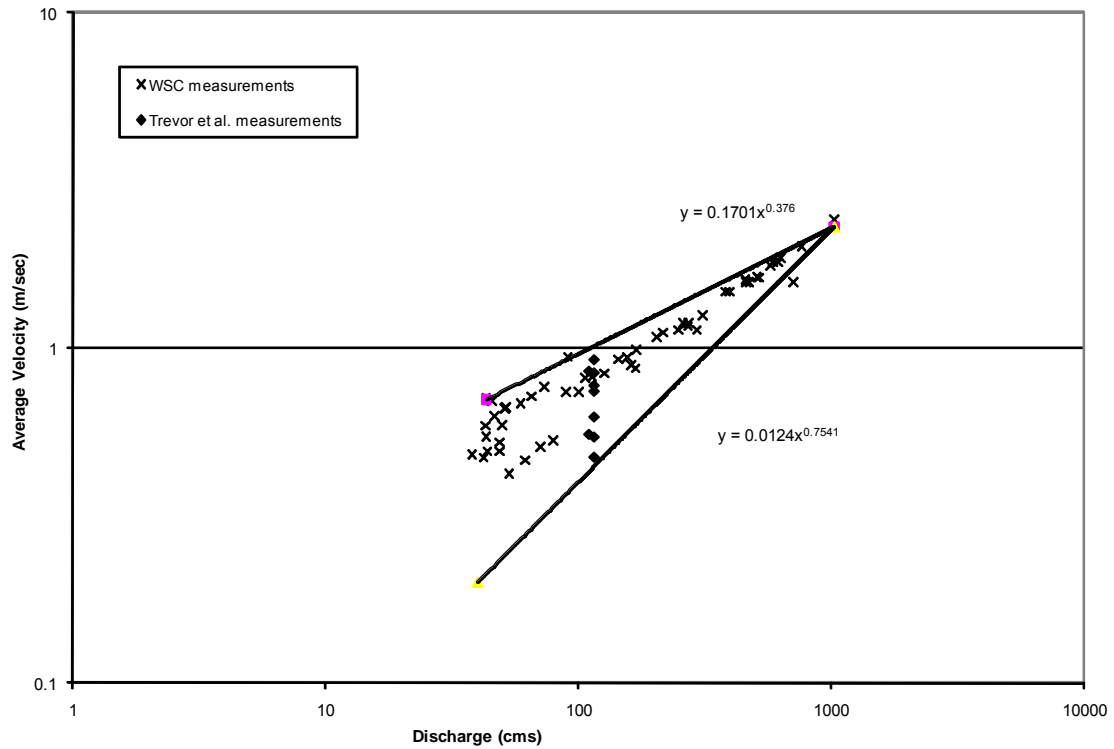
Figure 5.6a. Velocity reversal pattern for Windfall reach.

average distance between pools on the river is 530m.   Applying this insight concerning

the data at both stations, it is reasonable to construct velocity reversal patterns that

encompass the full spread of the average velocity-discharge data for the two reaches (Fig.

5.6 a, b).

The existence of the velocity reversal patterns is further reinforced for these

sections of river by the cross-section data of Trevor et al. (1988). Their channel survey

data for the two reaches that the stations at Windfall and Athabasca fall in are also plotted

on Figures 5.6a and b. Similar to the upper reach analysis, these average velocity-

discharge points vertically straddle the reversal patterns.
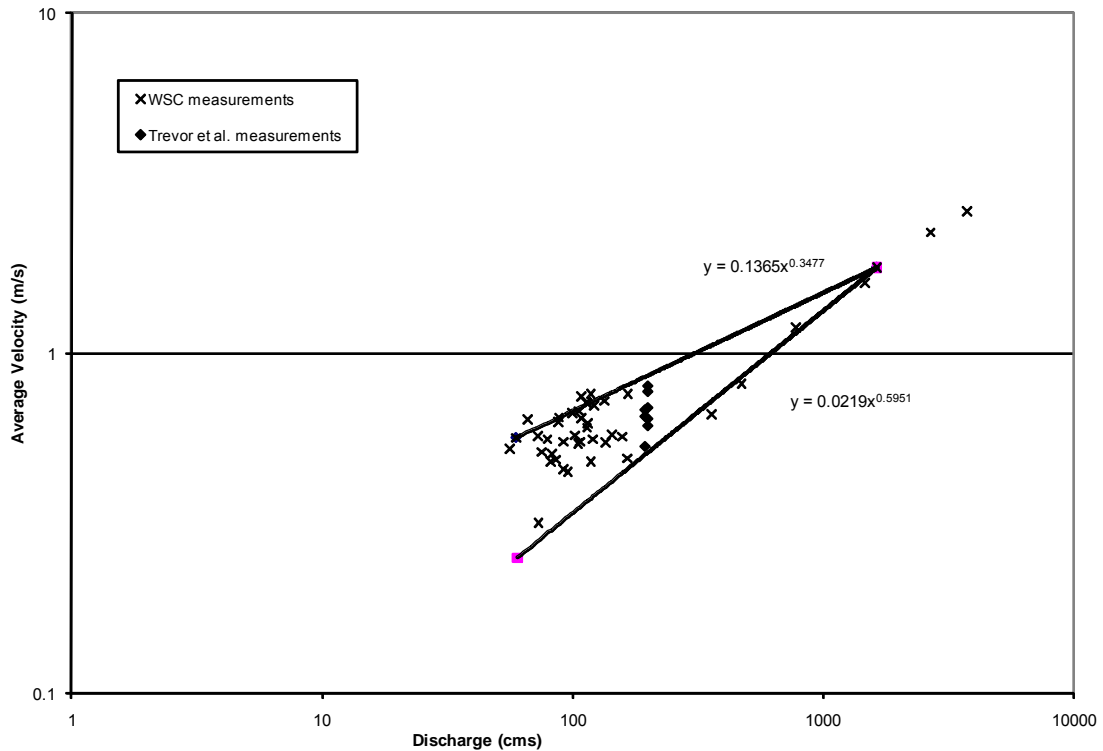
Figure 5.6b. Velocity reversal pattern for Athabasca reach.

    This analysis of station and reach data firmly establishes the velocity reversal

patterns for three reaches of the Athabasca River. These are the reaches from Hinton to

Berland River, Berland to McLeod River and Lesser Slave River to Athabasca. The

reversal patterns are overlaid on one graph in Figure 5.7. However, this still leaves the

middle two reaches without representation. These two reaches, McLeod River to

Pembina River and the Pembina River to Lesser Slave River, lack hydrometric station

data because there are no hydrometric stations operating along them. Therefore, their

velocity reversal pattern must be inferred by other means. Since no station data is

available for either reach and since they are contiguous and in the middle of the section

being investigated, it seems reasonable to use one pattern to represent hydraulic geometry

of both reaches.
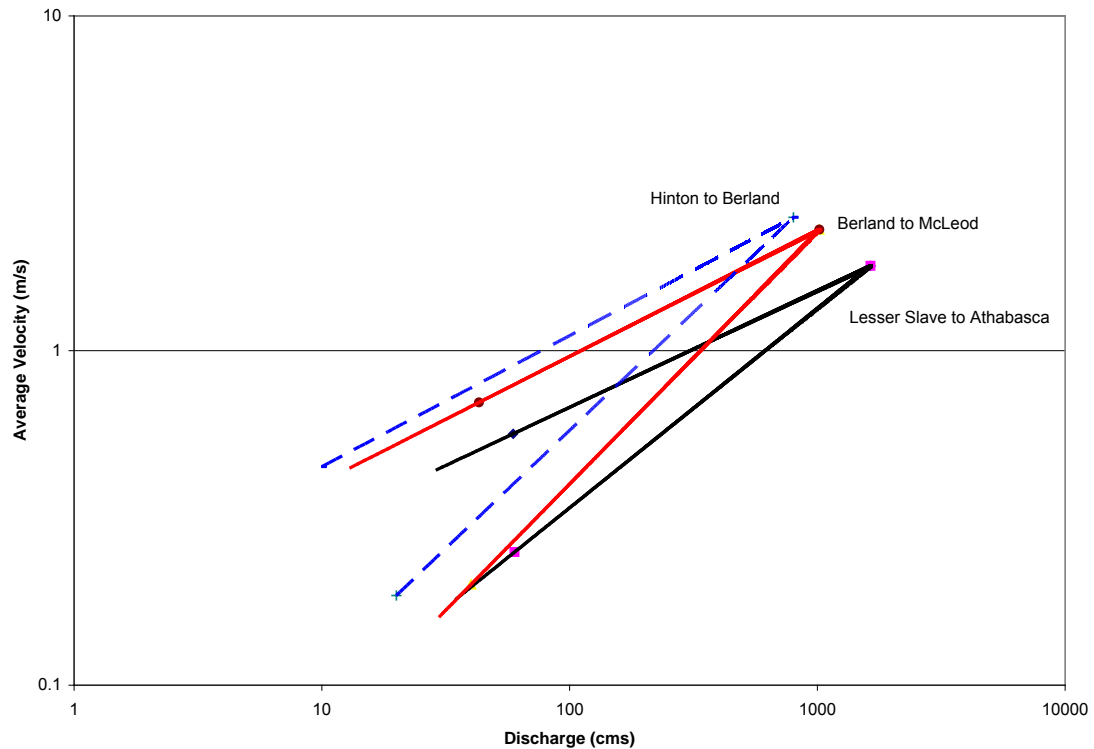
Figure 5.7. Velocity reversal patterns for the reaches from: Hinton to Berland River; Berland River to McLeod River and Lesser Slave River to Athabasca.

The only data available for both of these reaches is the channel survey data measured by Trevor et al. (1988). However, this data coupled to pattern analysis of the upstream and downstream reaches can be used to infer the velocity pattern for the reach in the following fashion.

Examination of the reversal patterns in Figure 5.7 suggests that there is a definite direction to the shift of the points of reversal for each pattern from reach to reach. A short curve could be drawn through these points. It seems reasonable to expect then that the missing reach's point of reversal would be located along this curve. Also, plotting of the cross-section data measured by Trevor et al. (1988) results in a vertical band that
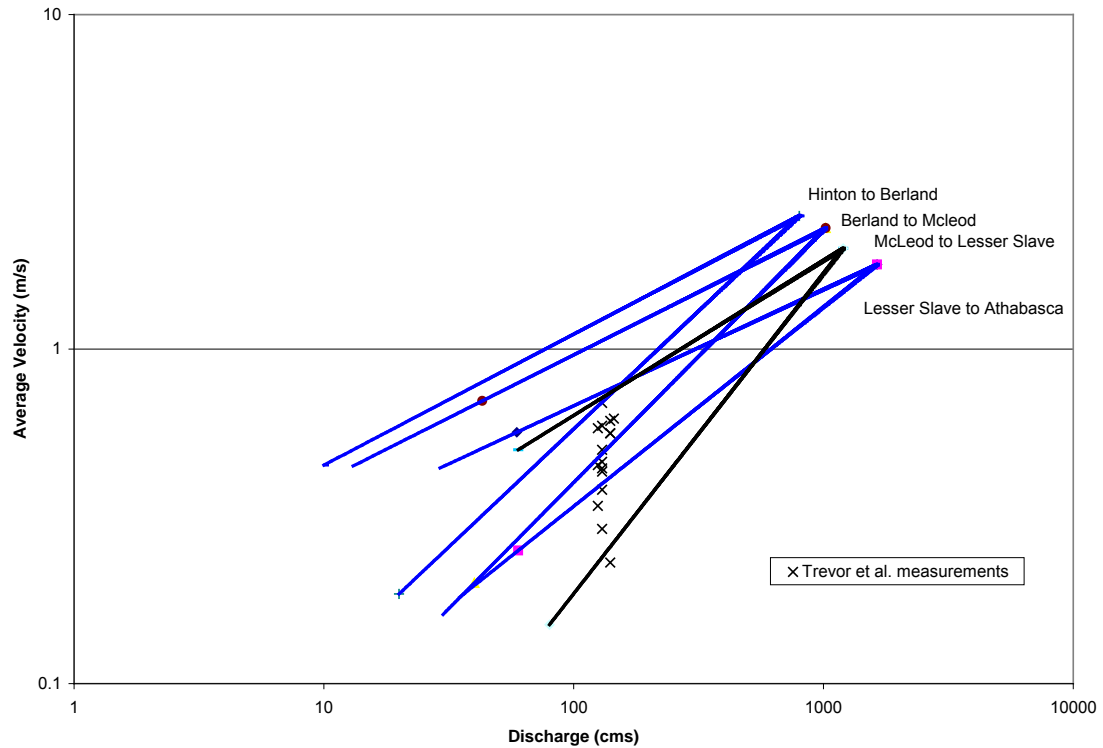
***Figure 5.8. Velocity reversal patterns for the reaches from: Hinton to Berland
River; Berland River to McLeod River; McLeod River to Lesser Slave River and
Lesser Slave River to Athabasca.***

encompasses the spread of the velocity reversal pattern for this middle reach. The

velocity reversal pattern constructed from this interpretation is shown in Figure 5.8.

To summarize, the Athabasca River is divided into four reaches for modelling.

These are: Hinton to the Berland River; Berland River to MacLeod River; Macleod River

to the Lesser Slave River; and the Lesser Slave River to the Town of Athabasca. Each of

these reaches has a distinct reversal pattern as shown in Figure 5.8.

5.5   Uncertainties

Before calibration begins, an understanding of the source of uncertainties in modelling

DO levels on the Athabasca River would seem prudent. There are usually a number of

sources of uncertainty that surround the application of water quality models. Besides

uncertainty in the model structure itself, there is also doubt surrounding the correct

estimation of the rate parameters and uncertainty in the accuracy of the input data as well

as the data against which the model will be tested against. It is often difficult to separate

the effect of parameter estimates and data uncertainties, and this is the case here. The

major uncertainties during the calibration and validation exercises stem mainly from the

following:

1. flow in the Athabasca River during the water quality survey period.

2. hydraulic geometry of the middle reach of the Athabasca, and

3. BOD5/BODu ratio.

    The flow levels during the water quality survey periods were calculated by

MacDonald and Hamilton (1988) from flow measurements made by Alberta

Environment. All major tributaries and five main-stem river locations were measured

during the water quality surveys. Addition of incoming flows with the main-stem flows

resulted in discrepancies between the computed flow at Athabasca and the measured flow

for the four water survey periods. MacDonald and Hamilton (1988) state that the

discrepancies amount to 23.5, 16.6, 14.1 and 4.3 per cent of the flow at the Town of

Athabasca for the four water quality survey periods, respectively. These discrepancies in

the flow balance were resolved by proportioning the missing flow to ungauged tributaries

or springs. Chambers et al. (1996) were able to better estimate the proportioning of these

flow discrepancies to the ungauged tributaries using average flows for these tributaries based on data from later years.

The lack of hydrometric stations between the MacLeod River and the Lesser Slave River led to the inference of the hydraulic geometry pattern for this stretch of river. There is uncertainty concerning the accuracy of the inferred hydraulic geometry, hence the velocities used in the model runs for this reach, but this uncertainty is mitigated to some extent by the cross-sectional data of Trevor et al. (1988) for this part of the river. The range of the velocities from the measured cross-sections is used to infer the variable velocity pattern caused by the pool and riffle planform. The cross-sectional velocity data correlate highly with the variable velocity patterns determined in other reaches of the river, and there is no reason to believe that this would not be the case for the middle reaches, although the data record does not yet exist to verify this.

The water quality surveys measure the BOD_5 level for all samples. However the analysis uses the BOD_u level. The ratio of BOD_u/ BOD_5 is used to convert the measured BOD_5 to BOD_u . The accuracy of the ratio is a source of uncertainty in all DO river modelling. However, the procedures used by Alberta Environment to determine these levels and the published reports of MacDonald and Radermacher (1993) serve to allay fears of large errors in the calculation of this ratio. Therefore, although the determination of the ratio is a source of uncertainty in DO modelling, it has been adequately scrutinized for this investigation.

5.6   Calibration

In order to properly assess the validity of the new transport model, the model's parameter set must be properly calibrated to the test environment, the Athabasca River. This usually involves a combination of procedures to determine the correct values for each parameter, ranging from field measurement, to comparison with parameters from other studies, to manipulation of the parameters in the model so that the results best fit observations. Once calibration is completed, the model is ready to be tested against measured data. The goodness of fit between the measured data and the models results then determine its validity.

In this case the calibration of the model to the Athabasca River is a fairly straight-forward process because of the ground covered by prior modelling investigations. The hydraulic parameters used by the model are predetermined from the velocity reversal pattern and the reaeration rate and SOD were determined from field measurement. This leaves only the BOD decay rate to be determined during calibration. However, bottle measurements for this rate are available as a guide. The following discussion describes in detail the calibration procedure for the model.

The total parameter set to be calibrated encompasses seven parameters in all, three directly related to the hydraulic condition of the river while the other four are biochemical rate parameters. Referring to Equations 5.3 and 5.4, the three hydraulic variables are a, the average velocity of flow in the channel reach, b, its amplitude, measured as the difference in velocity between pool and riffle sections, and L, the river distance between adjacent pools. The four rate parameters k, l, n and s are the rates for removal of BOD, decay of BOD, reaeration and SOD, respectively.

The water quality survey conducted by Alberta Environment on February 1-11, 1988 is the period chosen for calibration. The flow in the Athabasca River at this time was 25.1 cms at Hinton, collecting to 51.4 cms at the Town of Athabasca. The Athabasca River was ice covered during this period except for the open water zone, located below the effluent outflow from the pulp and paper mill at Hinton. This lack of reaeration along the majority of the river eliminates a major source of uncertainty in DO modelling, the accurate assessment of the reaeration coefficient. It could reasonably be assumed to be zero for the ice covered sections of the river. This is in line with the reasoning of MacDonald and Hamilton (1988) and Chambers et al. (1996) in their modelling of the Athabasca River. For the 10.5 km open water section below the Weldwood Mill, a reaeration rate of 0.58 day^{-1} at 0°C was used for calibration. This is the same value used by MacDonald and Hamilton (1988) and Chambers et al. (1996). Both of the reaeration values, under ice and open water, were determined from field study by MacDonald et al. (1989).

The hydraulic parameters a and b (Equations 5.3 and 5.4) are governed by the hydraulic geometry pattern of the reach. Once the flow level is known, both of these parameters are determined from the hydraulic geometry graphs presented in Section 5.4. A simple calculator was created in Excel for each reach. For each reach, a flow level could be entered and the average velocity and amplitude of the velocity variation determined and entered into the model.

The average length between pools and riffle sections, L, was calculated using the equation of Leopold and Wolman (1960) presented in Chapter 3. An average low flow channel width of 120 m was used in the calculation. With an average sinuosity of 1.17

for the river, the pool to pool spacing worked out to be approximately 800 m. This

spacing was verified by measuring the meander lengths on random sections of the river

on 1:50,000 NTS map sheets.

The SOD rates, s, used in the calibration of the model are the same as those used

by Chambers et al. (1996). The rate varies from 0.65 day^{-1} immediately downstream of

the Weldwood of Canada plant at Hinton to a low of 0.025 day^{-1} at the McLeod River and

points downstream. Chambers et al. (1996) derived these values from measurements of

SOD along the Athabasca River by Casey and Noton (1989), Casey (1990), Noton (1995)

and HBT AGRA Ltd. (1993 and 1994).

For the calibration, the BOD settlement rate, m, was set to 0.15 day^{-1} at 0°C for

the first 55 km downstream of the pulp and paper mill effluent discharge points. For the

rest of the river, it was assumed that settlement of the BOD was negligible. This

generally agrees with the approaches taken by MacDonald and Hamilton (1988) and

Chambers et al. (1996). They suggest that BOD settlement rate decreases in a linear

fashion in the downstream, the greatest rate of settlement occurring immediately

downstream of the mill's effluent pipe. MacDonald and Hamilton (1988) used a

maximum rate of settlement of 0.15 day^{-1} decreasing to zero at one hundred kilometres

downstream of the effluent source, while Chambers used a maximum settlement rate of

0.574 day^{-1}.

This left only the BOD decay rate, k, to be determined by calibration. MacDonald

and Hamilton (1988) adjusted this parameter in their calibration of the DOSTOC model

to best fit the measured data on the Athabasca. Chambers et al. (1996) used decay rates

determined from bottle tests of effluent in the laboratory. In this calibration, the BOD

decay rate was adjusted, keeping in mind the values used in those prior studies, to best fit

DO levels measured on the Athabasca River. Since BOD decay rate plus BOD

settlement rate *m* add to equal the BOD removal rate, the manipulation of the decay rate

also affects the BOD removal rate.

There are three scenarios that govern the BOD decay rate applied in the model:

1. the background BOD decay and removal rates for river and tributary water

    unaffected by effluent discharges;

2. BOD decay and removal rates for effluent from the two sewage treatment plants;

    and

3. BOD decay and removal rates for the pulp and paper mill effluents discharged to

    the river.

The background BOD decay rate for tributaries and along the main stem of the

river was set to 0.0104 day^{-1}. This rate was coupled to a settling rate of zero, thus the

BOD removal rate for all pristine waters was the same as the BOD decay rate. This is the

same interpretation and rate value used by MacDonald and Hamilton (1989) and

Chambers et al. (1996) in their modelling of the river. The BOD decay and BOD settling

rates for sewage outflows were also set to the same values as the background rates after

Chambers et al. (1996). MacDonald and Hamilton used the calibration exercise to

establish the BOD decay rate for sewage with no settlement.

The setting of the BOD decay rate for mill outflows is basically where the

difference lies between the calibrations of MacDonald and Hamilton (1988) and

Chambers et al. (1996). Chambers et al. (1996) based their BOD decay rates on average

BOD decay rates determined from daily samples of mill effluent collected and analyzed

by Alberta Environment. MacDonald and Hamilton (1989) and also MacDonald and Radermacher (1993) determined the BOD decay rate by varying it during calibration to best fit the measured data. In this calibration, paralleling the MacDonald and Hamilton (1989) approach, the BOD decay rate below the mill outfalls was adjusted to best fit the observed data, while holding all other parameters fixed. The BOD decay rate found to best fit the measured data from the February 1988 water quality survey was 0.07 day^{-1} at 0°C. This rate coupled to a settlement rate of 0.15 day^{-1} at 0°C results in a BOD removal rate of 0.23 day^{-1} at 0°C for the 55 kilometres of river immediately downstream of the mill outfall. For the next 22.5 kilometres, the BOD decay rate is reduced to 0.035 day^{-1} at 0°C, while the settling rate reverts to zero. For the rest of the river, the BOD rate is at a background value of 0.026 day^{-1} at 0°C.
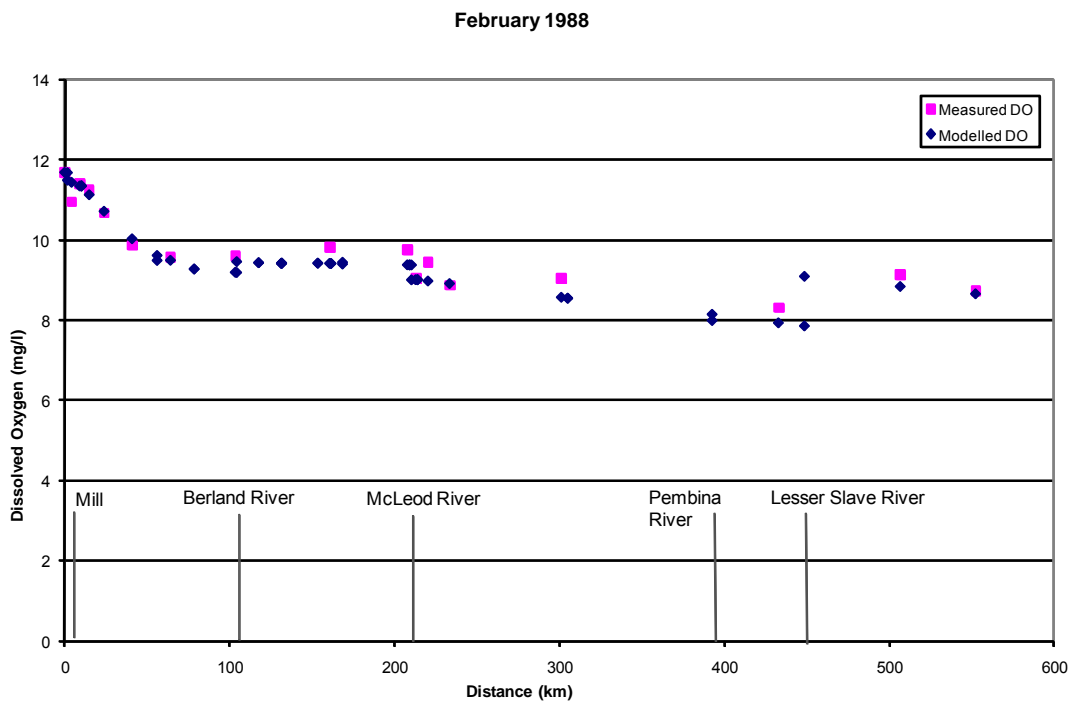
February 1988

Figure 5.9. Comparison of predicted DO levels to sampled DO levels on the Athabasca River for February, 1988 sampling period.

The model structure and layout for both calibration and verification are detailed in Appendix 2.

The results of the calibration of the model are shown in Figure 5.9. As can be seen from the figure, the model results fit the observed DO levels very well. The background DO above the mill is 11.69 mg/l. An oxygen sag is simulated below the Weldwood mill with a low value of 9.19 mg/l occurring just upstream of the Berland River. The flow from the Berland helps somewhat in the recovery of DO in the river to a level of 9.46 mg/l. From the Berland to the Lesser Slave River the DO level declines to 7.85 mg/l, the minimum value experienced along the river. The importance of the flow from the Lesser Slave in increasing DO levels is illustrated by the predicted and observed data, DO rising to 9.0 mg/l. The DO levels decline for the next 100 kilometers to the town of Athabasca where the level is 8.66 mg/l.

The BOD decay rates determined for mill effluent during calibration are now used in the three validation simulations. However, before this final step, a sensitivity and non-dimensional analysis are employed.

5.7   Sensitivity and Non-Dimensional Analysis

To appreciate the sensitivity of each parameter in Equation 5.3 and 5.4, a parameter perturbation analysis is conducted. This analysis was conducted for the 7Q10 flow at

Table 5.1. Value of parameters in Equations 5.3 and 5.4 for a ±25% perturbation.

Perturbation	a (m/s)	b (m/s)	L (m)	k (1/sec)	l (1/sec)	n (1/sec)	s (mg/l/sec)
	0.300	0.15	528	2.55E-06	8.10E-07	6.71E-06	7.52E-06
25%	0.375	0.19	660	3.18E-06	1.01E-06	8.39E-06	9.40E-06
-25%	0.225	0.11	396	1.91E-06	6.08E-07	5.03E-06	5.64E-06

Hinton which is 16 cms. Initial conditions for BOD and oxygen deficit are 22.8 mg/l and 1.51 mg/l, respectively. Four stations – 13202; 26404; 52808 and 105616 metres downstream of the effluent outfall at the Weldwood Mill – were used in the evaluation. The sensitivity analysis basically involves the perturbation of each of the parameters in Equations 5.3 and 5.4 by ± 25% while holding the other parameters constant. The corresponding variation in the state variable, oxygen deficit concentration, reflect the sensitivity of the solution to the parameter varied. This percentage difference in the state variable for a perturbation of ±25% in each parameter is shown in Table 5.2 for the station 105616 m downstream of Weldwood.

The parameter that is most sensitive to the prediction is average velocity, a, while varying S, sediment oxygen demand, and L, the pool and riffle spacing, by plus or minus twenty-five per cent has little or no effect on the prediction. The reaeration parameter, n, is quite sensitive too, a plus or minus 25 per cent perturbation causing a 30 per cent change in the result. However, the aeration value used in the analysis represents the short open-water zones directly downstream of the mill effluent sources. For the ice covered portions, the majority of the river, this parameter is zero. The BOD decay and removal rates are the next most sensitive parameters, while the velocity amplitude, b, also has a significant sensitivity, causing a nine per cent change in the result.

Table 5.2. Results of sensitivity analysis for Station 105616 m.

Perturbation	Oxygen Deficit Concentration (mg/l)						
	a (m/s)	b (m/s)	L (m)	k (1/sec)	l (1/sec)	n (1/sec)	s (mg/l/sec)
25%	1.53	1.08	1.21	1.04	1.49	0.92	1.17
-25%	0.60	1.30	1.21	1.43	0.93	1.67	1.25
Change in Oxygen Deficit Concentration (%)							
± 25% change	-38	9	0	16	-23	30	3

Table 5.3. Non-dimensional analysis for the Athabasca River.

	Q cms	u pool m/s	u riffle m/s	a m/s	b m/s	2b/a	A pool sq. m	A riffle sq. m	Ap/Ar
Reversal	600	2.042	2.066	2.054	0.012	0.01	293.897	290.445	1.0
	100	0.577	0.973	0.775	0.198	0.51	173.361	102.758	1.7
	50	0.354	0.727	0.541	0.187	0.69	141.341	68.746	2.1
	30	0.247	0.587	0.417	0.170	0.82	121.594	51.121	2.4
Calibration	25.1	0.218	0.544	0.381	0.163	0.86	115.371	46.098	2.5
	20	0.185	0.495	0.340	0.155	0.91	107.903	40.409	2.7
7Q10	16	0.158	0.451	0.305	0.146	0.96	101.038	35.505	2.8
	10	0.114	0.370	0.242	0.128	1.06	87.974	27.034	3.3

A point to note here is that a plus or minus 25 per cent perturbation in the parameters is not a realistic assessment of the sensitivity. The values of some of the parameters are known with a high degree of confidence while others are not. Therefore, a 25 per cent perturbation of a parameter that will never vary by 25 per cent does not reflect reality. This is the case for the reaeration coefficient which is zero under ice covered conditions and therefore should not be considered as sensitive at all. The 7Q10 flow on the Athabasca is close to the "rule-of-thumb" criteria for considering the use of the variable velocity model on the river to predict pollutant transport. A non-dimensional analysis, presented in Table 5.3, is used to confirm this suggestion. As can be seen from the table, at the 7Q10 flow level on the Athabasca, the *2b/a* value is close to one, 0.96 to be exact. This suggests that the pool and riffle planform significantly affects transport at this flow level.

5.8   Validation

Using the BOD decay rate and other rates determined from calibration, the variable velocity model was used to simulate DO conditions for the sampling periods of March

1988, January-February 1989 and February-March 1989. During these three periods, the

flow levels at Hinton in the Athabasca were 31.0, 31.1 and 28.0 cms, respectively, while

at Athabasca they were 63.5, 71.7 and 67.3 cms, respectively. These flow levels have

2b/a ratios that are around 0.80, which suggest that the impact of the pool and riffle

planform on transport will be significant.

Another interesting point of note here is that for the 1988 March survey, only the

Weldwood Mill at Hinton was operational and discharging effluent to the Athabasca, but

by the time of the next two sampling periods in 1989, the Miller Western mill at

Whitecourt had started operation and was also discharging effluent to the river. Since

now two mills are operating on the river, the effect of the pool and riffle planform on

transport may well be magnified.
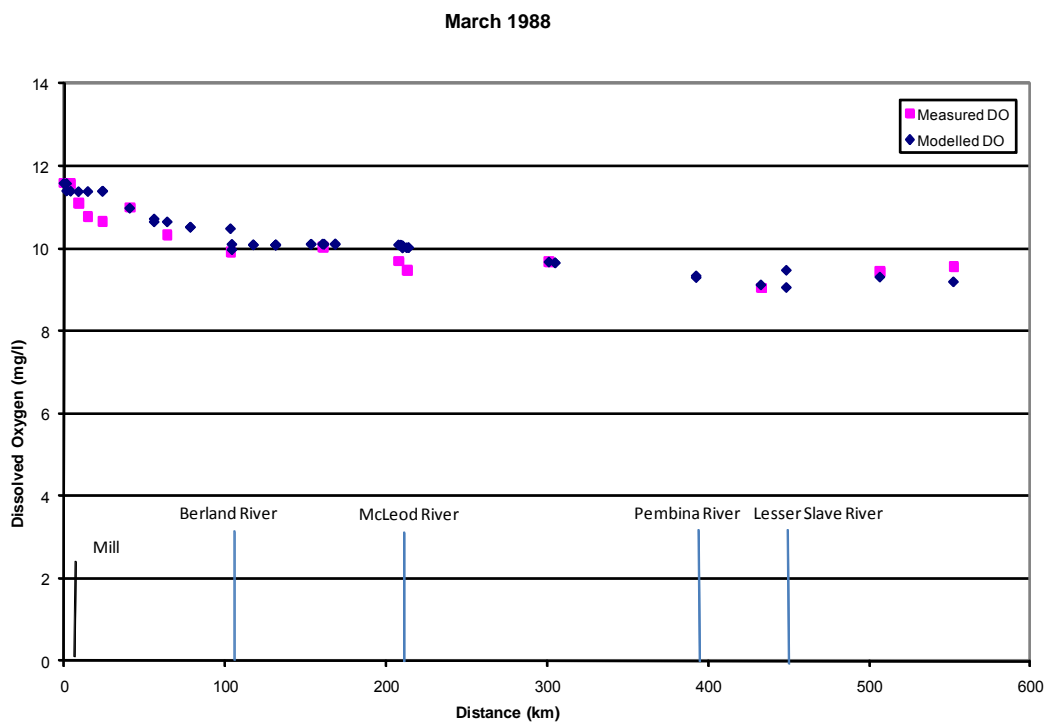
March 1988

***Figure 5.10. Comparison of predicted DO levels to sampled DO levels on the
Athabasca River, March 1988.***

January February 1989
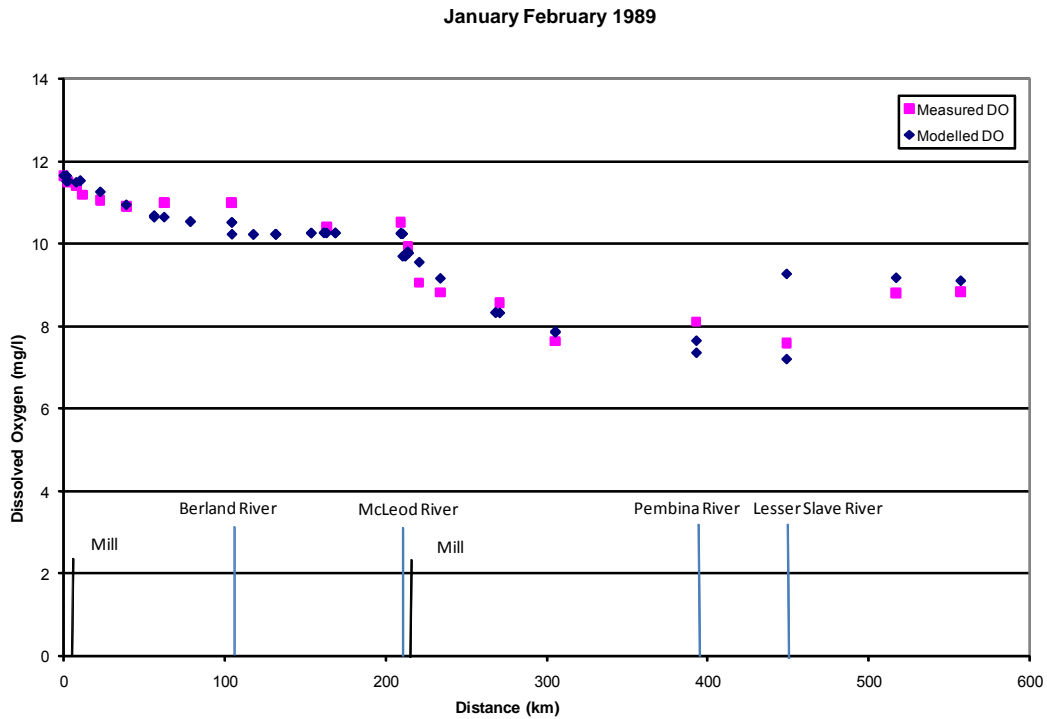
Figure 5.11. Comparison of predicted DO levels to sampled DO levels on the Athabasca River, January-February 1989.

February March 1989
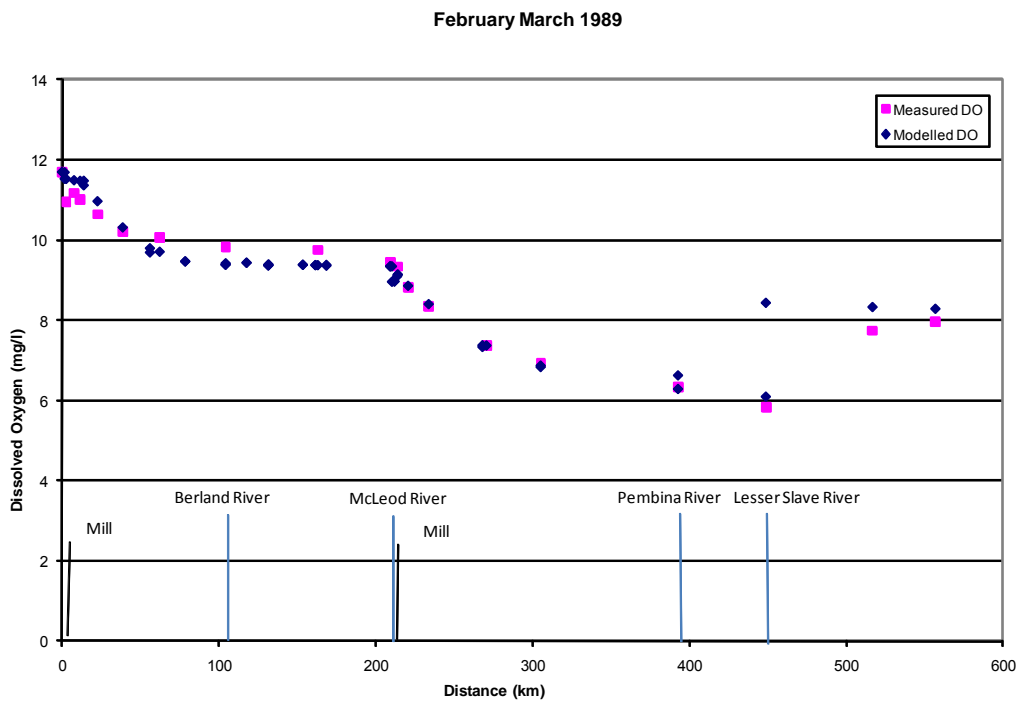
Figure 5.12. Comparison of predicted DO levels to sampled DO levels on the Athabasca River, February-March 1989.

Comparisons of the predictions using the new transport model and the measured DO levels in the river are shown by the graphs in Figures 5.10, 5.11 and 5.12.   A visual inspection of the graphs in Figures 5.10, 5.11 and 5.12 confirms that the predictions from the model fit the measured data for the river almost exactly in all cases. As a matter of fact, the fit is better for the 1989 scenarios which are affected by the discharges from two pulp and paper mills, than for the 1988 scenarios with only one mill operating.

At the confluence of major tributaries and effluent outfalls, the simulation predicts a step up or down in the DO level. These abrupt changes, although explaining the overall trend of the measured data, are not realistic.   The model assumes instantaneous mixing at these confluences, which is not necessarily the case in the river. Mixing would probably occur in a more gradual manner, complete mixing occurring a number of kilometres downstream of the confluence. However, apart from this issue the modeled simulations show a very good fit to the measured DO levels in this 555 kilometre section of the Athabasca River.

The March 1988 survey period shows a DO sag below the Weldwood effluent outfall. DO levels decrease gradually from the tail of the sag downstream to the confluence with the Lesser Slave River at 448.8 km downstream of Hinton. From here to the end a slight oxygen recovery is shown. For the 1989 survey periods, two pronounced DO sags form immediately downstream of the effluent outfalls at the Weldwood and Miller Western mills. Of particular note in Figures 5.11 and 5.12 is the influence of the Lesser Slave River in promoting a recovery in the DO levels in the River. At its confluence, the DO levels jump by slightly more than 2 mg/l.   This is in agreement with the measured data sampled downstream at Athabasca.

More rigorous statistical tests to aid in the assessment of the goodness of fit of the model predictions with the measured data are given by the root mean square (*RMS*):

$$RMS = \sqrt{\frac{1}{n}\sum(DO_{predicted} - DO_{measured})^2} \qquad (5.5)$$

and coefficient of determination (r^2):

$$r^2 = 1 - \frac{\sum(DO_{predicted} - DO_{measured})^2}{\sum(DO_{measured} - DO_{average})^2}. \qquad (5.6)$$

Both of these measures were used by Chambers et al. (1996) to measure the goodness of fit of their results and to contrast their results with the modelling results of MacDonald and Hamilton (1989). Basically, the closer the *RMS* value is to zero, the better the simulation fits the observed data; on the other hand with the r^2, the closer to one the better the fit. Incidentally, the r^2, or Nash Sutcliffe coefficient, is recommended by the ASCE Task Committee on Definition of Criteria for Evaluation of Watershed Models (ASCE, 1993) for continuous hydrograph modelling. It is used here to evaluate DO values instead of flow levels.

Table 5.4 presents the *RMS* and r^2 for the variable velocity model and for the DOSTOC runs of Chambers et al. (1996) and MacDonald and Hamilton (1989) for the four water quality survey periods. Comparison of the *RMS* and r^2 values for the DOSTOC modelling runs by both MacDonald and Hamilton (1989) and Chambers et al.

Table 5.4 Comparison of the root mean square and coefficient of determination for the Variable Velocity Model (VVM) and DOSTOC model simulations on the Athabasca River.

	Feb-88		Mar-88		Jan-Feb 1989		Feb-Mar 1989			
	RMS	r^2	RMS	r^2	RMS	r^2	RMS	r^2	average RMS	average r^2
VVM	0.09	**0.91**	0.09	**0.86**	0.09	**0.95**	0.10	**0.96**	0.09	**0.92**
DOSTOC (1996)	0.62	**0.51**	0.50	**0.53**	0.66	**0.79**	1.06	**0.56**	0.71	**0.60**
DOSTOC (1989)	0.35	**0.85**	0.44	**0.64**	0.09	**0.95**	0.05	**0.98**	0.23	**0.86**

(1996) with the new transport model establishes that the new model's results fit the measured data better than do the DOSTOC predictions. The average r^2 of the four runs using the variable velocity model is 0.92 with an *RMS* of 0.09. This is a very good fit.

Of note here is the very good performance of the model for both 1988 water quality survey periods. Chambers et al. (1996) and MacDonald and Hamilton (1989) had problems simulating these two periods. The new model's consistency of accurate predictions over all four survey periods bodes well for its future use as a predictive tool in water quality investigations.

5.10 Discussion

It is obvious from visual inspection of the graphs and comparison of statistical measures that the new variable velocity model more accurately predicts DO levels on the Athabasca River than does DOSTOC. The over-all goodness of fit, $0.86 \le r^2 \le 0.96$, of the calibration and three simulations prove that the model works correctly in predicting oxygen levels in the Athabasca River. Also, the model predictions are better than those forecast by the DOSTOC model. So then, what is the reason for this good fit? A good place to start looking for the answer to this question is to consider the conclusion and recommendations made by Chambers et al. (1996) to improve water quality modelling on the Athabasca River.

Chambers et al. (1996) point to three factors of the DO modelling on the Athabasca that should be investigated more fully to improve DOSTOC model predictions. First, they suggest that the SOD rates along the river may not be accurate, and thus could be the cause of part of the variance in the DOSTOC model results.

Second, they point out that the hydraulic geometry coefficients, determined from HEC-2 modelling may not be accurate. And third, they also allude to the fact that BOD decay rates for mill effluent, sewage and river water determined from laboratory analysis may not reflect the decay rates active in the Athabasca River.

First of all, the SOD rates used in the proposed Variable Velocity Model are the same as the SOD rates used by Chambers et al. (1996) in their model runs. These SOD rates are based on field measurements by Noton et al. (1995). Sensitivity analysis also establishes that variation in SOD rate does not have a great effect on the model predictions (Table 5.3). The proposed variable velocity model simulations close fit to the observed data suggests that these rates, although they may be in need of some fine tuning, are sound. For these reasons, the SOD rates would seem to accurately reflect the river environment and are not a great source of error in the DOSTOC modelling of the Athabasca River.

The difference in results between both models therefore must lie in the hydraulic interpretation of the Athabasca River, or the BOD decay rates, or some combination of these factors. Chambers et al. (1996) suggest that there may be a problem with the average velocity-discharge curves determined from HEC-2 analysis. They go on to point out that the travel times calculated from these curves do not correspond with the travel times calculated from the only tracer study on the river. There is definitely a marked difference between the HEC-2 calculated average velocity-discharge curves and the patterns determined for use in the variable velocity model, illustrated when one compares the two different sets of curves (Figures 5.2 and 5.8).

Table 5.5. Comparison of travel times calculated from HEC2 velocities and travel velocity u_T.

Distance Downstream of Hinton	50 cms flow		25.1 cms flow		16 cms flow	
	HEC 2 times	V V M times	HEC 2 times	V V M times	HEC 2 times	V V M times
Km	hr	hr	hr	hr	hr	hr
0.0	0.0	0.0	0.0	0.0	0.0	0.0
12.2	6.7	6.7	8.5	9.9	10.0	12.7
39.1	23.8	21.4	30.3	31.6	35.5	40.7
102.8	60.7	56.3	77.1	83.0	90.2	106.9
140.3	80.8	81.0	101.3	119.4	117.4	153.9
204.7	114.8	123.7	143.8	182.4	166.7	235.3
230.0	126.7	148.1	159.1	218.1	184.7	281.1
296.4	170.9	218.0	212.4	320.0	245.0	411.9
340.4	213.4	264.3	264.3	387.5	304.0	498.6
383.8	260.3	309.9	324.0	454.1	374.0	584.1
547.0	417.9	457.3	512.6	663.2	586.0	787.8

A comparison of travel times (Table 5.5) calculated from these different hydraulic interpretations at flow rates of 16 cms, 25.1 cms, and 50 cms confirms the considerable differences in travel time estimates between the two interpretations. The difference between the calculated travel times increases markedly with decreasing flow level. For the 16 cms flow level there is approximately a 200 hour difference in the travel times while at the 50 cms flow level the difference is 40 hours. This much longer residence time calculated by the VVM method, shown as travel velocity u_T in the table, is the cause of the increased decay of BOD and ultimately the lower DO levels estimated by the new model.

An important point to emphasize here is the observation made by Chambers et al. (1996, p.7.3) that states "Better simulations tended to occur in years of higher

114

discharges". This is a particularly insightful comment in light of the travel times and discussion of the theoretical analysis conducted in Chapter 4. The theoretical analysis suggests that as flow level declines the effect of the pool and riffle planform on transport becomes more pronounced, an effect not accounted for in the traditional approach. This is verified by Table 4.2, which shows that as flow level decreases, the differences between the predicted travel times become larger.

The better predictions of DO levels in the Athabasca River by the variable velocity model support the conclusion that travel times calculated from the variable velocity patterns are more accurate than those used by DOSTOC. However, how much of the difference in travel time is due to the average cross-sectional velocity, a, or the travel velocity, u_T? A comparison of travel times is shown in Table 5.6.

Table 5.6. Comparison of travel times calculated by average cross-sectional velocity, a, and travel velocity u_T.

Distance Downstream of Hinton	50 cms flow		25.1 cms flow		16 cms flow	
	a times	V V M times	a times	V V M times	a times	V V M times
Km	hr	hr	hr	hr	hr	hr
0.0	0.0	0.0	0.0	0.0	0.0	0.0
12.2	6.3	6.7	8.9	9.9	11.1	12.7
39.1	20.1	21.4	28.5	31.6	35.7	40.7
102.8	52.8	56.3	74.9	83.0	93.8	106.9
140.3	74.1	81.0	104.1	119.4	123.2	153.9
204.7	110.7	123.7	154.4	182.4	173.5	235.3
230.0	130.3	148.1	180.7	218.1	199.8	281.1
296.4	185.9	218.0	255.0	320.0	274.1	411.9
340.4	222.8	264.3	304.2	387.5	323.3	498.6
383.8	259.2	309.9	352.7	454.1	371.8	584.1
547.0	385.9	457.3	521.7	663.2	542.1	787.8

The important point of note here is that the travel times calculated using just the average velocity, *a*, are close to the travel times calculated using the HEC2 velocities, shown in the preceding table. Both of these tables establish that there is a great difference in travel time between the constant parameter approach to modelling and the variable velocity approach. This difference translates to a slower travel velocity through the pool and riffle channel that is not accounted for by a constant velocity approach. This manifests as a more rapid decrease in DO levels with distance downstream than is shown by the traditional approach.

This analysis clearly establishes that the pool and riffle planform, by setting up a fluctuation in the cross-sectional velocity dynamic, has a significant effect on transport. Importantly, there is a huge difference in travel times at the modelled flow levels on the Athabasca River. This is reflected in the ratio *2b/a*, which for the four periods modelled ranged between 0.86 to 0.91.

Beside the difference in travel times between the variable velocity model and DOSTOC, there is also a difference between the BOD decay rates used by the models. MacDonald and Hamilton (1998) used BOD decay rates for mill effluent, sewage and background river water determined from laboratory analysis at a standard temperature of 20°C. They determined the BOD sedimentation rate during calibration. Chambers et al.

Table 5.7. Flow level ranges and 2b/a ratios for the Athabasca River for the four survey periods.

	Feb-88		Mar-88		Jan-Feb 1989		Feb-Mar 1989	
	Hinton	*Athabasca*	*Hinton*	*Athabasca*	*Hinton*	*Athabasca*	*Hinton*	*Athabasca*
Flow (cms)	*25.00*	*51.00*	*31.00*	*63.50*	*31.10*	*71.70*	*28.00*	*67.30*
Average 2b/a	*0.91*		*0.90*		*0.86*		*0.89*	

(1996) based their BOD decay rates on laboratory analysis of mill effluents, sewages and Athabasca River waters collected and analyzed by Alberta Environment. Their rates were temperature corrected to 0^oC, the temperature of Athabasca River water during the winter survey periods. The BOD decay rate for mill effluent used in the variable velocity model was determined during calibration. Sewage and background rates used in the calibration and validation of the variable velocity model were the same as the rates used by Chambers et al. (1996), corrected to 0^oC. The only difference in rates between Chambers et al.'s (1996) modelling and the variable velocity model is the determination of mill effluent BOD rate. Chambers et al. (1996) use a laboratory determined rate while the rate used by the variable velocity model was determined during calibration.

Chambers et al. (1996) point out that their BOD decay rate for mill effluent, determined from laboratory bottle analysis, may not reflect the rate acting in the river. This observation is not surprising considering the numerous cascading biochemical reactions involved in BOD decay coupled to the difference between stilled bottle and open river environments. Differences in type and density of organisms between the river and mill treatment plant, turbulence, channel shape and roughness, are reasons that Thomman and Mueller (1997) suggest for the difference between bottle and river deoxygenation rates. Furthermore, they point out that the shallower the receiving environment the greater the difference between the rates, although for deep waters the bottle rate is a "useful first approximation to the deoxygenation rate."

In an early study, Wright and MacDonell (1979) suggest that for flows greater than 800 cfs, the bottle rate approaches the river rate. Their regression equation would however calculate a value of 0.41 day^{-1} for the mill effluent decay rate, well above the

0.07 found in this calibration. In a recent study that compares bottle to river BOD decay rates for seven different pulp mill effluents, Corn (2008) concludes that bottle rates never reflect the rate operating in the river, stating that "river deoxygenation rate for BOD cannot be measured in a laboratory BOD test. If bottle rates are used instead of the river rate, Corn goes on to warn that "another rate parameter would have to be adjusted in order to meet the target dissolved oxygen concentration in the river, thereby compounding the inaccuracies of the model." (Corn, 2008, p.2-3).

Considering the above reservations regarding the bottle calculated BOD decay rate, it was deemed a reasonable approach to estimate the BOD decay rate for mill effluent during calibration. Incidentally, it is also the approach used by MacDonald and Hamilton (1988) for determining settling rates on the river. Chambers et al. (1996), however, used the rate determined from laboratory bottle analysis. The BOD decay rate for mill effluent, established during calibration, was the only biochemical rate parameter that differed from the parameters in the DOSTOC model application to the Athabasca River.

The validation exercise clearly demonstrates that the new transport model predicts DO levels accurately along the Athabasca River. It also outperforms the DO modelling of the Athabasca River conducted by Chanbers et al. (1996) and MacDonald and Hamilton (1989) using DOSTOC, a model based on the assumption of a uniform channel shape. The VVM model outperforms the DOSTOC model because the estimates of travel times differ substantially from those of the previous studies. This results in a reduced travel velocity for a substance moving through a pool and riffle channel. It is the accurate estimate of travel time that is responsible for the good predictions of DO levels along the

Athabasca River. Therefore, the velocity reversal pattern, velocity amplitude and travel

velocity that describe the role of the pool and riffle planform on river transport, play a

significant role in accurately modelling DO levels along the Athabasca River.

Chapter 6   Summary and Conclusion

This thesis proposes that transport of pollutants in rivers is affected by the pool and riffle

bedform. The bedform causes a quasi-periodic fluctuation in average velocity along the

river channel. This phenomenon is often cited in the literature as the reason for the failure

of models that assume a uniform channel shape to accurately predict transport in rivers.

A review of the literature in Chapter 2 confirms that there are difficulties with the

application of the constant parameter model. The literature review draws attention to

three issues. They are:

1. the inability to derive a formula that can accurately determine the dispersion

    coefficient for rivers,

2. the spread of a pollutant pulse as it travels downstream does not conform to the Fickian dispersive behavior predicted by the constant parameter model; and

3. time-concentration curves measured from tracer studies have a different shape than those predicted by the constant parameter model.

The underlying reasons for the concerns have a common theme. That is natural channels never meet the required assumption of uniform cross-sectional shape which manifests itself as constant cross-sectional velocity in the transport equation. Instead, meandering river channels, where the pool and riffle bedform is the norm, experience a quasi-rhythmic change in average velocity as flow moves between pool and riffle sections. Many scientists including Aris (1959), Beer and Young (1983), Chapra and Runkel (1999), Day (1975), Day and Wood (1976), Deng et al. (2002), Nordin and Troutman (1980), Pedersen (1977), Singh (2002), Thackston and Schnelle (1970), Thompson et al. (1999), and Valentine and Wood (1977) recognize the role of irregular cross-sections along sinuous channels in influencing the transport mechanics in rivers. It is this irregularity in channel shape that is most commonly cited as the reason for the inability of the constant parameter form of the advection-dispersion equation to model transport in rivers.

Chapter 3 begins with a review of the literature concerning the pool and riffle planform. This review establishes that the pool and riffle sequence is periodic in nature and that it is regarded as the fundamental macro-scale bed-form of rivers irrespective of bed material type. The presence of the sequence is not only reported in streams that flow in their own alluvium, but also in bedrock streams and supraglacial streams.

There are evident physical and hydraulic differences between pools and riffles. During low to average flow stages, riffles are generally wider, about 15% to 30% wider than their counterpart pools. The average cross-sectional area of the riffle is less than that of the adjacent pool. Also, the average velocity in the riffle is greater than in the pool. Bed material is courser in the riffles than in the pools. These differences may influence the transport competence between pools and riffles that are not accounted for in constant parameter water quality models. Accounting for the possible transport differences between pool and riffle is the main goal of this thesis.

Hydraulic geometry relationships are used by water quality models to evaluate average velocity at particular flow levels along a river. A singular averaged relationship between average velocity and discharge is used to characterize a reach's response to flow variation. This approach masks the differences between pool and riffle sections since hydraulic geometry investigations reported in literature also establish that there are differences between the relationships for pool and riffle sections.   Keller (1970) suggested that the different responses were the cause for the stability of the pool and riffle planform over time. This is now known as the velocity reversal hypothesis. The literature on reversal establishes that the differences between the average velocity in a pool and riffle increases as flow level declines. This is important because it is at low flow levels that TMDLs are calculated.

Work presented in Chapter 3 establishes that the reversal pattern occurs on the Assiniboine River. The pattern is different for the two reaches of the Assiniboine examined. From this evidence and analysis of data from other rivers, it is hypothesized that a reversal pattern is not only characteristic of a pool and riffle sequence within a

reach, but that its location and spread when plotted on a log-log graph is a characteristic of the reach's hydraulic condition.

In Chapter 4, the development of a new river transport model starts with the derivation of an equation, based on the velocity reversal pattern, which can describe the variation in average cross-sectional velocity between a pool and riffle. This periodic equation is then incorporated into a mass balance analysis for a representative element of a pool and riffle channel and a new pollutant transport model is developed. This new transport model incorporates the periodic changes in channel cross-sectional shape due to pool and riffle planform in a velocity expression that can be readily ascertained from stream-flow records and surveyed cross-sections. Theoretical analysis, using measured data from the Assiniboine River, suggests that a variable cross-sectional velocity due to pool and riffle planform does have an effect on pollutant transport. It promotes an enhanced decay of contaminant than is not accounted for by an approach that assumes a uniform channel shape. Theoretical analysis in Chapter 4 shows that the enhanced decay is a result of the increased travel time owing to pool and riffle planform that is not predicted by a uniform channel approach. The effect of the pool and riffle on velocity is given by the expression

$$u_T = \sqrt{a^2 - b^2} \ ,$$

where u_T is the travel velocity, a is average cross-sectional velocity and b is the velocity amplitude. This expression can be used to simply modify the traditional uniform flow advection equation to account for a pool and riffle channel. As a matter of fact, a general formula for the calculation of travel velocity is

$$u_T = \frac{QL_p}{V} \ .$$

It is clear that the enhanced decay attributable to a pool and riffle channel is a result of the increase in travel velocity. Furthermore, the enhanced decay becomes more significant as flow in the river declines. Analysis clearly suggests that this fact has important implications for TMDL modelling, since these regulatory limits are usually set at the 7Q10 flow level. The finding of enhanced decay due to the pool and riffle planform of a river and the method described to model the effect add a new dimension to water quality investigations.

In Chapter 5, the new model's predictions are tested against measured data. The validation exercise is based on a 555 kilometre long section of the Athabasca River. In 1988 and 1989, four separate water quality surveys were conducted along the river. These surveys measured BOD and DO levels from Hinton to Athabasca. In order to apply the model to the Athabasca River it was modified to reflect the Streeter Phelps form. After calibrating the model for the February, 1988 water quality survey of the river, the new transport model was used to simulate DO conditions for the three other water quality survey periods: March 1988, January-February 1989 and February-March 1989. The model results are also compared to DOSTOC simulations of Chambers et al. (1996) and MacDonald and Hamilton (1989) for these survey periods. The new variable velocity model not only accurately predicts DO levels along the Athabasca River, but outperforms the modelling of both previous investigations.

Analysis of the results shows that the estimate of the travel times based on the new approach to modelling transport are very different from those of the previous studies. The pool and riffle planform of the Athabasca River causes an increase in travel time which translates to a travel velocity which is lower than the average cross-sectional

velocity. It is this predicted increase in travel time that accounts for the success of the

model in predicting DO levels along the river.

The new model is intuitively simple in architecture, yet complex enough to model

the effect of pool and riffle planform on the transport of pollutants. The analysis clearly

shows that as flow level declines, the effect of the pool and riffle becomes more prevalent

and leads to the enhanced decay of a substance. Non-dimensional analysis suggests it

should be used to assess the transport of pollutants when the cross-sectional area of the

pool is three times the size of the riffle. This commonly occurs when rivers experience

low flows conditions, usually around the 7Q10 level. Therefore, the use of the model is

suggested for TMDL calculations.

6.1   Future Directions

The four DO simulation runs on the Athabasca River have Nash Sutcliffe coefficients of

0.86 or better, suggesting that the model is accounting for more than 86 per cent of the

variation in the DO levels measured in the Athabasca River. This result is achieved by

using a fluctuating advection component with a constant biochemical reaction term.

However, the reaction term in the variable velocity model should also be influenced by

channel geometry of the pool and riffle. For instance, BOD loss rate depends on two

factors: decay and settling. It is obvious that settling rate is influenced by the pool and

riffle planform of the river. Riffles, because of their relatively higher velocities and

shallower depths, would experience a different settling dynamic than that acting in the

pool. Whether this difference in behavior has an effect on oxygen levels will be a future

focus of studies.

A similar effect can also be outlined for reaeration. This study has focused on winter ice cover conditions in the Athabasca River. However, during open water conditions, the effect of the pool and riffle planform on aeration is of interest. How does the structure affect aeration as flow decreases to the 7Q10 level? Certainly there is a dynamic here due to the greater velocities and surface widths in the riffle relative to the pool that may affect aeration. Quantifying this dynamic is also a future focus of study.

Another area of interest is peryphyton growth and nutrient dynamics during the summer months. Peryphton growth is usually restricted to riffles because of their courser beds and shallower depths. Peryphyton absorbs nutrients and there is good evidence on the Assiniboine River to suggest that nutrient concentration downstream of riffles that are colonized by peryphyton is significantly lowered. This phenomenon is difficult to model accurately with QUAL2E because it uses a constant reach velocity approach. The new transport model, adapted to account for nutrient dynamics, may provide insight into this situation. These modifications and applications of the new transport model will form the basis for some interesting future studies.

6.2   Conclusion

This thesis advances the science of water quality modelling by showing that the pool and riffle bedform has a quantifiable effect on transport in rivers. The effect is at a maximum at low flow levels and therefore, it should be taken into account for TMDL calculations.

The literature on river channel morphology establishes that river channels are non-uniform in shape and are dominated by the pool and riffle bedform. The literature on river transport suggests that the role of the pool and riffle may be important in transport

mechanics, but until now the effect of the structure is not accounted for in one-dimensional water quality models, because of the uniform channel assumption. The hydraulic literature establishes that at low flow levels the riffle crest acts as a hydraulic control on the upstream pool, causing a backwater condition. The difference in water surface slopes over the pool and riffle causes a fluctuation in average cross-sectional velocity along the river channel. This fluctuation in turn causes an increased travel time for a substance moving along the channel, which manifests as an increased decay when a first order reaction is modelled.

The effect of a fluctuating average velocity is captured in a new equation that uses a periodic function to simulate the changes in average velocity experienced along pool and riffle sequences.   The equation that describes the average velocity fluctuation due to a pool and riffle planform is incorporated into a mass balance analysis and a new form of the advective transport model derived. The application of this new variable velocity model to the Assiniboine River establishes that the pool and riffle, by causing a periodic variation in average cross-sectional velocity, does have an effect on substance transport. It results in an increase in the travel time of a substance through a pool and riffle channel which results in a travel velocity that is less than the average cross-sectional velocity depending on the severity of the planform. The end result for substance transport in a river is an augmented decay. The decay becomes more pronounced as flow level declines because the influence of the pool and riffle becomes more severe. This effect is not accounted for in a model that assumes a uniform channel.   The ability of the new approach to simulate the increased decay that occurs at low flow levels is important because many TMDL calculations are set at these levels.

In this thesis, the new model is tested on the Athabasca River for four survey periods. The model predicts DO levels on the Athabasca River between Hinton and Athabasca with a high degree of accuracy. Also, the new transport model outperforms DOSTOC, a model based on the traditional assumption of a uniform channel shape.   The consistency of accurate predictions over all four survey periods suggests that the new model works. The effect of the pool and riffle planform on transport, often cited in the literature as a cause for the failure of the uniform channel approach to accurately model transport in rivers, is now accounted for in this new approach to modelling transport. Further research is required to extend the effect of a variable velocity into the biochemical reaction term in the model equation.

The excellent results obtained using the modified Streeter-Phelps form of the model show that this is a valuable new approach to modelling water quality in rivers. Analysis in this thesis suggests that the model should be used when simulating transport at low flow conditions on rivers. The model's simplicity and ease of use suggest it has great promise as a tool for water quality modelling on Canadian rivers, because of the great distances they span, the remoteness of the territory they flow in and the scarcity of hydrologic data.

Literature Cited

Andres, D. and Thompson, J. (1995). "Summary of existing hydraulic and geomorphic data on the Assiniboine River between Winnipeg, Manitoba and Preeceville, Saskatchewan." Trillium Engineering and Hydrographics Inc. Edmonton.

Andrews, E. D. (1979). "Scour and fill in a stream channel, East Fork River, Western Wyoming". *U.S. Geological Survey Prof. Paper* 1117, 49p.

Ashworth, P. J. (1987)."Bedload transport and channel change in gravel bed-rivers". PhD thesis, University of Stirling, UK.

Bathurst. J.C. and Thorne, C.R. (Eds.) Gravel-bed Rivers. Wiley, Chichester. 291-338.

Bansal, M. K. (1971). "Dispersion in natural streams." *Journal of the Hydraulics Division, ASCE,* 97(11), 1867-1886.

Beer, T. and Young, P. C. (1983). "Longitudinal dispersion in natural stream channels." *Journal of the Environmental Engineering Division, ASCE,* 109(5), 1049-1067.

Beltaos, S. and Day, T. J. (1976). "Longitudinal dispersion in a natural stream: Lesser Slave River, Alberta." *Internal Report* No. REH/76/1, *Transportation and Surface Water Engineering Division, Alberta Research Council, Edmonton, Alberta,* 30p.

Beltaos, S. and Day, T. J. (1978). "A field study of longitudinal dispersion." Canadian Journal of Civil Engineering, 5(4), 572-585.

Bencala, K. E. and Walters, R. A. (1983). "Simulation of transient storage in a mountain pool and riffle stream; A transient storage model." *Water Resources Research,* 19, 718-724.

Bencala, K.E., (1983). Simulation of solute transport in a mountain pool and riffle stream with a kinetic mass transfer model for sorbtion." Water resources Research 19(3), 732-738.

Beven, K. and Carling, P.A. (1992). "Velocities, roughness and dispersion in the lowland River Severn." In Carling, P.A. and Petts, G.E. (Eds.), *Lowland floodplain rivers.* Wiley, Chichester. 71-93.

Bhowmik, N.G. and and Demissie, M. (1982a). "Bed Material Sorting in Pools and Riffles". *Journal Hydraulis Division, ASCE,* 108, 1227-1231.

Bhowmik, N.G. and and Demissie, M. (1982b). "Closure". *Journal of the Hydraulics Division, ASCE,* 109, 1245-1247.

Booker, D.J., Sear, D.A. and Payne, A.J. (2001). "Modelling Three-Dimensional Flow Structures and Patterns of Boundary Shear stress in a Natural Pool-Riffle Sequence". *Earth Surface Processes and Landform,s* **26**: 553–576.

Boxall, J.B. and Guymer, I. (2003). "Analysis and prediction of transverse mixing coefficients in natural channels." Journal of Hydraulic Engineering, 129(2), 129-139.

Caamano, D., Goodwin, P., Buffington, J. M., Liou, J.C. and Daly-Laursen, S. (2009). "Unifying Criterion for the velocity reversal hypothesis in gravel-bed rivers." *Journal of Hydraulic Engineering*, 135 (1), 66-70.

Cao, Z., Carling P.A. and Oakey.R. (2002). "Flow reversal over a natural pool-riffle sequence: a computational study." *Earth Surface Processes and Landforms,* 28. 689–705.

Carling, P.A. (1991). "An appraisal of the velocity reversal hypothesis for stable pool/riffle sequences in the River Severn, England". *Earth Surface Processes and Landform,s* **16**: 19–31.

Carling P.A. and Orr H.G. (2000). "Morphology of riffle-pool sequences in the river Severn England." *Earth Surface Processes and Landforms,* 24. 369–384.

Carling P.A. and Wood N. (1994). Simulation of flow over pool-riffle topography: a consideration of the velocity reversal hypothesis. *Earth Surface Processes and Landforms* **19**: 319–332.

Casey, R.J. and Noton, L. R. (1989). "Method Development and Measurement of Sediment Oxygen Demand during the Winter on the Athabasca River." Prepared for the Standards and Approvals Division, Alberta Environment, Edmonton Alberta.

Casey, R.J. (1990). "Sediment Oxygen Demand during the Winter in the Athabasca River and Wapiti-Smoky River, 1990." Prepared for the Standards and Approvals Division, Alberta Environment, Edmonton Alberta.

Chambers, P.A., Pietroniro, A., Scrimgeour, G.J. and Ferguson, M. (1996). "Assessment and Validation of Modelling Under-ice Dissolved Oxygen Using DOSTOC, Athabasca River, 1988 to 1994." *Northern River Basins Study Profect Report #95*, Northern River Basins Study, Edmonton, Alberta.

Chapra, S. C. (1997). Surface water-quality modeling. McGraw-Hill, New York.

Chapra, S. C. and Runkel, R.L. (1999). "Modeling impact of storage zones on stream dissolved oxygen." *Journal of Environmental Engineering*, May 1999, 415-419.

Chatwin, P.C. (1980). "Presentation of longitudinal dispersion data." *Journal of the Hydraulics Division, ASCE,* 106(HY1), 71-83.

Church, M. and Jones, D. (1982). "Channel bars in gravel-bed rivers" In Hey, R.D.,

Clifford, N.J. (1993). "Differential bed sedimentology and the maintenance of riffle-pool sequences." *Catena* 20, 447–468.

Clifford, N.J and Richards K.S. (1992). The reversal hypothesis and the maintenance of pool-riffle sequences: a review and field appraisal. In Carling, P.A. and Petts, G.E. (Eds.), *Lowland floodplain rivers*. Wiley, Chichester. 43-70.

Cooley, M., Schneider-Vieira, F., and Towes, J. (2001). Assiniboine River Monitoring Study Water Quality Component: Water Quality Assessment and Model for the Open Water Season. North/South Consultants Inc. Winnipeg, Manitoba. 156pp.

Corn, M. (2008) "Comparison of CBODu Time Series Bottle Rates with Actual Stream CBODu Deoxygenation Rates." The Aquaeerian, V. 10, 2-3.

Czernuszenko, W. and Rowinksi, P. M. (1997) "Properties of the dead-zone model of longitudinal dispersion in rivers." Journal of Hydraulic Research, 35(4), 491-505.

Elder, J.W. (1954). "The dispersion of marked fluid in turbulent shear flow." *Journal of Fluid Mechanics 5(4),* 544-560.

133

Day, T. J.,(1975). "Longitudinal dispersion in natural channels." *Water Resources Research* 11(6), 909-918.

Deng, Z. Q., Bengtsson, L., Singh, V.P. and Adrian, D. D.(2002). "Longitudinal dispersion coefficient in single-channel streams." *Journal of Hydraulic Engineering* 128(10). 901-916.

Dozier, J. (1974). "Channel adjustments in Supraglacial streams." in Icefield ranges research project, scientific results, v. 4. *Geological Society of America,* 189-205.

Dozier, J. (1976). "An examination of the variance minimization tendencies of a supragalcial stream." *Journal of Hydrology* 31. 359-380.

Elliot, A. H. and Brooks, N. H. (1997). "Transfer of nonsorbing solutes to a streambed with bedforms: Theory." *Water Resources Research* 33(1), 123-136.

Fischer, H. B. (1967). "The mechanics of dispersion in natural streams." *Journal of the Hydraulics Division, ASCE,* 93(6). 187-216.

Fischer, H. B., List, E. J., Koh, R. C., Imberger, J. and Brooks, N. H. (1979). "Mixing in inland and coastal waters". *Academic Press Inc., New York, N.Y.*

Galay, V.J. (1974). "Assiniboine River degradation study." Manitoba Department of Mines, Resources and Environmental Management; *Water Resources Branch Report,* 74-27.

Godfrey, R. G. and Fredrich, B. J. (1970). "Stream dispersion at selected sites." *U.S. Geological Survey, Professional Report* 433-K.

Guymer, I. (1998). Longitudinal dispersion in sinuous channel with changes in shape" *Journal of Hydraulic Engineering,* 124(1). 33-39.

Hack, J.T. (1957). Studies of longitudinal stream profiles in Virginia and Maryland. *U.S. Geological. Survey Prof. Paper* 294-B, 97p.

Halket, I . H. (2003). "Hydraulic characteristics of the upper Assiniboine River in Manitoba." Report submitted to *Manitoba Conservation, Water Quality Division.* 31p.

Harrison, L.W. and Keller, E.A. (2007). "Modeling forced pool-riffle hydraulics in a boulder-bed stream, southern California." *Geomorphology*, 83, 232-248.

Harrison, R. W. (2002). "Assiniboine River bankfull occurrences". Memorandum. Surface Water Management, Manitoba Conservation.

Harvey, J. W. and Bencala, K. E. (1993). "The effect of streambed topography on surface-subsurface water exchange in mountain catchments." *Water Resources Research* 29 (1), 89-98.

Hudson, P. F. (2002). "Pool-Riffle morphology in an actively migrating alluvial channel: The lower Mississippi River". *Physical Geography*, 23 (2), 154-169.

Jackson, W.L. and Beschta. R.L. (1982). "A Model of Two-Phase Bedload Transport in a Oregon Coast Range Stream". *Earth Surface Processes Landform,* 7, 517-527.

Jowett, I.G. (2003). "Hydraulic constraints on habitat suitability for benthic invertebrates in gravel-bed rivers." *River Research and Applications,* 19, 495-507.

Kashefipour, S. E. and Falconer, R. A. (2002). Longitudinal dispersion coefficients in natural channels." *Water Research,* 36, 1596-1608.

Keller E.A. (1970). "Bed load Movement Experiments: Dry Creek, California." *Journal od Sedimentary Petrology,* 40, 1339-1344.

Keller E.A. (1971). "Areal sorting of bed material: the hypothesis of velocity reversal." *Geological Society of America, Bulletin,* 83, 915–918.

Keller E.A. (1972). "Development of alluvial stream channels, a five stage model." *Geological Society of America Bulletin* 83, 1531–1536.

Keller E.A. (1978). "Pools, riffles and channelization" *Environmental Geology* 2, 119-127.

Keller, E.A. and Melhorn, W.N. (1978). "Rhythmic spacing and the origin of pools and riffles." *Geological Society of America Bulletin* 89, 723-730.

Keller E.A, Florsheim J.L. (1993). "Velocity reversal hypothesis: A model approach." *Earth Surface Processes and Landforms* 18, 733–740.

Knighton, D. (1998). "Fluvial forms and processes." Oxford University Press, New York.

Leopold, L.B. and Maddock, T.Jr. (1953). "The hydraulic geometry of streams and some physiographic implications". *U.S. Geological Survey Prof. Paper* 252, 58p.

Leopold, L. B. and Wolman, M.G. (1957). "River channel patterns – Braided, meandering and straight." *U.S. Geological Survey Prof. Paper* 282-B, 85p.

Leopold, L. B. and Wolman, M.G. (1960). "River meanders" *Geological Society of America Bulletin* 71, 769-794.

Leopold, L.B., Wolman, G.M. and Miller, J.P. (1964). "Fluvial processes in geomorphology." Freeman, San Francisco. 522p.

Lisle, T.E. (1979). "A sorting mechanism for a riffle-pool sequence". *Geological Society of America Bulletin* **90**: 1142-1157.

Liu, H. and Cheng, H. D. (1980). Modified fickian model for predicting dispersion, *Journal of the Hydraulics Division, ASCE,* 106(HY6), 1021-1040.

Lowe, S. A. and Groninger, T. J. (2005). "Discussion of 'Estimation of the longitudinal dispersion coefficient using the velocity profile in natural streams' by ll Won Seo and Kyong Oh Baek". Journal of Hydraulic Engineering , 131(10), 927-928.

 MacDonald, G. and Hamilton, H.R. (1989) "Model Calibration and Receiving Water Evaluation for Pulp Mill Developments on the Athabasca River 1. Dissolved Oxygen." Prepared for the Standards and Approvals Division, Alberta Environment, Edmonton Alberta.

MacDonald, G. and Radermacher, A. (1993) "An evaluation of Dissolved Oxygen Modelling of the Atahbasca River and Wapiti Smoky River Systems." Prepared for the Standards and Approvals Division, Alberta Environment, Edmonton Alberta.

MacDonald, G., Holley, E.R. and Goudey, S. (1989). "Athabasca River Winter Reaeration Investigation." Prepared for the Standards and Approvals Division, Alberta Environment, Edmonton Alberta.

McQuivey, R.S. and Keefer, T. N. (1976). Dispersion-Mississippi River below Baton Rouge, La." Journal of the Environmental Engineering Division, ASCE, 102(10), 1425-1437.

Mermillod-Blondin, F., Creuze Des Chatelliers, M., Marmonier, P. and Dole-Olivier, M. J. (2000). "Distribution of solutes, microbes and invertebrates in river sediments along a riffle-pool sequence". *Freshwater Biology* 44, 255-269.

Milan D.J., Heritage, G.L., Large, A.R.G. and Charlton, M.E. (2001). Stage dependent variability in tractive force distribution through a riffle-pool sequence." *Catena* 44, 85-109.

Milne, J.A. (1982). "Bed material size and the pool-riffle sequence." *Sedimentology* 29, 267-287.

Nordin, C. F. and Sabol, G. V.,(1974) "Emperical data on longitudinal dispersion in rivers." U.S. Geological Survey, Water Resource Investigations, 20-74

Nordin, C. K. and Troutman, B.F. (1980). "Longitudinal Dispersion in Rivers: The persistence of skewness in observed data. *Water Resources Research,* 16(1), 123-128.

Noton, L.R. (1995) "Investigations of Streambed Oxygen Demand in the Athabasca River, Fall-Winter1994-1995." Prepared for the Standards and Approvals Division, Alberta Environment, Edmonton Alberta.

Noton, L.R. and Allan, D. (1994) "Oxygen Conditions in the Athabasca River System with emphasis on Winters 1990-93." Prepared for the Standards and Approvals Division, Alberta Environment, Edmonton Alberta.

O'Connor. J.E., Webb, R.H. and Baker, V.R. (1986). "Paleohydrology of Pool-Riffle Pattern Development: Boulder Creek, Utah". *Geological Society of America Bulletin* **97**: 410-420.

Palancar, M. C., Aragon, J. M., Sanchez, F. and Gil, R., (2003). "The determination of longitudinal dispersion coefficients in rivers." *Water Environment Research,* 75(4), 324-335.

Pasternack, G.B., Bourisavong, M.K. and Parikh, K.K. (2008). "Backwater control on riffle-pool hydraulics, fish habitat quality, and sediment transport regime in gravel-bed rivers." *Journal of Hydrology*, 357, 125-139.

Petit. F., (1987). "The Relationship Between Shear Stress and the Shaping of the Bed of a Pebble-Loaded River, La Rulles-Ardenne". *Catena,* 14, 453-468.

Richards, K.S. (1976a). "The morphology of riffle-pool sequences." *Earth Surface Processes* 1, 71-88.

Richards, K.S. (1976b). "Channel width and the riffle-pool sequence." *Geological Society of America Bulletin* 87, 883-890.

Richards, K.S. (1978). "Simulation of flow geometry in a pool-riffle stream." *Earth Surface Processes* 3. 345-354.

Robert, A. (1997). "Characteristics of velocity profiles along riffle-pool sequences and estimates of bed shear stress." *Geomorphology* 19, 89-98.

Runkel, R. L. (1998). One-dimensional transport with inflow and storage (OTIS): A solute transport model for streams and rivers. *Water Resources Investigations Report No. 98-4018.* U.S. Geological Survey, Denver, Colo.

Runkel, R. L., McKnight, D. M., and Andrews, E. D. (1998). "Analysis of transient storage subject to unsteadyflow: diel flow variation in an Antarctic stream." *Journal of the North American Benthological Society*, 17(2), 143-154.

Rutherford, J.E. and MacKay, R.J. (1985). "The vertical distribution of hydropsychid larvae and pupae (Trichoptera: Hydropsychidae) in stream substrates." *Canadian Journal of Zoology*, 63, 1306-1315.

Sawyer, A.M., Pasternack, G.B., Moir, H.J. and Fulton, A.A. (2010). "Riffle-pool maintenance and flow convergence routing observed on a large gravel-bed river." *Geomorphology*, 114, 143-160.

Schmid, B. H. (1995). "On the transient storage equations for longitudinal solute transport in open channels: temporal moments accounting for the effects of first order decay." *Journal of Hydraulic Research*, 33(5), 595-610.

Singh, S. K. (2003). Treatment of stagnant zones in riverine advection-dispersion. *Journal of Hydraulic Engineering, ASCE,* 129(6), 470-473.

Sear, D. A. (1996). "Sediment transport processes in pool–riffle sequences." *Earth Surface Processes and Landforms* 21, 241–262.

Seo, W. I. and Cheong, T. S. (2001) "Moment- based calculation of parameters for the storage zone model for river dispersion." Journal of Hydarulic Engineering 127(6), 453-465.

Seo, W. I. and Baek, K. O. (2004), "Estimation of the longitudinal dispersion coefficient using the velocity profile in natural streams." Journal of Hydraulic Engineering, 130(3), 227-336.

Shepherd, R.G. and Schumm, S.A. (1974). "Experimental study of river incision". *Geological Society of America Bulletin* 85, 257-268.

Stefan, H. G. and Demetrapolous, A. C. (1981). Cell-in –series simulation of riverine transport." *Journal of the Hydraulics Division, ASCE,* 107(6), 675-697.

Taylor, G.I.(1954). "The dispersion of matter in turbulent flow through a pipe." *Proceedings Royal Society of London. Ser.A. 219,* 186-203.

Teissyre, A.K. (1984). "The River Bobr in the Blazkowa study reach (central Sudetes): a case study in fluvial processes and sedimentology." Geologia Sudetica 19(1), 7-71.

Thackston, E. L. and Schnelle, K. B. (1970). "Predicting effects of dead zones on stream mixing." *Journal of the Sanitary Engineering Division, ASCE,* 96(SA2), 319-331.

Thomman, R. V. and Mueller, J. A. (1997) 'Principals of Surface Water Quality Modeling and Control.". Prentice Hall, 656 pp.

Thompson, D.M. (2000). "Random controls on semi-rhythmic spacing of pools and riffles in constriction-dominated rivers". *Earth Surface Processes and Landforms* 26, 1195-1212.

Thompson, D.M., Wohl, E.E. (2009). "The linkage between velocity patterns and sediment entrainment in a forced-pool and riffle unit. *Earth Surface Processes and Landforms*, 34, 177-192.

Thompson, D.M., Wohl, E.E. and Jarret, R.D. (1999). "Velocity reversals and sediment sorting in pools and riffles controlled by channel constrictions". *Geomorphology* 27, 229-241.

Thompson, M.V. and Fitch, M. (1989). "Athabasca River Update of Hydraulic Parameters for Water Quality Modelling." Prepared for the Standards and Approvals Division, Alberta Environment, Edmonton Alberta.

Toprak, Z. F. and Savci, M. E. (2007). "Longitudinal Dispersion Coefficient Modeling in Natural Channels using Fuzzy Logic." Clean, 35(6), 626-637.

Trevor, B., Thompson, J. and Andres, D. (1988) "Low Flow Hydraulic Characteristics of the Athabasca River, Hinton to Athabasca" Alberta Research Council Report No. SWE-88/13, Edmonton, Alberta.

Valentine E. M. and Wood, I. R, (1977), "Longitudinal dispersion with dead zones." *Journal of the Hydraulics Division, ASCE,* 103(HY9), 975-990.

Valentine E. M. and Wood, I. R, (1979), "Experiments in longitudinal dispersion with dead zones." *Journal of the Hydraulics Division, ASCE,* 105(HY8), 999-1016.

Ward, J.V., Bretschko, G., Brunke, M., Danielopol, D., Gibert, J., Gonser, T. and Hildrew, A.G. (1998). "The boundaries of river systems: the metazoan perspective. *Freshwater Biology* 40, 531-569.

Wohl, E. and Legleiter, C.J. (2003). "Controls on pool characteristics along a resistant-boundary channel". *Journal of Geology 111*, 103-114.

Worman,A. (2000). "Comparison of models for transient storage of solutes in small streams." Water Resources Research, 36(2), 455-468.

Yalin, M.S. (1971). "On the formation of dunes and meanders" *International Association Hydraulic Research, 14th Congress, Paris, Proceedings* 3, paper C13, 1-8.

Yang C.T. (1971). Formation of riffles and pools." Water Resources Research 7, 1567-1574.

Yotsukura, N., Fischer, H. B. and Sayre, W.W. (1970). "Measurement of mixing characteristics of the Missouri River between Sioux City, Iowa and Plattsmouth, Nebrasksa." U.S. Geological Survey, Water Supply Paper 1989G, 29p.

Zand, S. M., Kennedy, G. W., Zellwweger, G.W. and Avanzino, R. J. (1976). "Solute transport and modeling of water quality in a small stream." Journal of Research, U.S. Geological Survey 4(2), 233-240.

APPENDIX 1   Description of Model Structure

The model is based on the Equations 5.3 and 5.4, the Streeter-Phelps form of the new

transport model. These equations describe the interplay of the major sources and sinks of

oxygen in a river coupled to the transport of DO and BOD: the consumption of DO by

the decay of organic matter in the water and river-bed and replenishment of oxygen from

the atmosphere.

The simulation uses an Excel worksheet to order the data while the simultaneous

calculations of BOD and DO are computed in Maple 11 using the Ordinary Differential

Equation Analyzer. The simulation works in the following fashion. Initial conditions are

entered first. These are the initial flow and BOD and DO levels. Values for the coefficients that describe the reach conditions are also entered. These are average velocity and velocity amplitude and the rate coefficients. The model calculates the BOD and DO levels for points of interest downstream. Where a new point source load or tributary is encountered, the model re-calculates new mixed initial BOD and DO levels for that point. If required, new hydraulic geometry and rate coefficients are entered. The model then runs under these conditions until another point source, new reach or change in rate coefficients is encountered. All input data, BOD and DO simulation results, as well as the BOD and DO levels measured during the survey periods are shown in the four Excel files of Appendix 1. The following section provides a general description of the structure of these files.

Much of the preliminary modelling work needed to calibrate and validate the model was completed by MacDonald and Hamilton (1989). Especially pertinent to this study, they constructed the river distance framework for the simulation runs. This framework, also adopted by Chambers et al. (1996) in their modelling of the river, describes in kilometres downstream of Hinton the location of points of interest to the modelling such as mill and town effluent discharge points, tributary confluences and open water zones. Incidentally, the length of these open water zones encountered below the mill effluent outfalls was determined by MacDonald and Hamilton (1988) from aerial photographs.

All river distances are listed in kilometres and measured to the nearest hundred metres. River distances that have two decimal places are used as markers. They show where the simulation ends for a section governed by one set of parameters and a new

section starts under new initial conditions and, if required, a new set of parameters. The

BOD_u and DO levels at the end of a section, recorded at the two decimal place station,

are used in the computation of the initial conditions for the next section. A mass balance

approach which assumes instantaneous mixing across the channel is used to calculate the

new initial condition. For example, the model is run under an initial set of parameters

from Hinton to the 1.7 km mark, where the effluent from the Weldwood Mill discharges

to the river. The BOD_u and DO levels at the end of the 1.7 km section, before the

effluent is encountered, are entered into the 1.69 km station. The effluent and main

channel conditions are mixed and new initial levels for the next reach entered in the

appropriate cells at the 1.7 km station. The model is run for this next section until the

10.2 km mark where open water now changes to ice cover.

Columns C and D detail the hydraulic conditions along the river for the particular

time frame. Column C shows the flow in the main channel and column D shows the

incoming flow from tributaries and point sources. These flow levels are the same as the

ones used by Chambers et al. (1996) and differ from the flow levels used by MacDonald

and Hamilton (1989). Basically, Chambers et al., using measurements of the small

tributary flows obtained after MacDonald and Hamilton's work was completed, were able

to more accurately assess the flow levels along the river for the periods of record.

Columns E, F and G list the measured water quality data along the river. The

BOD_u loads contributed by industrial/municipal point sources are listed in Column E.

The BOD_u loads contributed from tributaries are listed in Column F. All of the loadings

are entered at the beginning of the section that they pour into. These loading values are

the same as those used by MacDonald and Hamilton (1989) and Chambers et al. (1996)

and were measured and calculated by Alberta Environment. In all cases, BOD_5 levels were measured by Alberta Environment and the procedures for the conversion of the BOD_5 to BOD_u are discussed by MacDonald and Radermacher (1993) and Chambers et al. (1996). DO concentrations for all sources contributing to the main flow are listed in Column G. Some BOD_u and DO measurements were not available for some of the minor tributaries for various reasons. Where this occurs, historical mean values have replaced the missing data. These BOD_u and DO levels are taken from Chambers et al. (1996).

Columns H to T list the reaction rate constants. These rate constants are entered at the beginning of the section and remain constant until a new condition is encountered. The rate constants are corrected to a river temperature of $0^{o}C$ and converted to sec^{-1} units for computational purposes. The rate for pulp and paper mill and sewage treatment plant effluent BOD decay is shown in Columns H, I and J and the rate for BOD decay in tributary inflows is shown in Columns L, M and N. These columns show the rate constants at $20^{o}C$, and $0^{o}C$ with units of day^{-1} and sec^{-1}. The BOD decay rates for mill effluent were measured by Alberta Environment and the Mill in question. There is some discrepancy between the values reported by each agency, and a good discussion of this issue is given in Chambers et al. (1996). The BOD removal rate (the sum of decay and settling) for effluent discharges is shown in Column K while the settling rate of BOD from these sources is shown in Columns Q and R. Tributaries loads are considered to have no settle-able fraction and therefore their removal rate is equal to the decay rate. For more discussion on this point, see MacDonald and Hamilton (1988).

The reaeration rate for open water and under-ice conditions are shown in Columns O and P. For under ice conditions, reaeration is considered to be zero, while for the open water zones downstream of mill discharge points, a value of 0.58 day^{-1} at 0°C is used.

Column T lists the SOD values used in the model. These are the values used by Chambers et al. (1996) and are derived from multiple investigations of SOD along the Athabasca River by Casey and Noton (1989), Casey (1990), Noton (1995) and HBT AGRA Ltd. (1993 and 1994).

Columns U and V list the initial conditions for BOD$_u$ and DO levels upstream of Hinton. Column W lists the saturation level for dissolved oxygen along the Athabasca River. Note that the values increase downstream as the river descends towards the town of Athabasca.

Columns X, Y and Z are used to enter the parameters for the variable velocity equation (Eq. 4.2) Column X is reserved for average distance between pools (L). Column Y is the average cross-sectional velocity of the pool and riffle sequence (a), while column Z lists the velocity amplitude (b).

Columns AA, AB, and AC list the results of the simulation. AA is the predicted BOD$_u$ level, while AB is the predicted oxygen deficit and BC the DO level.

Appendix 2

The following four Excel spreadsheets contain the detailed model structure and

calculations.

Using MacDonald's river distances. Flows from Chambers. Chambers BODu and DO. Rates from Chambers + two rate model for decay of mill effluent

A	B	C	D	E	F	G	H	I	J	K	L	M	N	O	P	Q	R	S	T	U	V	W	X	Y	Z	AA	AB	AC	AD	AE
February 1-11				**1988** Inputs			**Rates**													**Headwater Initial**						**Variable Velocity Model**			**Samples**	

Column headers:
- A: Name or description notes
- B: Distance d/s
- C: River Flow cms
- D: Tributary/ Point Source inflows cms
- E: Point Source BODu (XLD1) mg/l — chamber's values
- F: Tributary BODu (XLD3) mg/l
- G: Point Source and Tributary DO (XLD2) mg/l
- H: Point Source BOD decay 1/day @20C (XK1)
- I: Point Source BOD decay 1/day @0C
- J: Point Source BOD decay 1/sec @0C
- K: BOD removal rate 1/sec
- L: BOD decay rate for tributaries 1/day @20c (XK4)
- M: BOD decay rate for tributaries 1/day @0c
- N: BOD decay rate for tributaries @0c 1/sec
- O: Reaeration 1/day @0C (XK2)
- P: Reaeration 1/sec @0C
- Q: BOD settling rate @0c 1/day (XK3)
- R: BOD settling rate @0c 1/sec (XK3)
- S: SOD @0c 1/day XRES
- T: SOD @0c 1/sec XRES
- U: BOD u (XO3)
- V: DO (XO2)
- W: O sat (XDS)
- X: pool to pool spacing sinuosity*5.4w^ 1.01 (m)
- Y: Average velocity (a) (in m/s)
- Z: Velocity Amplitude (b) (m/s)
- AA: BOD result
- AB: D result
- AC: DO result
- AD: Distance d/s
- AE:

Name	Dist	Flow	Inflow	XLD1	XLD3	XLD2	XK1	@0C	@0C	Kremove	XK4	M	N	XK2	P	XK3d	XK3s	XRESd	XRESs	XO3	XO2	XDS	spacing	vel	amp	BOD	D	DO	Dist	AE
Hinton	0	25.1								1.2E-07	0.026	0.010376	1.20095E-07	0	0	0	0		0	13.89	11.69	13	528.080959	0.381	0.163	13.890	1.310	11.690	0	11.69
	1	25.1									0.026											13							1	
	1.69	25.1																				13				13.882	1.318	11.682	1.69	
Weldwood	1.7	24.176	0.924	255		6.3		0.07	8.1E-07	2.55E-06				0.58	6.71E-06	0.15	1.74E-06	0.65	7.52E-06			13.01				22.758	1.516	11.494	1.7	
open water	5	25.1																				13.015	8.5 km open water				1.574	11.441	4.2	10.95
																						13.015							5	
																						13.02					1.670	11.350	9.1	11.41
open water	10																					13.02							10	
open water	10.19																					13.03				21.195	1.689	11.342	10.19	
ice cover	10.2													0	0							13.03				21.369	1.672	11.358	10.2	
	15																					13.035				20.535	1.905	11.131	14.9	11.25
	20																					13.04							20	
	25																					13.045				19.024	2.323	10.717	23.9	10.67
	30																					13.05							30	
	35																					13.055							35	
	40																					13.06				16.434	3.029	10.031	40.9	9.87
	45																					13.065							45	
	50																					13.07							50	
	55																					13.07				14.369	3.580	9.490	55	
	56.09				note: value note: o																	13.07				14.369	3.580	9.490	56.09	
Old Man Creek	56.1	25.1	0.908		chambers saturation 20.87	13.07		0.035	4.05E-07	4.05E-07					0	0	0	0.118	1.37E-06			13.07				14.595	3.455	9.615	56.1	
	60	26.008																				13.078							60	
	65																					13.086				14.426	3.592	9.494	64.2	9.575
	70																					13.094							70	
	75																					13.102							75	
	78.59				from point source to background - maybe is fast a decline																	13.11				14.126	3.835	9.275	78.59	
Spring 1	78.6	26.008	0.022		8.03	11.59		0	0		1.20095E-07				0	0	0	0.098	1.13E-06			13.11				14.121	3.833	9.277	78.6	
	80	26.03																											80	
	85																												85	
	90																												90	
	95																												95	
	100																					13.15				13.915	3.956	9.194	103.5	9.596
	104.39																					13.15				13.907	3.961	9.189	104.39	
Berland River	104.4	26.03	6.43		11.24	10.56					1.20095E-07				0	0	0	0.084	9.72E-07			13.15		0.473	0.164	13.378	3.689	9.461	104.4	
	105	32.46																											105	
	110																												110	
	115																												115	
	117.69																					13.17				13.301	3.737	9.433	117.69	
Spring 2	117.7	32.46	0.018		4.58	11.86					1.20095E-07				0	0	0	0.095	1.1E-06			13.17				13.296	3.735	9.435	117.7	
	120	32.478																											120	
	125																												125	
	130																												130	
	131.49																					13.2				13.213	3.784	9.416	131.49	
Marsh Creek	131.5	32.478	0.225		4.58	11.86					1.20095E-07							0.081	9.38E-07			13.2				13.153	3.784	9.416	131.5	
	131.69	32.703																				13.2				13.152	3.785	9.415	131.69	
Pine Creek	131.7	32.703	0.165		4.66	11.85					1.20095E-07							0.081	9.38E-07			13.2				13.109	3.772	9.428	131.7	
	135	32.868																											135	
	140																												140	
	145																												145	
	150																												150	
	153.59																					13.27				12.986	3.849	9.421	153.59	
Spring 3	153.6	32.868	0.018		3.21	11.3					1.20095E-07							0.059	6.83E-07			13.27				12.981	3.848	9.422	153.6	
	155	32.886																											155	
	160																					13.29				12.945	3.873	9.417	160.7	9.81
	161.59																					13.29				12.941	3.876	9.414	161.59	
Two Creek	161.6	32.886	0.012		7.63	9.07					1.20095E-07							0.042	4.86E-07			13.29				12.939	3.876	9.414	161.6	
	165	32.898																											165	
	168.59																					13.3				12.907	3.900	9.400	168.59	
Windfall	168.6	32.898	0.49		5.62	12.51					1.20095E-07							0.025	2.89E-07			13.3				12.800	3.855	9.445	168.6	
	170	33.388																											170	
	175																												175	
	200																					13.37				12.640	3.990	9.380	207.9	9.75
	209.29																					13.37				12.634	3.994	9.376	209.29	
Sakwatamau Riv	209.3	33.388	0.923		3.61	9.57					1.20095E-07							0.025	2.89E-07			13.37				12.391	3.989	9.381	209.3	
	210.39	34.311																				13.37				12.387	3.993	9.377	210.39	
McLeod River	210.4	34.311	3.68		7.79	5.54					1.20095E-07							0.025	2.89E-07			13.37		0.295	0.188	11.941	4.364	9.006	210.4	
	211.99	37.991																											211.99	
Miller West	212	37.991																				13.39				11.922	4.380	9.010	212.9	9.046
open water	214.09																					13.4				11.913	4.387	9.013	214.09	
White STP	214.1	37.931	0.06	99.84		5.1												0.025				13.4				12.052	4.393	9.007	214.1	
	225	37.991																				13.41				12.004	4.433	8.977	220.4	9.456
	235																					13.43				11.904	4.516	8.914	233.5	8.873
	250																												250	
	275																												275	
	300																					13.5				11.405	4.930	8.571	301.3	9.046
	305.19																					13.5				11.377	4.953	8.547	305.19	
Freeman River	305.2	37.991	0.118		8.03	8.65					1.20095E-07											13.5				11.366	4.953	8.547	305.2	
	350	38.109																											349.3	
	392.79																					13.61				10.743	5.465	8.145	392.79	
Pembina River	392.8	38.109	1.02		8.83	2.21																13.61				10.693	5.619	7.991	392.8	
	400	39.129																				13.62				10.419	5.688	7.932	433	8.31
	448.79																					13.63				10.312	5.775	7.855	448.79	
Lesser Slave Riv	448.8	39.129	12.3		22.48	13.03																13.63		0.38	0.154	13.222	4.537	9.093	448.8	
	500	51.429																				13.64				12.910	4.800	8.840	506.9	9.13
u/s of Athabasca	600	51.429																				13.66				12.670	5.003	8.657	552.6	8.737

Using MacDonald's river distances. Flows from Chambers. Chambers BODu and DO. Rates from Chambers + two rate model for decay of mill effluent

A	B	C	D	E	F	G	H	I	J	K	L	M	N	O	P	Q	R	S	T	U	V	W	X	Y	Z	AA	AB	AC	AD	AE
	March 4-9			**1988** Inputs			Rates													Headwater Initial						Variable Velocity Model			Samples	
Name or description notes	Distance d/s	River Flow cms	Tributary/ Point Source inflows cms	Point Source BODu (XLD1) chamber's values	Tributary BODu (XLD3)	Point Source and Tributary DO (XLD2)	Point Source BOD decay 1/day @20C (XK1)	Point Source BOD decay 1/day @0C	Point Source BOD decay 1/sec @0C	BOD removal rate 1/sec	BOD decay rate for tributaries 1/day @20c (XK4)	BOD decay rate for tributaries 1/day @0c	BOD decay rate for tributaries 1/day @0c 1/sec	Reaeration 1/day @0C (XK2)	Reaeration 1/sec @0C	BOD settling rate @0c 1/day (XK3)	BOD settling rate @0c 1/sec (XK3)	SOD @0c 1/day XRES	SOD @0c 1/sec XRES	BOD u (XO3)	DO (XO2)	O sat (XDS)	pool to pool spacing sinuosity*5.4w^ 1.01 (m)	Average velocity (a) (in m/s)	Velocity Amplitude (b) (m/s)	BOD result	D result	DO result	Distance d/s	
headwater	0	31						0.026	0.010376	1.2E-07	0.026	0.010376	1.20095E-07	0	0	0	0		0	12.05	11.59	13	800	0.424	0.171	12.05	1.410	11.59	0	11.59
	1	31							0.026													13							1	
	1.69	31																				13				12.050	1.416	11.584	1.69	
Weldwood	1.7	30.026	0.974	127.8		5.6		0.07	8.1E-07	2.55E-06				0.58	6.71E-06	0.15	1.74E-06	0.65	7.52E-06			13.01				15.687	1.605	11.405	1.7	
	4.2																					13.015				15.388	1.616	11.399	4.2	11.58
open water	5	31																				13.015	22.5 km open water						5	
	9.1																					13.02				14.810	1.633	11.387	9.1	11.105
open water	10																					13.02							10	
	10.19																					13.03							10.19	
	10.2																					13.03							10.2	
	14.9																					13.035				14.140	1.644	11.391	14.9	10.78
	20																					13.04							20	
open water	23.9																					13.045				13.155	1.644	11.396	23.9	10.665
ice cover	24.2													0	0							13.05				13.132	1.644	11.401	24.2	
	35																					13.055							35	
	40																					13.06				11.459	2.073	10.987	40.9	11
	45																					13.065							45	
	50																					13.07							50	
	55																					13.07							55	
	56.09																					13.07				10.092	2.414	10.656	56.09	
Old Man Creek	56.1	31	1.33	17.67	12.38		0.035	4.05E-07	4.05E-07							0	0	0	0.118	1.37E-06		13.07				10.403	2.343	10.727	56.1	
	60	32.33																				13.078							60	
	65																					13.086				10.288	2.430	10.656	64.2	10.325
	70																					13.094							70	
	75																					13.102							75	
	78.59					from point source to background - maybe to fast a decline																13.11				10.084	2.583	10.527	78.59	
Spring 1	78.6	32.33	0.022	8.43	11.59			1.2E-07	1.2E-07			1.20095E-07				0	0	0	0.098	1.13E-06		13.11				10.082	2.582	10.528	78.6	
	80	32.352																											80	
	85																												85	
	90																												90	
	95																												95	
	100																					13.15				9.931	2.660	10.490	103.5	9.92
	104.39																					13.15				9.331	3.169	9.981	104.39	
Berland River	104.4	32.352	7.69	9.64	10.66							1.20095E-07				0	0	0	0.084	9.72E-07		13.15		0.473	0.164	9.390	3.039	10.111	104.4	
	105	40.042																											105	
	110																												110	
	115																												115	
	117.69																					13.17				9.328	3.072	10.098	117.69	
Spring 2	117.7	40.042	0.018	4.58	11.86							1.20095E-07				0	0	0	0.095	1.1E-06		13.17				9.326	3.071	10.099	117.7	
	120	40.06																											120	
	125																												125	
	130																												130	
	131.49																					13.2				9.257	3.106	10.094	131.49	
Marsh Creek	131.5	40.06	0.225	4.66	11.85							1.20095E-07							0.081	9.38E-07		13.2				9.231	3.106	10.094	131.5	
	131.69	40.285																				13.2				9.230	3.106	10.094	131.69	
Pine Creek	131.7	40.285	0.165	3.21	11.3							1.20095E-07							0.081	9.38E-07		13.2				9.206	3.101	10.099	131.7	
	135	40.45																											135	
	140																												140	
	145																												145	
	150																												150	
	153.59																					13.27				9.097	3.156	10.114	153.59	
Spring 3	153.6	40.45	0.018	3.21	11.02							1.20095E-07							0.059	6.83E-07		13.27				9.094	3.155	10.115	153.6	
	155	40.468																											155	
	160																					13.29				9.066	3.172	10.118	160.7	10.035
	161.59																					13.29				9.062	3.175	10.115	161.59	
Two Creek	161.6	40.468	0.012	7.63	9.7							1.20095E-07							0.042	4.86E-07		13.29				9.062	3.175	10.115	161.6	
	165	40.48																											165	
	168.59																					13.3				9.037	3.192	10.108	168.59	
Windfall	168.6	40.48	0.479	16.06	11.47							1.20095E-07							0.025	2.89E-07		13.3				9.119	3.176	10.124	168.6	
	170	40.959																											170	
	175																												175	
	200																					13.37				8.997	3.273	10.097	207.9	9.69
	209.29																					13.37				8.992	3.276	10.094	209.29	
Sakwatamau Riv	209.3	40.959	0.923	3.61	9.57							1.20095E-07							0.025	2.89E-07		13.37				8.874	3.288	10.082	209.3	
	210.39	41.882																				13.37				8.871	3.291	10.079	210.39	
McLeod River	210.4	41.882	7.5	16.06	9.71							1.20095E-07							0.025	2.89E-07		13.37		0.295	0.188	9.963	3.347	10.023	210.4	
	211.99	49.382																											211.99	
Miller West	212	49.382																				13.39				9.946	3.361	10.029	212.9	9.47
open water	214.09	49.382																				13.4				9.938	3.367	10.033	214.09	
White STP	214.1	49.345	0.037	99.84		5.1													0.025			13.4				10.006	3.370	10.030	214.1	
	225	49.382																				13.41							220.4	
	235																					13.43							233.5	
	250																												250	
	275																												275	
	300																					13.5				9.447	3.818	9.682	301.3	9.67
	305.19																					13.5				9.423	3.837	9.663	305.19	
Freeman River	305.2	49.382	0.151	11.24	8.98							1.20095E-07										13.5				9.428	3.839	9.661	305.2	
	350	49.533																											349.3	
	392.79																					13.61				8.892	4.263	9.347	392.79	
Pembina River	392.8	49.533	1.37	12.05	7.81							1.20095E-07										13.61				8.977	4.304	9.306	392.8	
	400	50.903																				13.62				8.738	4.492	9.128	433	9.046
	448.79																					13.63				8.645	4.565	9.065	448.79	
Lesser Slave Riv	448.8	50.903	12.6	9.64	11.17																	13.63		0.38	0.154	8.842	4.147	9.483	448.8	
	500	63.503																				13.64				8.618	4.322	9.318	506.9	9.45
u/s of Athabasca	600	63.503																				13.66				8.445	4.457	9.203	552.6	9.556

note: value note: o chambers saturation

Using MacDonald's river distances. Flows from Chambers. Chambers BODu and DO. Rates from Chambers + two rate model for decay of mill effluent.

9 January 15 February 1989 Inputs — **Rates** — **Headwater Initial** — **Variable Velocity Model** — **Samples**

Column legend:
- A: Name or description notes
- B: Distance d/s
- C: River Flow cms
- D: Tributary/Point Source inflows cms
- E: Point Source BODu (XLD1) chamber's values
- F: Tributary BODu (XLD3)
- G: Point Source and Tributary DO (XLD2)
- H: Point Source BOD decay 1/day @20C (XK1)
- I: Point Source BOD decay 1/day @0C
- J: Point Source BOD decay 1/sec @0C
- K: BOD removal rate 1/sec
- L: BOD decay rate for tributaries 1/day @20c (XK4)
- M: BOD decay rate for tributaries 1/day @0c
- N: BOD decay rate for tributaries 1/sec
- O: Reaeration 1/day @0C (XK2)
- P: Reaeration 1/sec @0C
- Q: BOD settling rate @0c 1/day (XK3)
- R: BOD settling rate @0c 1/sec (XK3)
- S: SOD @0c 1/day XRES
- T: SOD @0c 1/sec XRES
- U: BOD u (XO4)
- V: DO (XO3)
- W: O sat (XDS)
- X: pool to pool spacing sinuosity*5.4w^1.01 (m)
- Y: Average velocity (a) (in m/s)
- Z: Velocity Amplitude (b) (m/s)
- AA: BOD result
- AB: D result
- AC: DO result
- AD: Distance d/s (Samples)
- AE: Sample value

A	B	C	D	E	F	G	H	I	J	K	L	M	N	O	P	Q	R	S	T	U	V	W	X	Y	Z	AA	AB	AC	AD	AE
headwater	0	31.1								1.2E-07	0.026	0.010376	1.20095E-07	0	0			0		9.64	11.65	13	528.080959	0.424	0.171	9.640	1.350	11.650	0	11.65
	1	31.1									0.026											13				9.635	1.355	11.645	1	
	1.69																					13				9.635	1.355	11.645	1.69	
Weldwood	1.7	30.13	0.97	105		7	0.07		8.1E-07	2.55E-06				0.58	6.71E-06	0.15	1.74E-06	0.65	7.52315E-06			13.01				12.609	1.500	11.510	1.7	
	2.7	31.1																				13.015	8.5 open water observed			15.905	1.497	11.518	2.7	11.5
open water	7.7																					13.015				15.260	1.531	11.484	7.7	11.4
	10																					13.02							10	
open water	10.19													0	0							13.02				11.765	1.496	11.524	10.19	
ice cover	10.2													0	0							13.02				11.765	1.496	11.524	10.2	
	11.6																					13.03							11.6	11.185
	15																					13.035							15	
	20																					13.04							20	
	22.65																					13.045				10.609	1.787	11.253	22.65	11.055
	30																					13.05							30	
	35																					13.055							35	
	38.75																					13.06				9.250	2.120	10.940	38.75	10.9
	45																					13.065							45	
	50																					13.07							50	
note: value chambers's values; note: o saturation	55																					13.07							55	
	56.09																					13.07				7.934	2.432	10.639	56.09	
Old Man Creek	56.1	31.1	0.7		8.03	12.36	0.035		4.05E-07	4.05E-07								0.118	1.36574E-06			13.07				7.936	2.394	10.676	56.1	
	60	31.8																				13.078							60	
	65																					13.086				7.863	2.445	10.641	62.3	11
	70																					13.094							70	
	75																					13.102							75	
	78.59																					13.11				7.673	2.577	10.533	78.59	
Spring 1	78.6	31.8	0.015		8.83	11.63	from point source to background - maybe to fast a decline		0	0			1.20095E-07			0	0	0.098	1.13426E-06			13.11				7.674	2.577	10.533	78.6	
	80	31.815																											80	
	85																												85	
	90																												90	
	95																												95	
	100																					13.15				7.538	2.637	10.513	104.2	10.987
	104.39																					13.15				7.537	2.638	10.512	104.39	
Berland River	104.4	31.81	5.67		7.23	8.61							1.20095E-07			0	0	0.084	9.72222E-07			13.15				7.491	2.926	10.224	104.4	
	105	37.48																						0.505	0.168				105	
	110																												110	
	115																												115	
	117.69																					13.17				7.440	2.951	10.219	117.69	
Spring 2	117.7	37.48	0.02		0.8	11.7							1.20095E-07			0	0	0.095	1.09954E-06			13.17				7.436	2.950	10.220	117.7	
	120	37.5																											120	
	125																												125	
	130																												130	
	131.49																					13.2				7.378	2.976	10.224	131.49	
Marsh Creek	131.5	37.5	0.066		6.42	10.46							1.20095E-07					0.081	9.375E-07			13.2				7.377	2.976	10.224	131.5	
	131.69	37.566																				13.2				7.376	2.976	10.224	131.69	
Pine Creek	131.7	37.566	0.019		2.41	10.51							1.20095E-07					0.081	9.375E-07			13.2				7.373	2.976	10.224	131.7	
	135	37.585																											135	
	140																												140	
	145																												145	
	150																												150	
	153.59																					13.27				7.289	3.017	10.253	153.59	
Spring 3	153.6	37.585	0.015		1.61	10.74							1.20095E-07					0.059	6.8287E-07			13.27				7.287	3.016	10.254	153.6	
	155	37.6																											155	
	160																					13.29							160	
	161.59																					13.29				7.261	3.031	10.259	161.59	
Two Creek	161.6	37.6	0.01		9.64	7.67							1.20095E-07					0.042	4.86111E-07			13.29				7.262	3.031	10.259	161.6	
	165	37.61																				13.29				7.258	3.034	10.256	163.1	10.407
	168.59																					13.3				7.242	3.044	10.256	168.59	
Windfall	168.6	37.61	0		10.44	9.12							1.20095E-07					0.025	2.89352E-07			13.3				7.242	3.044	10.256	168.6	
	170	37.61																											170	
	175																												175	
	200																												200	
	209.29																					13.37				7.144	3.117	10.253	209.29	
Sakwatamau Riv	209.3	37.61	0.923		3.61	9.57							1.20095E-07					0.52	6.01852E-06			13.37				7.060	3.133	10.237	209.3	10.53
	210.39	38.533																				13.37				7.044	3.135	10.235	210.39	
McLeod River	210.4	38.533	4.76		12.85	5.28							1.20095E-07					0.52	6.01852E-06			13.37		0.312	0.194	7.683	3.680	9.690	210.4	
	211.99	43.293																				13.39				7.638	3.686	9.704	211.99	
Miller West	212	43.152	0.141	2450.8		5.8	0.05		5.79E-07	2.31E-06				0.58	6.71E-06	0.15	1.74E-06	0.388	4.49074E-06			13.39				15.595	3.699	9.691	212	
		43.293																					open water			15.340	3.601	9.799	213.49	
open water	213.49													0	0											15.382	3.606	9.794	213.5	
ice cover	213.5													0	0											15.357	3.611		213.7	9.925
	213.7																									15.2896	3.6264		214.09	
	214.09	43.293																				13.4				15.332	3.862	9.768	214.1	
White STP	214.1	43.255	0.038	63.2		3.2								0	0	0	0	0.276	3.19444E-06			13.4				14.318	3.864	9.546	220.7	9.055
	225	43.293																				13.41				12.495	4.277	9.153	233.8	8.822
	235																					13.43							235	
	268.09							0.036		4.17E-07	4.17E-07				0	0	0	0	0.157	1.81713E-06			13.45				8.647	5.127	8.323	268.09	
	268.1																						13.45	up to here			8.647	5.127	8.323	268.1	
	300																						13.48				8.590	5.165	8.315	270.65	8.572
	305.19																						13.5				7.872	5.634	7.866	305.19	
Freeman River	305.2	43.293	0.48		4.02	5.56						0.026	0.010376	1.20095E-07	0	0	0	0	0.157	1.81713E-06			13.5				7.786	5.659	7.841	305.2	7.635
	350	43.773																											349.3	
	392.79																						13.61				6.832	5.970	7.640	392.79	8.107
Pembina River	392.8	43.773	2.8		4.02	2.77																	13.61				6.663	6.262	7.348	392.8	
	400	46.573																					13.62				6.071	6.437	7.193	400	
	448.79																						13.63				6.071	6.437	7.193	448.79	
Lesser Slave Riv	448.8	46.573	25.107		7.23	13.1												0.146	1.68981E-06			13.63		0.44	0.162	6.477	4.368	9.262	448.8	7.592
	500	71.68																					13.64				6.141	4.472	9.168	516.8	8.805
u/s of Athabasca	556.9	71.68																					13.66				5.833	4.564	9.096	556.9	8.838

Using MacDonald's river distances. Flows from Chambers. Chambers BODu and DO. Rates from Chambers + two rate model for decay of mill effluent

A	B	C	D	E	F	G	H	I	J	K	L	M	N	O	P	Q	R	S	T	U	V	W	X	Y	Z	AA	AB	AC	AD	AE
13 February 16 March				**1989** Inputs			**Rates**													**Headwater Initial**						**Variable Velocity Model**			**Samples**	
Name or description notes	Distance d/s	River Flow cms	Tributary/ Point Source inflows cms	Point Source BODu (XLD1) chamber's values	Tributary BODu (XLD3)	Point Source and Tributary DO (XLD2)	Point Source BOD decay 1/day @20C (XK1)	Point Source BOD decay 1/day @0C	Point Source BOD decay 1/sec @0C	BOD removal rate 1/sec	BOD decay rate for tributaries 1/day @20c (XK4)	BOD decay rate for tributaries 1/day @0c	BOD decay rate for tributaries 1/day@0c 1/sec	Reaeration 1/day @0C (XK2)	Reaeration 1/sec @0C	BOD settling rate @0c 1/day (XK3)	BOD settling rate @0c 1/sec (XK3)	SOD @0c 1/day XRES	SOD @0c 1/sec XRES	BOD u (XO4)	DO (XO3)	O sat (XDS)	pool to pool spacing sinuosity*5.4w^1.01 (m)	Average velocity (in m/s) (a)	Velocity Amplitude (b) (m/s)	BOD result	D result	DO result	Distance d/s	
headwater	0	28							1.2E-07		0.026	0.010376	1.20095E-07	0	0	0		0		13.89	11.69	13	528.080959	0.4	0.17	13.890	1.310	11.690	0	11.69
	1	28									0.026											13							1	
	1.69	28																				13				13.882	1.318	11.682	1.69	
Weldwood	1.7	26.98	1.02	73.15		7	0.07		8.1E-07	2.55E-06				0.58	6.71E-06	0.15	1.74E-06	0.65	7.52315E-06			13.01				16.041	1.489	11.521	1.7	
	2.7	28																				13.015	12.2 km open water			15.905	1.497	11.518	2.7	10.96
open water	7.7	28																				13.015				15.260	1.531	11.484	7.7	11.177
	10																					13.02							10	
open water	11.6																					13.02				14.759	1.551	11.469	11.6	11.01
open water	13.89																					13.03				14.482	1.559	11.471	13.89	
ice cover	13.9													0	0							13.03				21.369	1.672	11.358	13.9	
	15																					13.035							15	
	20																					13.04							20	
	22.65																					13.045				19.914	2.077	10.963	22.65	10.64
	30																					13.05							30	
	35																					13.055							35	
	38.75																					13.06				17.471	2.748	10.312	38.75	10.21
	45																					13.065							45	
	50																					13.07							50	
	55																					13.07							55	
	56.09			note: value chambers values	note: o saturation																	13.07				15.123	3.380	9.690	56.09	
Old Man Creek	56.1	28	0.95		5.62	12.84	0.035		4.05E-07	4.05E-07					0	0		0.118	1.36574E-06			13.07				14.811	3.277	9.793	56.1	
	60	28.95																				13.078							60	
	65																					13.086				14.685	3.380	9.706	62.3	10.06
	70																					13.094							70	
	75																					13.102							75	
	78.59			from point source to background - maybe to fast a decline																		13.11				14.359	3.645	9.466	78.59	
Spring 1	78.6	28.95	0.03		8.03	11.55			0	0			1.20095E-07		0	0		0.098	1.13426E-06			13.11				14.352	3.642	9.468	78.6	
	80	28.98																											80	
	85																												85	
	90																												90	
	95																												95	
	100																					13.15				14.148	3.765	9.385	104.2	9.827
	104.39																					13.15				14.146	3.766	9.384	104.39	
Berland River	104.4	28.98	5.52		8.03	9.61							1.20095E-07		0	0		0.084	9.72222E-07			13.15		0.45	0.16	13.168	3.730	9.420	104.4	
	105	34.5																											105	
	110																												110	
	115																												115	
	117.69																					13.17				13.088	3.737	9.433	117.69	
Spring 2	117.7	34.5	0.015		5.62	12.01							1.20095E-07		0	0		0.095	1.09954E-06			13.17				13.084	3.736	9.434	117.7	
	120	34.515																											120	
	125																												125	
	130																												130	
	131.49																					13.2				12.997	3.830	9.370	131.49	
Marsh Creek	131.5	34.515	0.173		5.62	11.7							1.20095E-07					0.081	9.375E-07			13.2				12.960	3.830	9.370	131.5	
	131.69	34.688																				13.2				12.959	3.831	9.369	131.69	
Pine Creek	131.7	34.688	0.31		4.02	12.09							1.20095E-07					0.081	9.375E-07			13.2				12.880	3.807	9.393	131.7	
	135	34.998																											135	
	140																												140	
	145																												145	
	150																												150	
	153.59																					13.27				12.750	3.888	9.382	153.59	
Spring 3	153.6	34.998	0.02		4.82	11.29							1.20095E-07					0.059	6.8287E-07			13.27				12.745	3.887	9.383	153.6	
	155	35.018																											155	
	160																					13.29							160	
	161.59																					13.29				12.703	3.916	9.374	161.59	
Two Creek	161.6	35.018	0.014		5.62	10.47							1.20095E-07					0.042	4.86111E-07			13.29				12.700	3.915	9.375	161.6	
	165	35.032																				13.29				12.698	3.917	9.373	163.1	9.75
	168.59																					13.3				12.667	3.940	9.360	168.59	
Windfall	168.6	35.032	0.503		3.21	10.78							1.20095E-07					0.025	2.89352E-07			13.3				12.533	3.920	9.380	168.6	
	170	35.535																											170	
	175																												175	
	200																					13.37							200	
	209.29																					13.37				12.403	4.029	9.341	209.29	
Sakwatamau River	209.3	35.535	0.923		3.61	9.57							1.20095E-07					0.52	6.01852E-06			13.37				12.180	4.023	9.347	209.3	9.46
	210.39	36.458																				13.37				12.161	4.027	9.343	210.39	
McLeod River	210.4	36.458	4.63		6.42	5.95							1.20095E-07					0.52	6.01852E-06			13.37		0.305	0.192	11.514	4.409	8.961	210.4	
	211.99	41.088																				13.39				11.464	4.418	8.972	211.99	
Miller West	212	40.964	0.124	2450.8		7.3	0.05		5.79E-07	2.31E-06				0.58	6.71E-06	0.15	1.74E-06	0.388	4.49074E-06			13.39				18.826	4.423	8.967	212	
open water	213.49																									18.494	4.294	9.096	213.7	9.343
ice cover	213.5																													
	214.09	41.088																				13.4				18.402	4.259	9.141	214.09	
White STP	214.1	41.053	0.035	63.2		4.4								0	0			0.276	3.19444E-06			13.4				18.440	4.263	9.137	214.1	
	225	41.088																				13.41				17.203	4.550	8.860	220.7	8.813
	235																					13.43				15.139	5.026	8.405	233.8	8.343
	268.09																					13.45				10.324	6.110	7.340	268.09	
	268.1						0.036		4.17E-07	4.17E-07				0	0	0	0	0.157	1.81713E-06			13.45				9.518	6.069	7.381	268.1	
	300																					13.48				9.466	6.105	7.375	270.65	7.375
	305.19																					13.5				8.642	6.660	6.840	305.19	
Freeman River	305.2	41.088	0.59		9.64	9.45					0.026	0.010376	1.20095E-07	0	0	0	0	0.157	1.81713E-06			13.5				8.520	6.623	6.877	305.2	6.94
	350	41.678																											349.3	
	392.79																					13.61				7.494	6.978	6.632	392.79	6.332
Pembina River	392.8	41.678	2.91		11.24	1.46																13.61				7.739	7.315	6.295	392.8	
	400	44.588																				13.62							400	
	448.79																					13.63				7.099	7.526	6.105	448.79	
Lesser Slave River	448.8	44.588	22.692		3.21	13.02												0.146	1.68981E-06			13.63		0.428	0.161	5.787	5.193	8.437	448.8	5.827
	500	67.28																				13.64				5.381	5.308	8.332	516.8	7.74
u/s of Athabasca	556.9	67.28																				13.66				5.146	5.372	8.288	556.9	7.955